N73-18568

REPORT NO. GDCA 632-3-169
CONTRACT NAS 8-27203

AFS-17311

CASE FILE
COPY

CHARACTERISTICS OF A GELLED LIQUID HYDROGEN POLYPHENYLENE OXIDE (PPO) FOAM OPEN-CELL INSULATION SYSTEM

FINAL REPORT (PHASE ONE)

MAY 1973
NASA STI FACILITY
INPUT BRANCH

GENERAL DYNAMICS
Convair Aerospace Division

REPORT NO. GDCA 632-3-169
CONTRACT NAS 8-27203

CHARACTERISTICS OF A GELLED LIQUID HYDROGEN POLYPHENYLENE OXIDE (PPO) FOAM OPEN-CELL INSULATION SYSTEM

FINAL REPORT (PHASE ONE)

15 February 1973

Submitted to
National Aeronautics and Space Administration
GEORGE C. MARSHALL SPACE FLIGHT CENTER
Huntsville, Alabama

Prepared by
CONVAIR AEROSPACE DIVISION OF GENERAL DYNAMICS
San Diego, California

ABSTRACT

Phase I of a program to investigate the characteristics of a gelled liquid hydrogen (gel)/ polyphenylene oxide (PPO) foam open-cell insulation system is presented. Convair Aerospace has developed a large-scale gel production and storage facility and a small-scale facility, the latter used for detailed visual examination of the gel/PPO foam interface. The Aerojet Liquid Rocket Company of Sacramento, California, was subcontracted to investigate techniques for the production of gelled liquid hydrogen, develop a process design for scale-up to a 1.89 m^3 (500 gallon) gel production and storage facility, determine gel transfer characteristics, determine the solubility rate of gaseous helium in the gel, and investigate the gross gel/PPO foam interfacial phenomena. An "inside-tank" process for scaled-up production of gelled liquid hydrogen was selected. No detectable gel structure degradation occurred during repeated shearing. The viscosity of gelled liquid hydrogen at shear rates of 300 sec^{-1} and higher is 2 to 5-fold greater than that of neat liquid hydrogen. No clogging problems were encountered during the transfer of gelled liquid hydrogen through warmed transfer lines. The solubility rate of helium in liquid hydrogen was significantly reduced by the presence of gel structure. The boil-off rates from gelled liquid hydrogen were reduced from 25 to 50 percent compared to those observed for the neat liquid hydrogen under compatible conditions. The polyphenylene oxide (PPO) foam insulation was found to be compatible with liquid ethane.

FOREWORD

This report describes the accomplishments of Phase I of Contract NAS8-27203, "Investigation of the Characteristics of a Gelled Liquid Hydrogen Polyphenylene Oxide (PPO) Foam Open-Celled Insulation System." This is a final contract report due to NASA cancellation of the program at the completion of Phase I for budgetary reasons. The program was managed by F. O. Bennett of the Convair Aerospace Division of General Dynamics under the overall direction of R. E. Tatro, Thermodynamics Group Engineer. A major portion of the Phase I activity was subcontracted to the Aerojet Liquid Rocket Company of Sacramento, California, where it was managed by Dr. S. D. Rosenberg, Manager of the Chemical Processes and Materials Laboratories Department. Experimental work at Aerojet was directed by Dr. E. M. VanderWall.

This contract was administered under the technical direction of E. H. Hyde, the Contracting Officer's Representative, S&E-ASTN-PF, Astronautics Laboratory of the NASA George C. Marshall Space Flight Center.

In addition to the above named, the contributions to this program of the following Convair Aerospace and Aerojet personnel are gratefully acknowledged:

Convair Aerospace	Aerojet
M. H. Blatt	R. E. Anderson
H. G. Brittain	R. L. Beegle, Jr.
M. D. Campbell	J. A. Cabeal
G. E. Copeland	
B. A. Ganoe	
R. W. Jennings	
R. L. Otwell	
K. I. Sleigh	

TABLE OF CONTENTS

Section		Page
LIST OF ILLUSTRATIONS		xi
LIST OF TABLES		xiii
NOMENCLATURE		xv
SUMMARY		xvii
1	INTRODUCTION	1-1
2	GELLED LIQUID HYDROGEN (WBS 1100)	2-1
2.1	GEL CHARACTERISTICS AND PRODUCTION APPARATUS	2-1
2.2	GEL PRODUCTION FACILITY DEVELOPMENT	2-16
3	TRANSFER AND SOLUBILITY (WBS 1200)	3-1
3.1	GEL TRANSFER	3-1
3.2	HELIUM SOLUBILITY	3-19
4	INTERFACIAL PHENOMENA (WBS 1300)	4-1
4.1	COMPATIBILITY AND GROSS EFFECTS	4-1
4.2	INTERFACIAL EFFECTS	4-5
5	REFERENCES	5-1
6	NEW TECHNOLOGY	6-1

LIST OF ILLUSTRATIONS

Figure		Page
1-1	Work Breakdown Structure	1-3
1-2	Program Schedule	1-4
1-3	Density Impulse of Chemical Propulsion	1-6
1-4	Comparison of Nuclear and Chemical Propulsion Systems Performance	1-8
2-1	Outside- and Inside-Tank Gel Production Methods	2-3
2-2	Schematic Diagram of Apparatus for Preparation of Gelled Liquid Hydrogen	2-4
2-3	Flowing Gel Preparation Device	2-5
2-4	Results of "Flowing LH_2" Gel Production Tests	2-7
2-5	Apparatus for Storage of Gelled Liquid Hydrogen	2-8
2-6	Basic Apparatus for Preparation of Gelled Liquid Hydrogen	2-8
2-7	Results of "Static LH_2" Gel Production Tests	2-10
2-8	Schematic of Vacuum-Jacketed Internally Heated Injection Tube	2-12
2-9	Vacuum-Jacketed, Internally Heated Injection Tube	2-12
2-10	Gel Production Rate Versus Composition of Injected Gas Mixture	2-18
2-11	LH_2 Use Efficiency Versus Composition of Injected Gas Mixture	2-18
2-12	Twin-Orifice Injection Tube Operating in Liquid Hydrogen	2-19
2-13	Large Scale Gel Production Facility Schematic	2-21
2-14	Large Scale Gel Production Facility	2-22
2-15	Cover of Gel Production and Storage Tank	2-22
2-16	Pesco Liquid Hydrogen Pump	2-23
2-17	Gelant Injection Tube	2-24
2-18	Schematic of Gelant Injection Tube	2-26
2-19	View Into Gel Tank Through Viewport	2-27
3-1	Gel Shear Degradation Test Apparatus	3-2
3-2	Test Apparatus in Test Box	3-3

LIST OF ILLUSTRATIONS, CONTD

Figure		Page
3-3	Characteristic Flow Curve, Neat Liquid Hydrogen	3-4
3-4	Characteristic Flow Curve, Gelled Liquid Hydrogen (12.75% Ethane	3-4
3-5	Characteristic Flow Curve, Gelled Liquid Hydrogen (9.5% Ethane)	3-6
3-6	Segment of Flow Curve for Gelled Liquid Hydrogen (8.4% Ethane)	3-6
3-7	Characteristic Flow Curves for Gelled and Neat Liquid Hydrogen, 7.87 mm Tubing	3-8
3-8	Characteristic Flow Curves for Gelled and Neat Liquid Hydrogen, 3.25 mm Tubing	3-9
3-9	Gel Transfer Tubes	3-12
3-10	Schematic Diagram of Thermocouple Locations in Transfer Tubes	3-12
3-11	Transfer of Neat Liquid Hydrogen Through a 4.6 mm I.D. Tube Surrounded by Gaseous Nitrogen	3-14
3-12	Transfer of Liquid Hydrogen Gelled With 9.6 Weight Percent Ethane Through a 4.6 mm I.D. Tube Surrounded by Gaseous Nitrogen	3-14
3-13	Transfer of Neat Liquid Hydrogen Through a 4.6 mm I.D. Tube Surrounded by Liquid Nitrogen	3-15
3-14	Transfer of Liquid Hydrogen Gelled With 5.6 Weight Percent Ethane Through a 4.6 mm I.D. Tube Surrounded by Liquid Nitrogen	3-15
3-15	Transfer of Liquid Hydrogen Gelled With 24 Weight Percent Ethane Through a 4.6 mm I.D. Tube Surrounded by Liquid Nitrogen	3-17
3-16	Transfer of Liquid Hydrogen Gelled With 17.4 Weight Percent Ethane Through a 4.6 mm I.D. Tube Surrounded by Liquid Nitrogen	3-17
3-17	Restart of Transfer of Liquid Hydrogen Gelled With 17.4 Weight Percent Ethane Through a 4.6 mm I.D. Tube Surrounded by Liquid Nitrogen	3-18
3-18	Transfer of Neat Liquid Hydrogen Through a 7.0 mm I.D. Tube Surrounded by Gaseous Nitrogen	3-18
3-19	Transfer of Liquid Hydrogen Gelled With 10.2 Weight Percent Ethane Through a 7.0 mm I.D. Tube Surrounded by Gaseous Nitrogen	3-20
3-20	Transfer of Neat Liquid Hydrogen Through a 7.0 mm I.D. Tube Surrounded by Liquid Nitrogen	3-20

LIST OF ILLUSTRATIONS, CONTD

Figure		Page
3-21	Transfer of Liquid Hydrogen Gelled With 10.2 Weight Percent Ethane Through a 7.0 mm I.D. Tube Surrounded by Liquid Hydrogen	3-21
3-22	Flask Arrangement Used to Measure the Rate of Solubilization of Helium in Liquid Hydrogen	3-22
3-23	Relative Rate of Dissolution of Helium in Neat and Gelled LH_2	3-22
4-1	Apparatus Used for Immersion Testing of PPO Foam in Liquid Ethane	4-2
4-2	PPO Foam Samples in As-Received Condition and After Exposure to Liquid Ethane	4-2
4-3	Flask for Boil-off Tests With PPO Foam Present	4-3
4-4	Comparative Boiloff Rates	4-3
4-5	Interface Test Facility Schematic	4-6
4-6	Interface Test Apparatus	4-7
4-7	Interface Test Facility	4-7
4-8	Liquid Hydrogen in Test Container	4-8
4-9	Gel in Test Container	4-8

LIST OF TABLES

Table		Page
1	Chemical Propulsion System Performance	1-6
2	"Flowing LH_2" Gel Production Test Conditions	2-7
3	"Static LH_2" Gel Production Test Conditions	2-10
4	Summary of Gel Preparation Parameters	2-17
5	Apparent Viscosity of Gelled and Neat Liquid Hydrogen, 7.87 mm Tubing	3-8
6	Apparent Viscosity of Gelled and Neat Liquid Hydrogen, 3.25 mm Tubing	3-10
7	Apparent Viscosity of Gelled and Neat Liquid Hydrogen, 4.83 mm Tubing	3-10
8	Flow Test Parameters	3-13
9	Interface Effects Test Bubble Data	4-15

NOMENCLATURE

a	acceleration (m/sec^2)
A	area (m^2)
Bo	Bond number
C_p	specific heat (J/kg K)
C_v	flow coefficient
D	diameter (m)
F	force (N)
h	height (m)
h_{fg}	heat of vaporization (J/kg)
H	enthalpy (J/kg)
ΔH_f	heat of formation (J/mole)
I_{sp}	specific impulse (sec)
k	specific heat ratio
L	length (m)
$\dot{m}$	mass flow rate (kg/sec)
$\bar{M}$	molecular weight (kg/mole)
p	pressure (N/m^2)
P	pressure (N/m^2)
$\bar{q}$	volumetric flow rate (m^3/sec)
$\dot{Q}$	heat flow (watt)
R	radius (m)
T	temperature (K)
U	bubble rise velocity (m/sec)
V	velocity (m/sec)
$\dot{W}$	mass flow rate (kg/sec)

ϵ	area ratio
ρ	density (kg/m^3)
σ	surface tension (N/m)

Subscripts

b	bubble (subject to buoyancy), buoyancy
B	bubble (total)
c	chamber, combustion
E	exit
L	liquid
o	orifice
s	surface
T	throat
u	ullage
v	vapor

SUMMARY

Convair Aerospace Division of General Dynamics Corporation has completed the first phase of a planned three phase program to investigate the characteristics of a gelled liquid hydrogen/polyphenylene oxide (PPO*) foam open-cell insulation system. The program has been terminated by the NASA at the completion of Phase I for budgetary reasons. This report documents the activities of Phase I of this effort performed by Convair Aerospace with major subcontract participation by the Aerojet Liquid Rocket Company. Phase I, entitled "Interfacial Phenomena and Transfer," involved an investigation of techniques for producing gelled liquid hydrogen (gel) on a large scale, a study of gel transfer characteristics, and an investigation of the phenomena occurring at the gel/PPO foam interface.

Aerojet evaluated two techniques for gelling liquid hydrogen with small particles of ethane based on the gelant gas condensation process. The "inside-tank," or "static" technique, where the gelant gas is injected below the liquid surface of a tank of LH_2, was found to produce gel having a lower gelant weight concentration than that produced by the "outside-tank," or "flowing" technique, where the gelant is injected into a flowing stream of LH_2 and the resulting gel is collected in a tank. A process design was then written for scale up of the "static" technique and a large scale, 1.90 m^3 (500 gal), gel production facility was developed. During checkout of the system, 0.30 m^3 (80 gal) of gel containing 12-14 weight percent ethane gelant was produced. Two injection tubes, each containing four gelant injection orifices, will produce 1.33 m^3 (350 gal) of ten weight percent gel in approximately eleven hours.

True gels "shear thin" rapidly when exposed to a shearing stress, flow like a liquid, and then set back up when the stress is removed. The effect of repeated shearing, or transfer, of gelled liquid hydrogen on its at-rest structure was investigated, and it was concluded there is no significant shear degradation of the gel structure. Gel and neat liquid hydrogen flow viscosities were measured at various stress (ΔP) levels, in various tube sizes, and with various incident heat flux levels. In all cases under the same conditions the viscosity of flowing gelled liquid approaches that of flowing neat liquid hydrogen as the flow rate increases. During this investigation the rates of dissolution of helium in both neat and gelled liquid hydrogen were measured. It was concluded that, although the total quantity dissolved is the same for both systems, the rate of dissolution of helium in gel is many times less than that in neat liquid hydrogen.

*General Electric Co. trademark

A small-scale apparatus to evaluate the PPO foam/gelled LH_2 and PPO foam/neat LH_2 interfacial phenomena was fabricated and tested. Hydrogen gas bubble departure diameters and frequencies and bubble rise rates were predicted and measured. Heat transfer data were taken and temperature profiles were measured at two heater power settings.

SECTION 1

INTRODUCTION

The objective of this program is to evaluate analytically and experimentally the compatibility and characteristics of a propellant/insulation system consisting of liquid hydrogen gelled with solid ethane particles and polyphenylene oxide (PPO) open-cell foam. This system is being compared with a neat liquid hydrogen/PPO foam system to evaluate its applicability to large, cryogenic, launch and space transportation vehicles.

1.1 PROGRAM BACKGROUND AND OBJECTIVES

Liquid hydrogen has been used as a high-energy propellant for a number of years, and its characteristics have been thoroughly studied and documented. Among its shortcomings are low density, severe temperature stratification, low heat of vaporization per unit of volume, and sloshing during launch. Since before the first flight of the liquid-hydrogen-fueled Centaur upper stage vehicle, studies have been conducted in an effort to improve the handling and flight characteristics of hydrogen. One of the more promising developments has been the preparation of gels of both liquid and slush hydrogen which possess semi-solid structure when at rest and which shear-thin rapidly when stressed, with flow behavior closely approaching that of neat hydrogen (Ref. 1). These gels are prepared by suspending sub-micron-size particles of matter in the liquid in sufficient quantity so that the particle-particle attraction forces are great enough to impart the gel structure to the mixture.

A limited amount of research has been conducted involving the gelation of liquid hydrogen during the last several years. Until 1968, the most extensive investigations were conducted by Technidyne (Ref. 1 and 2). They were successful in gelling liquid hydrogen with several particulate gelants such as silica, carbon black, aluminum flake, lithium, and lithium borohydride. The respective concentration levels require for gelation were 35, 45, 73, 61 and 59 weight percent. In 1968, an Aerojet IRAD program demonstrated the successful gelation of liquid hydrogen with particles of methane, ethylene, butane, and ammonia. In this early study, less than 30 weight percent methane was required for gelation. Subsequently, under contract to the NASA, Aerojet formulated liquid hydrogen fuels which contain various quantities of hydrocarbons in a uniform suspension. By optimizing the gelant preparation techniques, liquid hydrogen was gelled using 10 weight percent ethane (Ref. 3).

The principal potential advantages of the gelled hydrogen system over the corresponding liquid system are that (1) the evaporation, or boiloff rate, is significantly lower (Ref. 2); (2) the frequency of slosh modes is higher and the amplitude lower; (3) the

semi-solid structure when at rest could eliminate the need for positive expulsion devices for zero-g transfer; and (4) leakage through cracks or punctures may be significantly lower (Ref. 4). For the Modular Nuclear Vehicle, liquid hydrogen gelled with carbon containing compounds has an advantage in that the corrosion of the carbonaceous reactor core by hydrogen can be reduced by the presence of carbon in the gelled hydrogen. Gelled liquid hydrogen does possess several potential disadvantages. Adding the gelant can reduce the specific impulse of the propellant unless a high-energy compound is used. This is discussed in more detail below. In this regard, it has been determined that the addition of beryllium or lithium metals to an H_2-O_2 or H_2-F_2 system can actually cause the specific impulse to increase (Ref. 5). If the gelant is nonvolatile at the system operating temperatures, solid residues can be deposited in lines, valves, pumps, etc., increasing system pressure drops and inhibiting engine restart. Residual propellant quantities are increased due to gel coring and hang-up during outflow although these effects may be reduced by an efficient outlet baffle design.

The two primary functions of an insulation system on a cryogenic propellant tank are to minimize liquid loss due to vaporization by minimizing heat flow into the tank, and to prevent cryopumping of air while in the atmosphere. Both internal and external closed-cell foam insulation systems have been used on the upper stages of the Saturn V launch vehicle, designed for a single mission cycle. More recently requirements have been developed for cryogenic storage systems which are reusable for up to 100 mission cycles. This demand has resulted in a need for a thorough re-evaluation of cryogenic insulation techniques and materials. An external system with its bond line cycled between ambient (or higher) and cryogenic temperatures on each mission is subjected to severe thermal stresses. Internal closed-cell foam systems have a warm bond line but must be covered with a potentially-unreliable liner which is designed to restrict hydrogen permeation of the cells. In addition, closed-cell foam systems in general undergo internal pressure cycling as the insulation is thermally cycled, a condition which can result in cracking, debonding, and possible complete structural failure.

An open-cell foam insulation system does not undergo internal pressure cycling and requires no liner. The open-cell insulation concept consists of small, elongated cells bonded to the inner tank wall at one end and open to the cryogenic liquid at the other end (Ref. 6). The cells are sized such that the forces due to liquid surface tension are large enough to prevent liquid entry into the cells, thus providing an insulating gas layer between the liquid and the tank wall. PPO open-cell foam is a unique, new material which has a density-conductivity (ρk) product competitive with that of existing systems (Ref. 7), is a tough material with good cryogenic properties (Ref. 8 and 9), and is a simple, two-component (foam and adhesive) system with the potential for maximum reliability and reusability. Its feasibility as a liquid hydrogen tank internal insulation system was demonstrated by Convair Aerospace in 1971 (Ref. 10).

The objectives of this program were to have been achieved with a three-phase study designed to evaluate gel/foam interfacial effects and gel transfer (Phase I), heat transfer and thermal stratification (Phase II), and the effect of sloshing and vibration

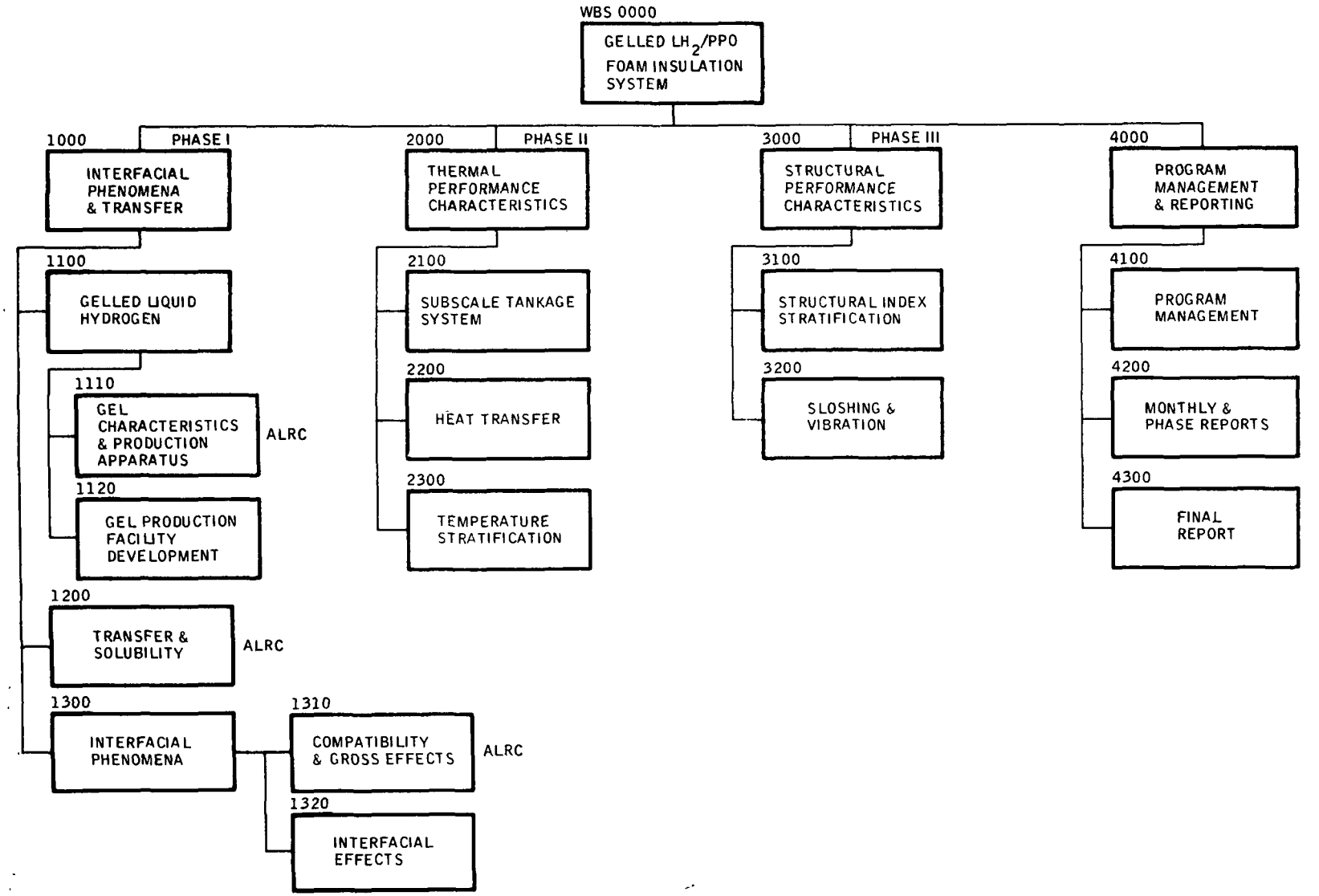

Figure 1-1. Work Breakdown Structure

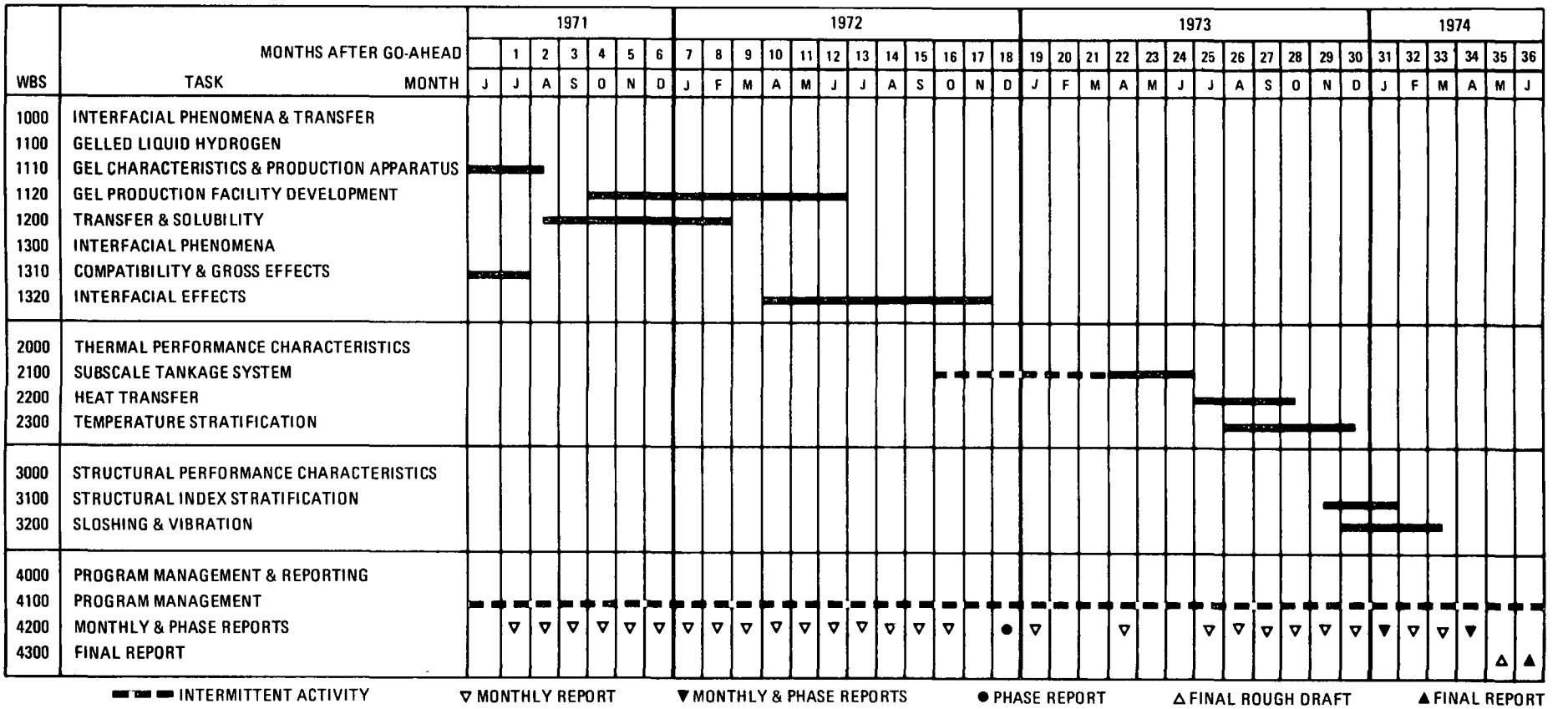

Figure 1-2. Program Schedule

on the structure of gelled liquid hydrogen (Phase III). However, NASA budgetary constraints caused termination of this contract at the completion of Phase I. A program work breakdown structure and schedule are shown in Figures 1-1 and 1-2, respectively. This report documents the results of the Phase I activity performed jointly by Convair Aerospace and the Aerojet Liquid Rocket Company. Although the English system of units (ft, lb, sec) has been used for all measurements and calculations, in this report the S.I. system of units is shown as the primary system with English units in parentheses.

1.2 THEORETICAL PROPELLANT PERFORMANCE

Potential applications for gelled liquid hydrogen include both chemical (H_2/O_2) and nuclear (H_2 expansion) propulsion systems. The effect of gelant addition to the hydrogen propellant on theoretical specific impulse is discussed below.

1.2.1 CHEMICAL PROPULSION SYSTEMS. One of the potential disadvantages of the use of gelled liquid hydrogen as a fuel is the specific impulse degradation that occurs due to the relatively low fuel value normally associated with the gelant. For example, with the hydrogen/oxygen bipropellant combination, the gelation of the liquid hydrogen with inert collodial silica (35 weight percent being required) with no inherent fuel value results in prohibitive performance losses (Ref. 11). In an effort to minimize the performance loss, a gelant with considerable fuel value, solid ethane, was used for gelation of liquid hydrogen in this investigation. It should be further noted that ethane was previously found to be the most effective hydrocarbon for the gelation of liquid hydrogen, 10 weight percent ethane produced gels having comparable structure to those obtained using 17 weight percent methane (Ref. 3). Theoretical performance data for the LO_2/LH_2 and LO_2/ethane-gelled LH_2 propellant combinations are presented in Table 1 and the data are plotted in Figure 1-3 in the form of specific impulse versus density impulse. The mixture ratio values are noted on the curves in Figure 1-3.

At the normal operating mixture ratio of 5, the specific impulse value is degraded 0.66% with the use of 4.7 weight percent ethane and the value is degraded 1.35 percent with the use of 9.4 weight percent ethane. On the other hand, the density impulse value is enhanced 2.8 percent with the use of 4.7 weight percent ethane and the value is enhanced 5.5 percent with 9.4 weight percent ethane. In order to assess the overall impact on performance by the use of gelled hydrogen, the mission must be clearly defined. The data presented herein provide the indication that the degradation is not prohibitive.

1.2.2 NUCLEAR PROPULSION SYSTEMS. Because of the extremely low molecular weight of hydrogen, the addition of relatively small amounts of gelants for the liquid hydrogen will produce significant degradation in the specific impulse value. The use of a hydrocarbon as gelant for the liquid hydrogen in a nuclear propulsion system has one advantage over other gelants in that it has been hypothesized that a hydrocarbon concentration equivalent to 0.5 weight percent of methane in hydrogen will significantly

Table 1. Chemical Propulsion System Performance

O/F	$I_{sp(1000/14.7)}$, sec	ρ_B, g/cm^3	$I_{sp}\ \rho_B$, g-sec/cm^3	T_c, K(R)
LO_2(NBP)/LH_2(NBP)				
2	370.69	0.1889	70.03	1800 (3240)
3	385.65	0.2387	92.05	2459 (4426)
4	389.42	0.2835	110.42	2957 (5322)
5	387.64	0.3241	125.65	3297 (5935)
6	382.16	0.3611	137.98	3498 (6297)
7	373.20	0.3948	147.34	3588 (6458)
8	361.07	0.4257	153.71	3603 (6485)
LO_2(NBP)/LH_2(NBP)+0.0469 C_2H_6				
2	369.06	0.1963	72.46	1815 (3267)
3	383.01	0.2476	94.82	2488 (4478)
4	386.83	0.2935	113.55	2992 (5385)
5	385.10	0.3350	129.01	3329 (5993)
6	379.11	0.3726	141.25	3518 (6332)
7	369.80	0.4068	150.45	3594 (6470)
8	356.88	0.4382	156.37	3599 (6478)
LO_2(NBP)/LH_2(NBP)+0.0937 C_2H_6				
2	366.98	0.2043	74.98	1832 (3297)
3	380.37	0.2571	97.79	2519 (4535)
4	384.25	0.3042	116.90	3028 (5451)
5	382.42	0.3466	132 54	3360 (6048)
6	376.09	0.3849	144.74	3536 (6365)
7	365.91	0.4196	153.54	3598 (6477)
8	352.54	0.4513	159.10	3593 (6467)

Note - The following heats of formation and densities were used in computing the performance data tabulated here

	ΔH_f, cal/mole	Density, g/cm^3
LO_2(NBP, 90.168 K)	-3102	1.1407
LH_2(NBP, 20.268 K)	-2154	0.070786
Ethane (solid @ 20.268 K)	-27,945	0.75 (estimated)

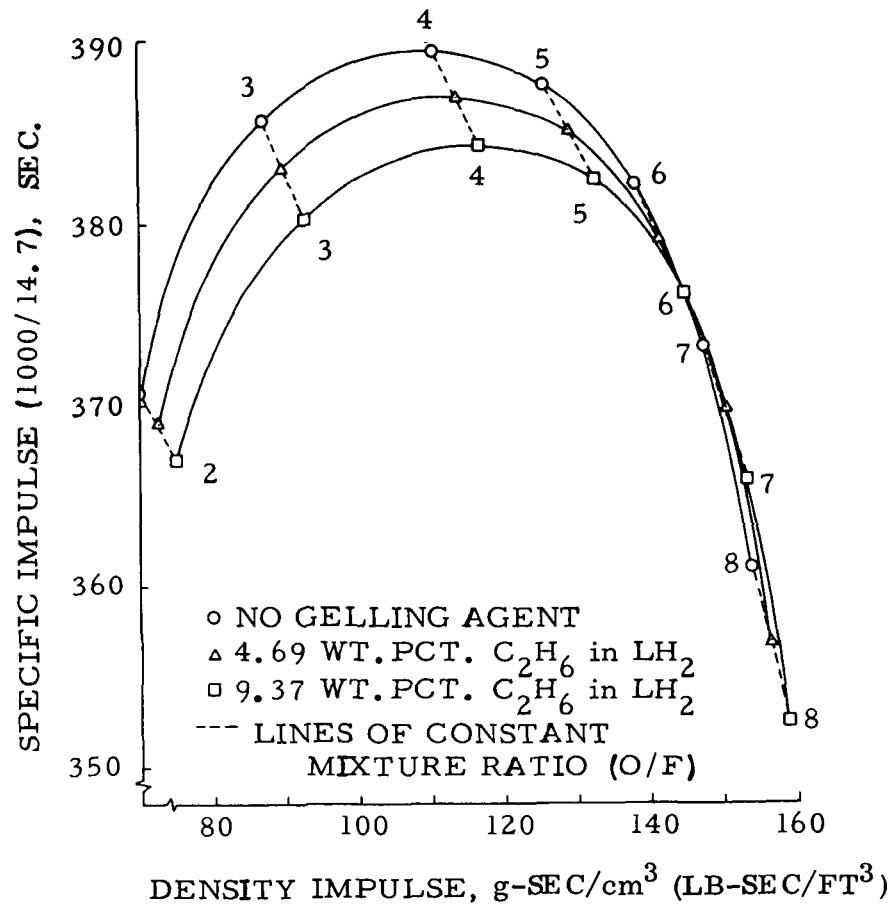

Figure 1-3. Density Impulse of Chemical Propulsion System

inhibit the core corrosion with graphitic fuel elements. However, considerably greater quantities of hydrocarbons are required to gel liquid hydrogen. It was found that approximately 17 weight percent methane is required to produce a stable liquid hydrogen gel (Ref. 3), while a comparable gel could be obtained with 10 weight percent ethane. A plot of the specific impulse decrease for a nuclear system versus the ethane concentration in the liquid hydrogen is shown in Figure 1-4. Equivalent values for a chemical system operating at a 5:1 mixture ratio are shown for comparison.

Assuming that 10 weight percent ethane is used to gel the hydrogen, the specific impulse performance degradation is 2.5% percent compared to that of neat liquid hydrogen at a 3.1 MN/m^2 (450 psia) chamber pressure, a 2500 K (4500R) chamber temperature and at an expansion ratio of 100:1. However, because of the corrosion inhibiting characteristics of the ethane, the nuclear reactor could be operated at a higher temperature to compensate for the specific impulse loss. An increase of approximately 110 C (200F) in the operating temperature of the nuclear reactor would compensate for the performance loss incurred by the use of 10 weight percent ethane as gelant for the liquid hydrogen.

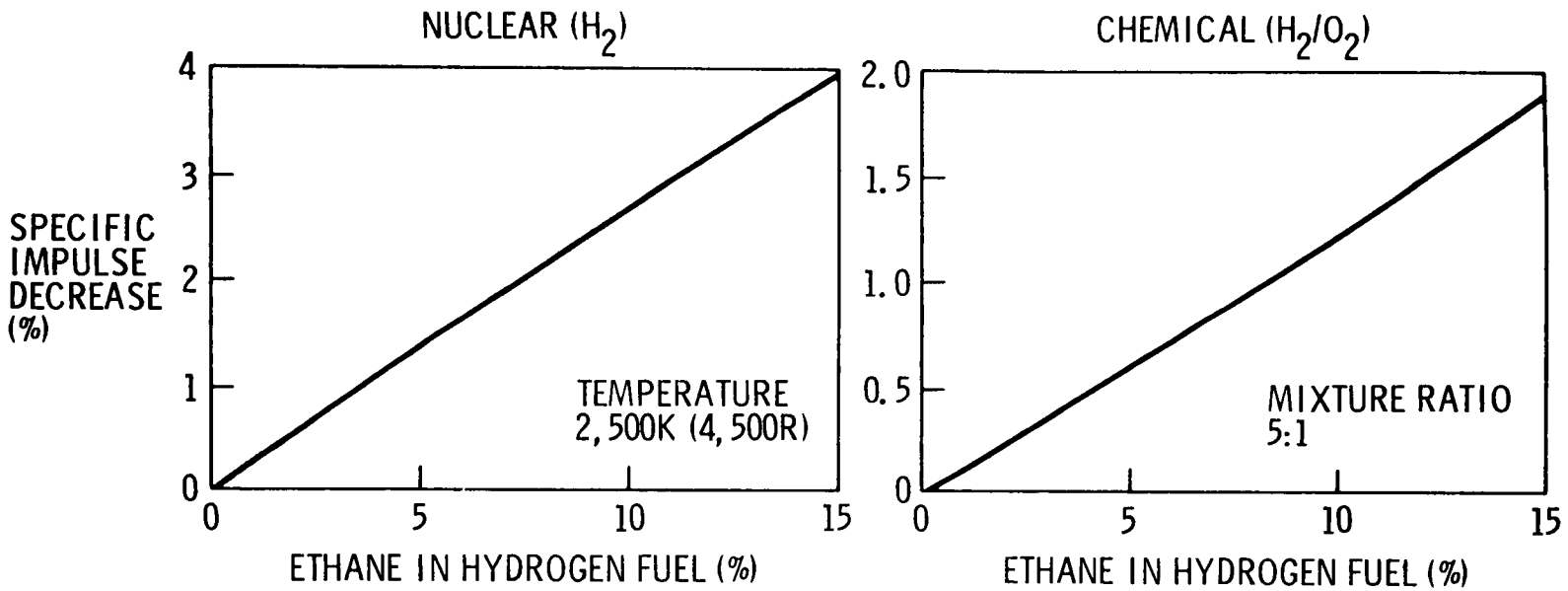

EQUILIBRIUM FLOW TO VACUUM
AREA RATIO 100:1
PRESSURE 3.1 MN/M^2 (450 PSIA)

Figure 1-4. Comparison of Nuclear and Chemical Propulsion Systems Performance

SECTION 2

GELLED LIQUID HYDROGEN

Two techniques for the production of gelled liquid hydrogen were investigated by Aerojet. The characteristics of the gels produced were evaluated and the "inside-tank," or "static" liquid hydrogen gel production process was selected for scale up. Convair Aerospace subsequently designed and fabricated a large-scale gelled liquid hydrogen production and storage facility.

2.1 GEL CHARACTERISTICS AND PRODUCTION APPARATUS

Prior to the initiation of testing a complete survey of literature pertinent to propellant gelation was made by Aerojet to maintain an awareness of the state-of-the-art in this field. Literature was found dating back to 1964 including work performed by Aerojet, Lockheed, NBS, and Technidyne. Work by Lockheed, NBS, and Union Carbide involving slush hydrogen was also reviewed. In addition a search of the Defense Documentation Center abstract bibliography was made with no new work being uncovered. As the program progressed a continuing awareness of developments in the field of liquid gelation was maintained.

2.1.1 GEL PRODUCTION TECHNIQUES. Based on available data, solid ethane particles appeared to be the most suitable gelant for liquid hydrogen. Significant gel structure can be produced using 10 weight percent ethane in the hydrogen (Ref. 3) and ethane is sufficiently volatile so that it will evaporate from feed lines under anticipated operating conditions. The latter characteristic, its volatility, circumvents a potential disadvantage of gelation of hydrogen; that is the clogging of propellant acquisition systems with residual gelants.

The general procedure for preparation of ethane gelant particles is to dilute gaseous ethane with gaseous hydrogen and then to inject the gaseous mixture into liquid hydrogen so that condensation and solidification of the gaseous ethane occurs immediately within the bulk of the liquid hydrogen (Ref. 12). In order to accomplish this, the gaseous mixture is passed through a small orifice to encourage the formation of micron-size ethane particles and to impart sufficient velocity to the gas-stream to prevent clogging of the orifice. In addition, the gaseous stream is heated upstream of the orifice to prevent the condensation of liquid ethane on the injector or orifice surfaces.

In the previous work with ethane as gelant for liquid hydrogen (Ref. 3), the gaseous ethane/hydrogen mixture was injected below the surface of the liquid hydrogen in a vacuum-jacketed glass flask which was immersed in either a liquid nitrogen or liquid hydrogen bath. The hydrogen boiloff produced by condensation of the ethane and

the gaseous hydrogen which served as the diluent for the ethane were vented through a port in the lid of the preparation flask. This method of preparation will be referred to as the inside-tank process or "static" method for preparation of gelled liquid hydrogen in subsequent discussion. An alternative method for preparation of gelled liquid hydrogen investigated in the current study was the outside-tank process or "flowing" liquid hydrogen method in which the feasibility of preparing the gel in a liquid hydrogen stream flowing into the tank was investigated. Schematics of the two methods are shown in Figure 2-1. The results obtained by the two methods are presented below.

2.1.1.1 Outside-Tank Process (Flowing Liquid Hydrogen Method). In the flowing liquid hydrogen process the gaseous mixture of ethane and hydrogen is injected directly into a stream of liquid hydrogen and flows into a receiver tank as gelled liquid hydrogen. The apparatus used to evaluate the process is shown in a schematic diagram in Figure 2-2. The gas and liquid feed systems and the liquid sampling system were used throughout the program. The parts of the apparatus that are unique to the flowing hydrogen process are the gas mixture heater and the mixing tee. They are shown in greater detail in Figure 2-3 as the flowing gel preparation device.

The gas mixture was introduced near the top of the heater tube and the gas was heated sufficiently so that condensation of ethane did not occur in the orifice at the outlet of the heated tube. The heater consisted of four strands of 127 μm (5 mil) Nichrome resistance wire in series supported in a four-hole Mullite insulator. The total resistance of the wire was 70 ohms and it was found experimentally that 2.0-2.5 amperes were required for heating the gas mixture to prevent clogging of the orifice.

The experimental procedure began with flowing gaseous helium through the injection tube to purge the system and subsequently to prevent the heating element from overheating and burning out. The heater was turned on and the flow of liquid hydrogen was initiated. As soon as the apparatus had equilibrated as evidenced by liquid hydrogen accumulating in the receiver flask immersed in a liquid nitrogen bath, the helium flow was stopped and the ethane/hydrogen flow initiated. The experiment was continued until sufficient ethane particles were formed to permit sampling of the liquid/solid mixture. The volumes of settled particles which were produced ranged from 65 to 300 cm^3.

The liquid/solid sample was removed from the receiver vessel via a dip tube which was fitted with a valve. A 300 cm^3 steel bomb was attached to the valve and the system was then evacuated to the valve. Opening the valve briefly caused a liquid-solid sample to be withdrawn from the receiver flask, the sample vaporized in the line, and collected in the evacuated bomb. The contents of the bomb were analyzed by vapor chromatography using a Perkin-Elmer Vapor Fractometer, Model 154D, with a flame ionization detector which is capable of detecting hydrocarbon concentrations down to less than one volume part per million.

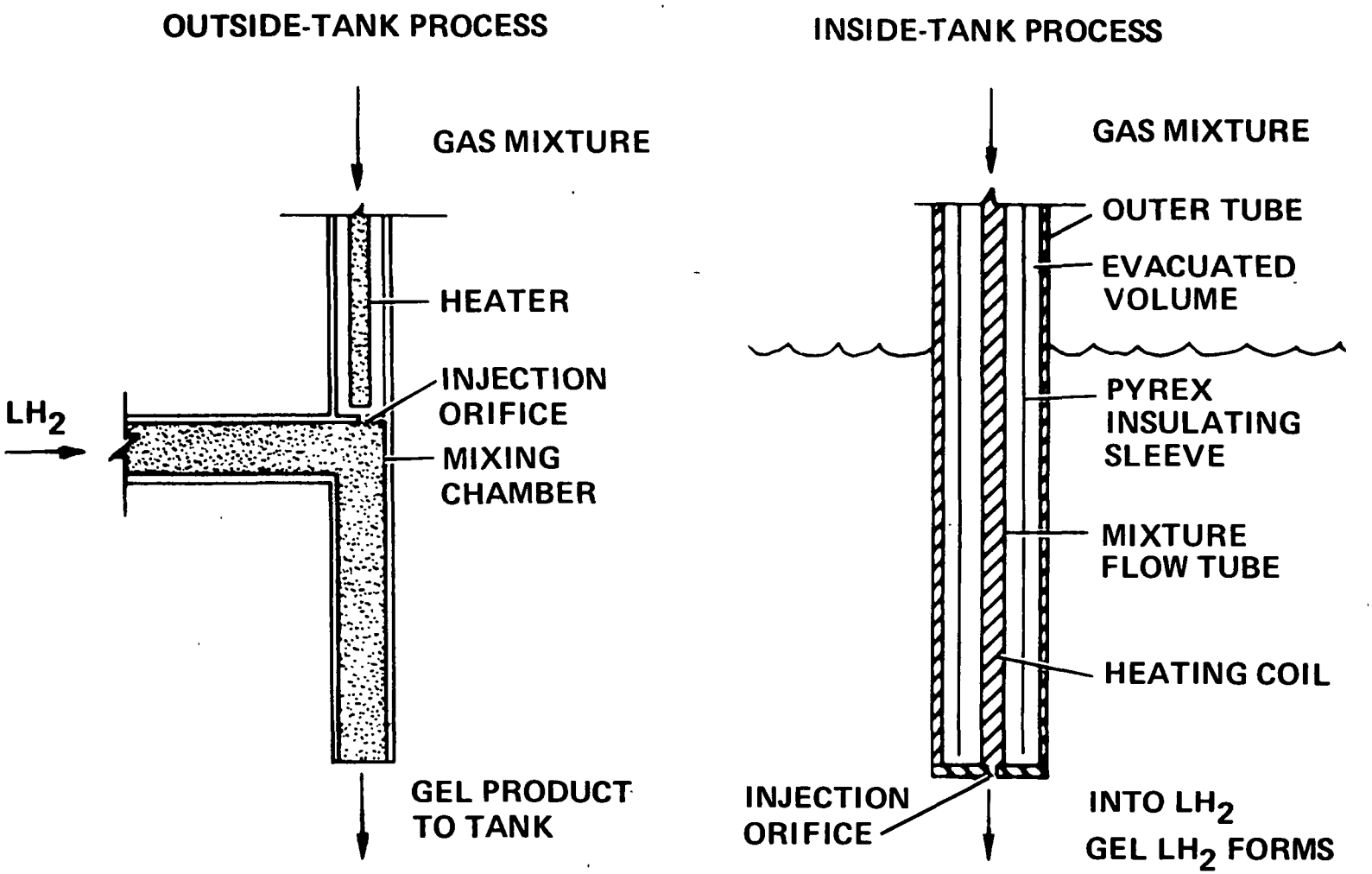

Figure 2-1. Outside- and Inside-Tank Gel Production Methods

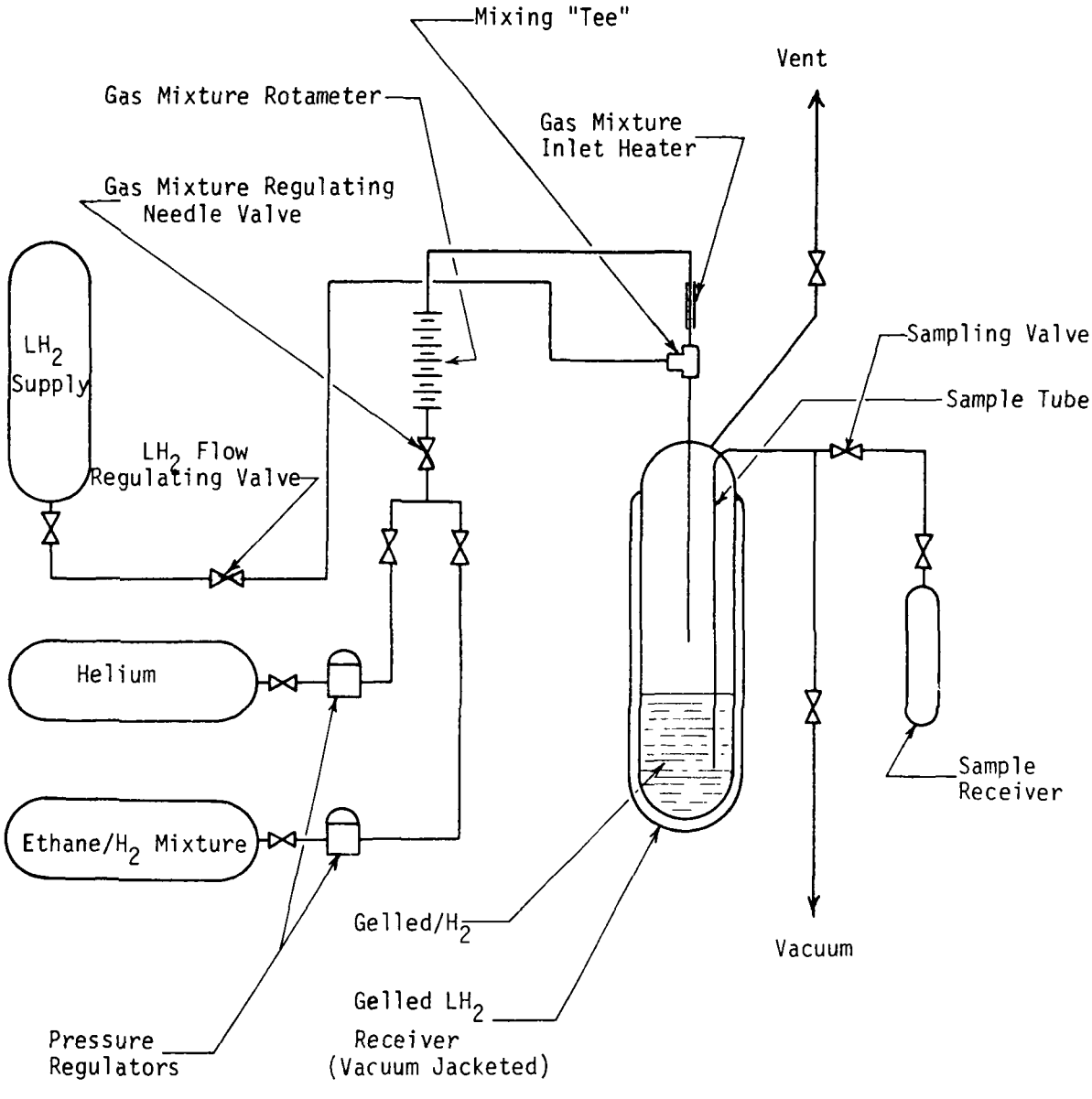

Figure 2-2. Schematic Diagram of Apparatus for Preparation of Gelled Liquid Hydrogen

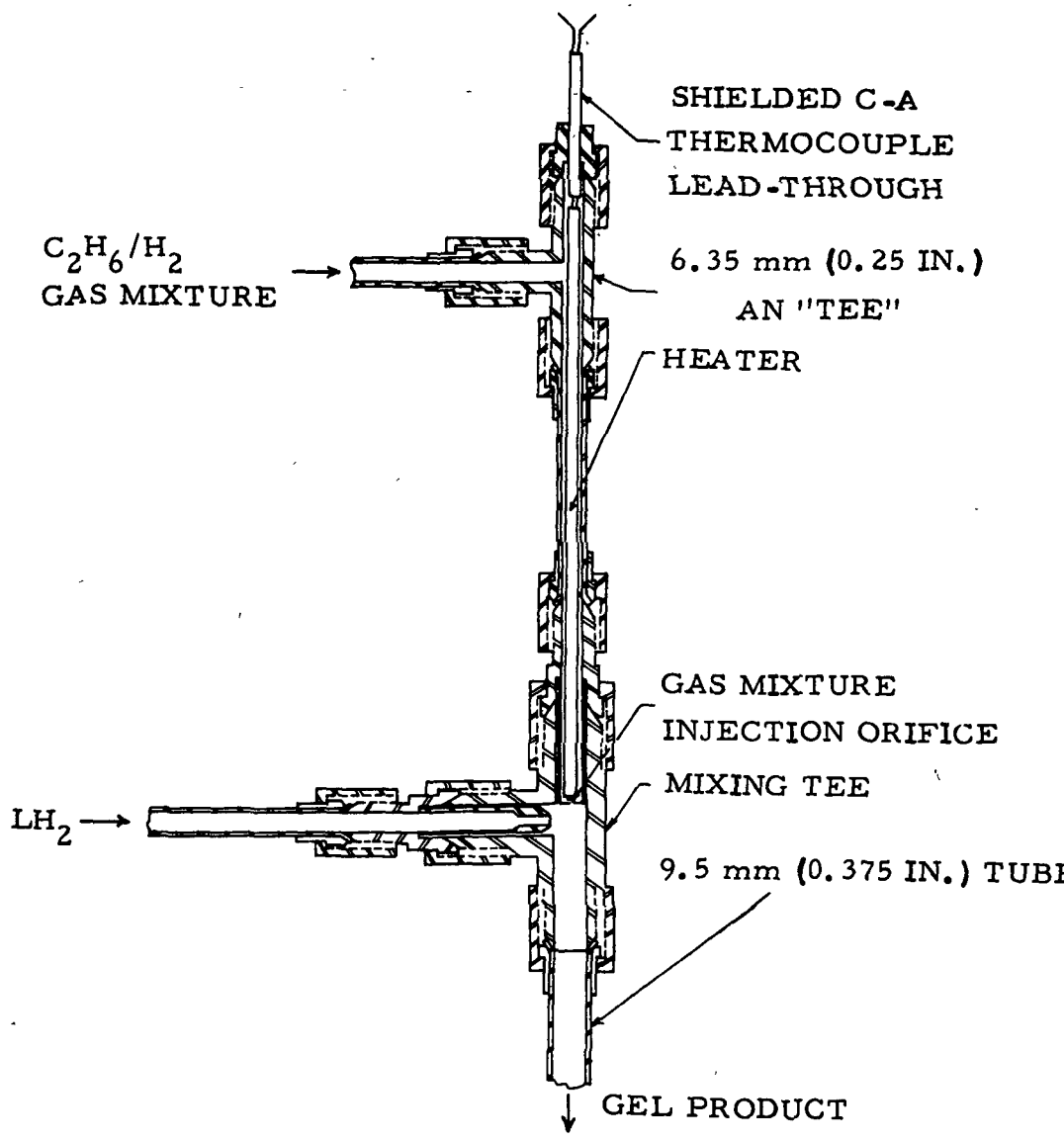

Figure 2-3. Flowing Gel Preparation Device

The quantity of gelant required for gelation with particulates is proportional to the size of the gelant particles; the smaller the particle size, the less gelant is required to impart structure to the liquid. Factors which were previously identified as affecting the gelant particle size were the size of the orifice through which the gaseous mixture is injected and the concentration of the hydrocarbon in the ethane/hydrogen gaseous mixture (Ref. 3). In this investigation, three sizes of orifices were used and three concentration levels of ethane in hydrogen were injected into the liquid hydrogen. The orifice diameters were 381, 508, and 635 μm (0.015, 0.020, and 0.025 in), and the ethane concentration levels were 2.5, 5, and 10 volume percent in hydrogen.

After preparation, the gelant particles of ethane were stored for 30 minutes in liquid hydrogen; the settled volume of the particles was measured and a sample was

withdrawn for analysis of the ethane concentration in the liquid hydrogen. From the data, a lower limit value for the minimum quantity of ethane necessary for gelation of liquid hydrogen can be calculated. The actual concentration of ethane required to impart "significant" structure to the gelled liquid hydrogen may be 1.5 to 2 times greater than the value obtained from the settled volume of particles. The data demonstrating the effect of orifice size and concentration of ethane in the gaseous hydrogen mixture on the minimum value of ethane required for gelation are shown in Figure 2-4. The conditions under which the predicting data were obtained are tabulated in Table 2.

The significant items to be noted from the data are that (1) as the orifice size is decreased, the quantity of ethane required for gelation decreases, and (2) as the concentration of ethane in the hydrogen carrier gas decreases, the quantity of ethane required for gelation decreases. However, below 5 mole percent ethane in gaseous hydrogen there is no significant decrease in the quantity of ethane required for gelation. The minimum value for the ethane required for gelation of liquid hydrogen by the flowing liquid hydrogen method is apparently 8 weight percent. Based on prior experience, that indicates that at least 12-15 weight percent ethane would be required to produce "significant" gel structure in liquid hydrogen using this process.

The data obtained in the preceding tests were based on a 30 minute settling period. Prior experience indicates that compaction of the particles may continue for periods up to 40 hours although the increase may be slight (Ref. 3). Because of this, a storage test of liquid hydrogen gelled with ethane was conducted for 48 hours. The apparatus used for the storage test is shown in Figure 2-5.

The gelled liquid hydrogen was prepared in the storage vessel while it was partially immersed in the liquid hydrogen storage dewar. The storage vessel was raised to boil off the excess hydrogen present and then capped and completely immersed in the liquid hydrogen bath. The volume of gel in the vessel was monitored through the view slot in the outer dewar. The ethane particles were prepared using a gas mixture containing 5 volume percent ethane in hydrogen and the gas mixture was injected through a 508 μm (0.020 in) orifice. The ethane concentration in the liquid hydrogen gel was 13.5 weight percent prior to the storage test. After storage for 48 hours, the gel was sampled again and the final concentration of the ethane was found to be 16.9 weight percent. In a comparable test conducted under a previous contract, a liquid hydrogen gel prepared by the in-tank process or static liquid hydrogen process contained 8.8 weight percent ethane immediately after preparation and 9.7 percent after five days of storage. The data indicate that smaller ethane gelant particles are produced by the in-tank process. Further confirmation of this is presented in the next section.

2.1.1.2 Inside-Tank Process (Static Liquid Hydrogen Process). The data for the static liquid hydrogen process was generated during a previous contract (Ref. 3) and is presented here to facilitate comparison with the flowing liquid hydrogen process. The apparatus used for the in-tank process is similar to that in Figure 2-2 except

Table 2. "Flowing LH_2" Gel Production Test Conditions

Exp. No.	Ethane Concentration In Injected Gas Mixture mole percent	Pressure Drop Across Orifice kN/m^2 (psi)		Orifice Diameter μm	LH_2 Flow Rate cc/sec	Gas Mixture Flow Rate cc/sec	Ethane Concentration in Settled Volume weight percent
11	10	152	(22.1)	635	5	128	16.6
12	10	154	(22.3)	635	5	129	14.6
13	10	411	(59.6)	381	5	100	13.6
14	10	410	(59.4)	381	5	112	11.4
15	10	377	(54.7)	381	5	118	11.4
18	10	188	(27.2)	508	5	144	13.3
20	10	194	(28.2)	508	5	148	12.3
21	10	192	(27.8)	508	5	146	12.4
5	5	345	(50.1)	381	6	130	8.4
6	5	364	(52.8)	381	6	126	6.8
22	5	183	(26.5)	508	5	162	6.5
31	5	189	(27.4)	508	5	165	8.4
8	5	147	(21.3)	635	6	128	10.9
9	5	153	(22.2)	635	6	146	10.4
27	2.5	400	(58.0)	381	5	171	8.1
28	2.5	400	(58.0)	381	5	170	9.6
24	2.5	183	(26.6)	508	5	174	9.3
25	2.5	187	(27.1)	508	5	175	8.0
33	2.5	153	(22.2)	635	5	153	11.1
34	2.5	153	(22.2)	635	5	151	9.1

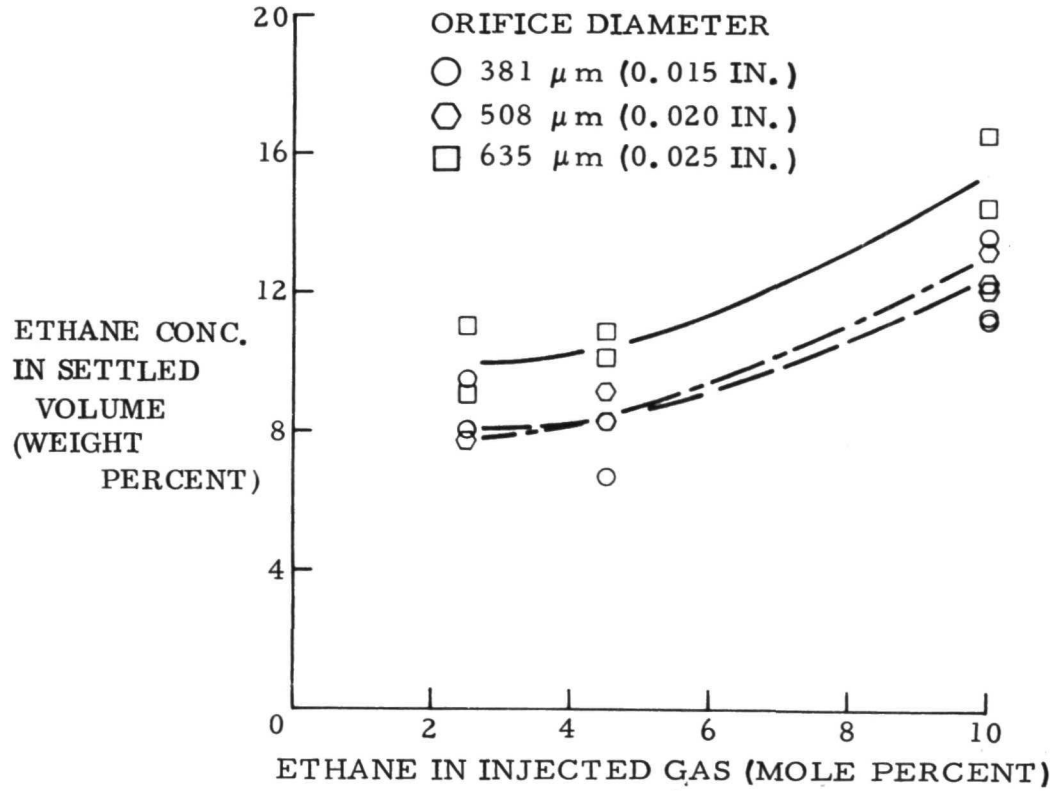

Figure 2-4. Results of "Flowing LH_2" Gel Production Tests

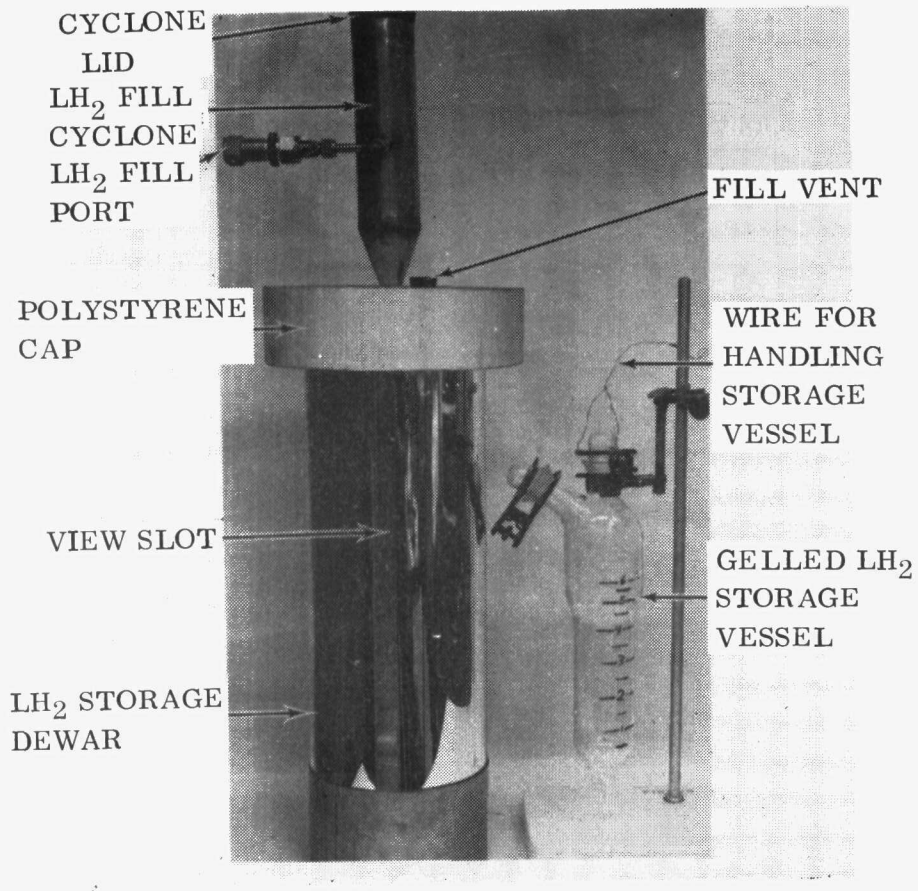

Figure 2-5. Apparatus for Storage of Gelled Liquid Hydrogen

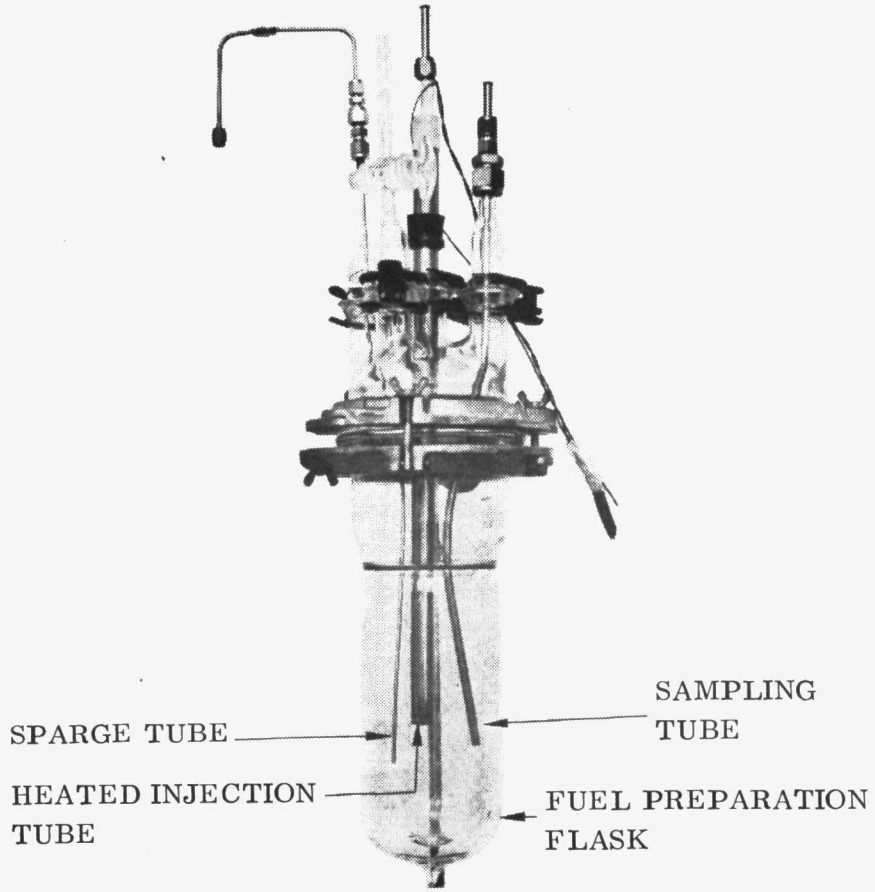

Figure 2-6. Basic Apparatus for Preparation of Gelled Liquid Hydrogen

for the injection tube arrangement. A typical injection tube arrangement used for the static liquid hydrogen process is shown in Figure 2-6. The experimental parameters investigated were comparable to those evaluated in the current program.

Three orifice diameters, 254, 635, and 1321 μm (0.010, 0.025, and 0.052 in), were used in the experiments. The ethane concentrations in the gas mixture which was injected into the liquid hydrogen to form ethane particles were 100, 50, 10, 5, 3, and 1 mole percent in hydrogen. The velocity of the injected stream is represented by the value of the pressure drop across the orifice. The particles were allowed to settle and age for 45 min after preparation in order to insure that a settled volume was attained. The data obtained from the experiments are presented in Table 3 and are also plotted in Figure 2-7.

The significant items to be noted from the data are that first, as the ethane concentration in the injected gas mixture decreases from 100 to 1 mole percent, the particle size decreases as evidenced by the decreasing concentration of ethane in the settled volume of particles. Below the 10 mole percent ethane level, the concentration effect is less pronounced. Second, as the orifice size decreases, the size of the particles also decreases significantly. At the 1 mole percent level however, the capture efficiency with the largest orifice was extremely low so that no significant quantity of gelant particles was accumulated in the liquid hydrogen. Capture efficiency refers to the percent of the injected ethane which remains in the liquid hydrogen in solid form, and is not swept out by the carrier gas bubbles. Third, the velocity of the injected stream is a secondary effect; comparing experiments 7JJ and 8JJ with 9JJ and 10JJ indicates that the average ethane concentration increases from 6.2 to 6.8 weight percent in the settled particles, but the difference in the values lies within the limits of experimental error. The trends to be noted from the data are that as the orifice size is decreased and the ethane concentration in the injected gas reduced, the ethane particles become more effective for gelling liquid hydrogen. The data indicate that the minimum quantity of ethane required for gelation is 4-6 weight percent. As mentioned above, the ethane concentration required for imparting "significant" structure to the gelled hydrogen may be 1-1/2 to 2 times the value obtained from settled volume data.

2.1.1.3 Comparison of Processes. The comparison of the data obtained from the flowing liquid hydrogen process and the static liquid hydrogen process demonstrates that the ethane gelant particles produced in the static process have a superior gelling capacity to those produced by the flowing process. The minimum obtainable ethane concentration in the settled volume of particles was found to be about 5 weight percent from the static process and about 8 weight percent for the flowing process. Thus "significant" structure may be expected to occur at a level of 10 weight percent ethane in the static process and 15 weight percent ethane in the flowing process. These values were confirmed in gel storage tests noted in the previous section.

The cause of the significant difference in the gel production "efficiency" of the two processes may be attributed to the two phase flow which exists beyond the injection

Table 3. "Static LH_2" Gel Production Test Conditions

Exp. No.	Ethane Concentration In Injected Gas Mixture mole percent	Pressure Drop Across Orifice kN/m^2 (psi)		Orifice Diameter μm	Ethane Concentration in Settled Volume of Particles in Liquid Hydrogen weight percent
15MM	100	48	(7.0)	1321	52.5
16MM	100	41	(5.9)	1321	52.5
5JJ	100	3	(0.5)	635	35.4
6JJ	100	7	(1.0)	635	37.5
17MM	100	503	(73)	254	18.0
18MM	100	517	(75)	254	16.5
13MM	50	39	(5.6)	1321	25.5
14MM	50	47	(6.8)	1321	34.5
9MM	50	25	(3.6)	635	13.5
10MM	50	21	(3.0)	635	14.8
11MM	50	538	(78)	254	12.4
12MM	50	552	(80)	254	11.7
5MM	10	21	(3.0)	635	7.4
6MM	10	455	(66)	254	5.7
7JJ	5	138	(20)	635	6.4
8JJ	5	124	(18)	635	6.0
9JJ	5	34	(5.0)	635	6.0
10JJ	5	24	(3.5)	635	7.5
11JJ	5	414	(60)	254	5.8
12JJ	5	400	(58)	254	4.2
13JJ	5	414	(60)	254	4.8
3JU	3	469	(68)	254	3.8
5JU	3	434	(63)	254	4.7
4JJ	1	8	(1.1)	635	6.4
2JJ	1	462	(67)	254	4.0
3JJ	1	441	(64)	254	4.0
19MM	1	496	(72)	254	4.3

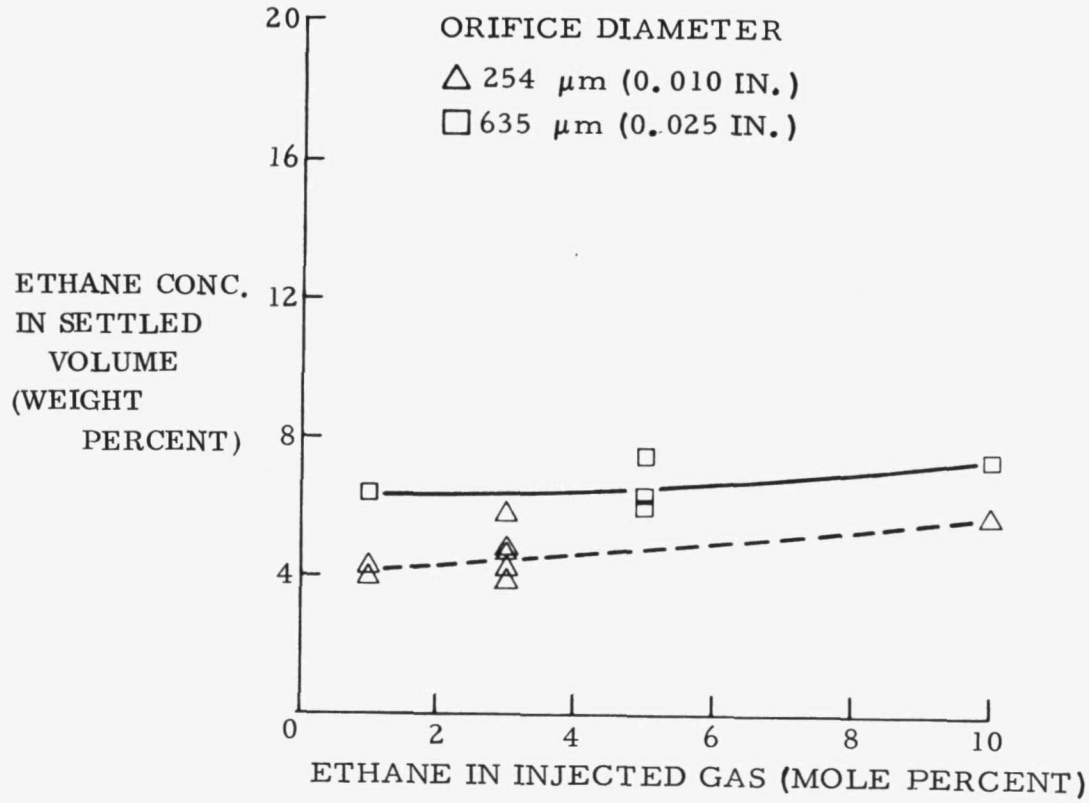

Figure 2-7. Results of "Static LH_2" Gel Production Tests

point in the flowing process. The particles may tend to accumulate along the tube surfaces and form more compact agglomerates rather than disperse uniformly in the liquid. The results clearly indicate that the static or in-tank process is preferred for scale-up. The maximum orifice size in the scale-up should be no greater than 635 μm (0.025 in.) in diameter and the ethane concentration in the injected gas mixture should not exceed 10 weight percent. A process design was developed accordingly and is discussed in the following section.

Because the "static" process was selected for the scaled up production of the gelled hydrogen, an improved injection tube was fabricated for use in the remainder of the laboratory investigation. A schematic diagram of the injection tube is shown in Figure 2-8 and a photograph of the tube in Figure 2-9. The principal improvements incorporated in the tube are: (1) a vacuum jacket with an internal radiation shield to minimize heat transfer through the walls of the tube and (2) an internal heating element which is in direct contact with the gas mixture. Previously, the comparable injection tubes required as much as 300 watts electrical power to prevent clogging in the injection orifice. Experiments with the new injection tube have indicated that less than 200 watts is sufficient.

2.1.2 PROCESS DESIGN FOR PREPARATION OF GELLED LIQUID HYDROGEN. The gelation of LH_2 is accomplished by the subsurface injection of a gaseous mixture of ethane (C_2H_6) and hydrogen (H_2) at sonic velocity directly into the LH_2 (in-tank process). The injection involves the use of a special vacuum jacketed injection tube with a small orifice and an electrical heater to prevent the condensation of ethane prior to its entry into the liquid hydrogen. This injection tube produces a subsurface plume of tiny bubbles of ethane and hydrogen which rapidly cool to liquid hydrogen temperature, producing minute particles of solid ethane. The minute particles of solid ethane cause the liquid hydrogen to gel with "significant" structure when the concentration of ethane particles reaches approximately 10 percent weight (~ 0.7 percent volume).

The process is shown schematically below.

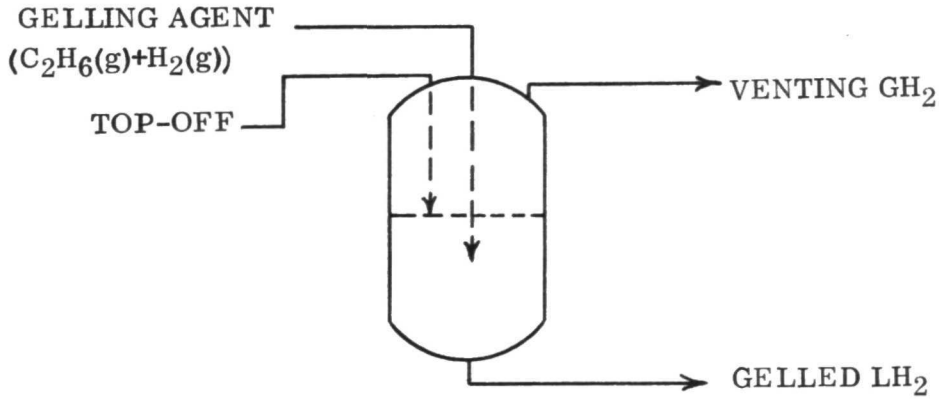

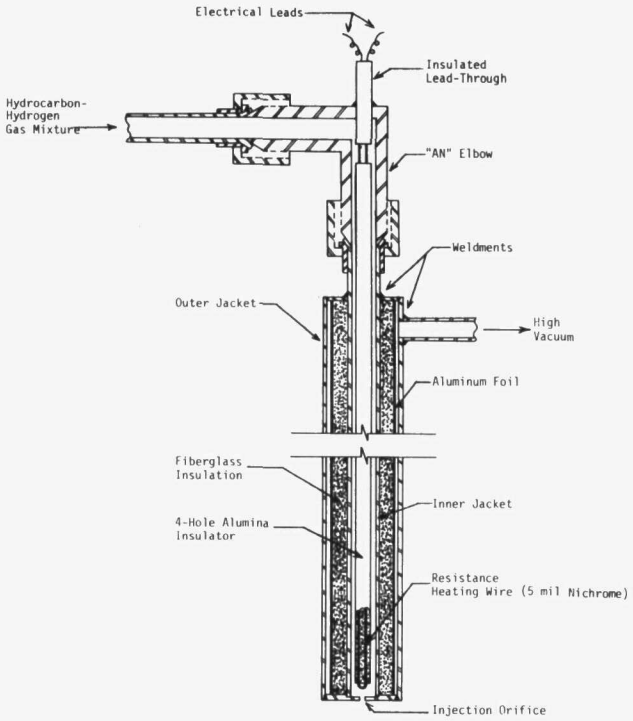

Figure 2-8. Schematic of Vacuum-Jacketed, Internally Heated Injection Tube

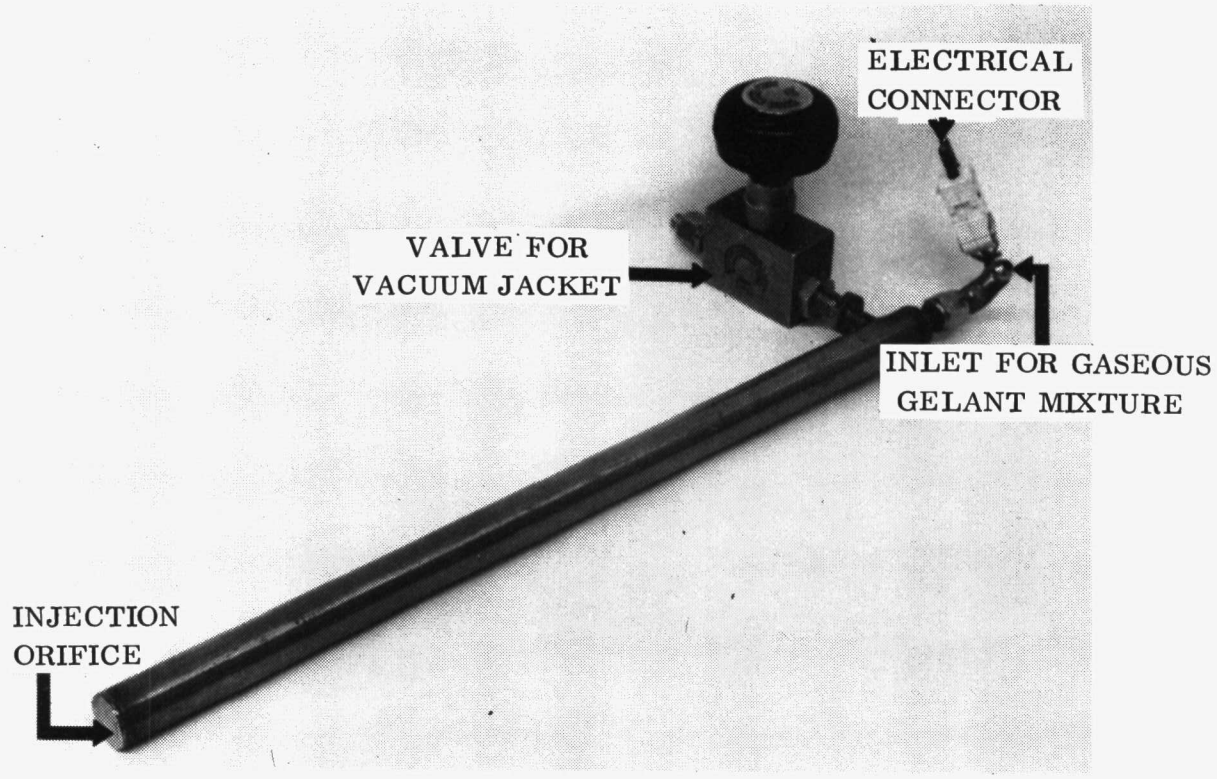

Figure 2-9. Vacuum-Jacketed, Internally Heated Injection Tube

The injection tube was assumed to have a 635 μm (0.025 in) orifice and the pressure and temperature of the ethane/hydrogen gaseous mixture immediately upstream of the orifice were 791 kN/m^2 (100 psig) and 294 K (70F), respectively. The maximum weight flow rate is then given approximately by the following equation

$$\dot{w}\,(\max) = C_v\, A_2\, p_1 \sqrt{\frac{g_c k \overline{M}}{R T_1} \left(\frac{2}{k+1}\right)^{k+1/k-1}}$$

where

$\dot{w}$ = flow rate, g/sec

C_v is taken as ~ 1

A_2 = 0.317 μ(m)^2 (0.00049 in.^{2}), the area of the orifice

p_1 = 791 kN/m^2 (114.7 psia), the pressure upstream of the orifice

g_c = 66.7 pN·m^2/kg^2

R = 8.31 J/mole K

T_1 = 294 K (530 R), gas temperature upstream of the orifice

$\overline{M}$ = mean molecular weight, kg/kg mole

k = ratio of specific heats $\approx C_p/(C_p-R)$

$\overline{M}$ and k are, however, functions of the composition of the gaseous ethane/hydrogen mixture and are tabulated below for several different compositions.

Injection Gas Composition				Mean Molecular Weight	Mean Molar C_p		
Mole or Vol%		Wt%					
C_2H_6	H_2	C_2H_6	H_2	kg/kg mole	kJ/kgK	k	$(\frac{2}{k+1})^{k+1/k-1}$
5	95	43.93	56.07	3.4156	31.27	1.362	0.3377
10	90	62.32	37.68	4.8151	32.44	1.345	0.3391
20	80	78.82	21.18	7.6142	34.79	1.314	0.3414

From the preceding table of data and the orifice flow equation, the following gelling agent injection rates were calculated:

Ethane Content of Gas Mixture, Mole % C_2H_6	Gas Injection Rate, g/sec		
	C_2H_6	H_2	Total
5	0.088	0.112	0.200
10	0.148	0.089	0.237
20	0.233	0.062	0.295

If the inlet pressure is different from 791 kN/m^2 (100 psig) but greater than about 205 kN/m^2 (15 psig), the above rates should be multiplied by the factor: $P_{(kN/m^2)}/791$. If the inlet temperature (just upstream of the orifice) is different from 294K (70F) but greater than the saturation temperature at inlet pressure and composition, the injection rates should be multiplied by $\sqrt{294/[T(K)]}$.

The above factors are not strictly correct because k varies with temperature (and pressure); however, that influence is negligible in the operating regions of interest.

Assuming the capture efficiency of the ethane from the injected gas mixture is ~100% (the actual value will depend on the ethane concentration in the gas mixture and depth of subsurface injection, and it could be as low as 50%), the production rates of gelled liquid hydrogen are calculated directly as follows for gels containing 5, 10 and 15% wt gelling agent (C_2H_6).

Ethane Content of Injected Gas Mole or vol % C_2H_6	Gelled LH_2 Production Rate, g/sec		
	5% Wt Gelling Agent	10% Wt Gelling Agent	15% Wt Gelling Agent
5	1.76	0.88	0.59
10	2.95	1.48	0.98
20	4.65	2.33	1.55

The densities of the gelled liquid hydrogen (at the NBP of LH_2) containing 5, 10 and 15% wt gelling agent are approximately 74.1, 77.8 and 81.9 kg/m^3 (4.629, 4.860 and 5.114 lb/ft^3), respectively. Volumetric production rates are thus calculated to be as follows:

Ethane Content of Injected Gas Mole or vol % C_2H_6	Gelled LH_2 Production Rate, $\mu(m)^3/sec$		
	5% Wt Gelling Agent	10% Wt Gelling Agent	15% Wt Gelling Agent
5	23.7	11.3	7.2
10	39.8	18.9	12.0
20	62.8	29.9	18.9

Three heat loads are imposed steadily on the system and an additional load is imposed upon startup. Each of these heat loads contributes to LH_2 boiloff. The three steady loads are

(1) Gelling agent solidification and carrier hydrogen cooldown.

(2) Injection tube heater output.

(3) Heat leak into the total gel preparation system.

The startup heat load involves chilldown of the total gel preparation system. The heat loads imposed by overall heat leak and initial chilldown are system dependent and their contributions to total boiloff have been neglected in the following evaluation of boiloff rates.

The heat load imposed by the addition of the ethane component of the injected gas mixture is defined by $(H_{(g)294K} - H_{(s)20.3K})$ and has been found to be approximately 1.066 MJ/kg (458.6 Btu/lb). This value accounts for sensible enthalpy changes in gaseous, liquid, and solid phases plus the heats of vaporization and fusion. The change in the enthalpy of C_2H_6 in going from the gas phase at 294K (70F) and a partial pressure in the range of approximately 41 to 159 kN/m^2 (6 to 23 psia) to the solid phase at 20.3K (36.5R) is defined as follows:

		kJ/kg	Btu/lb
$[H_{(g)294K} - H_{(\ell)133K}] = 1059 - 273$	=	786 [13]	338.0
$[H_{(\ell)133K} - H_{(\ell)90K}] = (\bar{C}_p)(\Delta T) = (2.31)(43)$	=	100 [14]	43.0
$[H_{(\ell)90K} - H_{(s)90K}] = \Delta H_{fusion}$	=	95 [14][15]	41.0
$[H_{(s)90K} - H_{(s)20K}] = (\bar{C}_p)(\Delta T) = (1.23)(70)$	=	86 [14]	37.0

The heat load imposed by the addition of the hydrogen component of the injected gas mixture is assumed to be $(H_{(g)294K} - H_{(g)20.3K})$ and by a similar procedure has been found to be approximately 3.917 MJ/kg (1685.2 Btu/lb). The heat load imposed by the injection tube heater could be analytically defined by a detailed heat transfer analysis. However, an approximate value is available from laboratory experience with an injection tube very similar to the one recommended and that experience is used as a basis for the present evaluation. The maximum heater input found from the laboratory effort is 300 watts (1024 Btu/hr) and is accepted here as a reasonable maximum that could be expected in the larger scale facility for each injection tube used.

In summary, the heat loads to be offset by LH_2 boiloff are as follows:

(1) 1.07 MJ per kg (459 Btu per lb) of C_2H_6 injected and captured.

(2) 3.92 MJ per kg (1685 Btu per lb) of carrier H_2 injected.

(3) 300 w (1024 Btu/hr) per injection tube.

The total heat loads per hour of operation contributed by these sources vary with the composition of the injected gas mixture and cause varying amounts of boiloff as summarized in the following table. The heat of vaporization of the liquid hydrogen which counteracts these heat loads is taken to be 443 kJ/kg (190.5 Btu/lb) of H_2 boiled off. Sensible heat change of the vaporized hydrogen was assumed not to occur.

Ethane Content of Injected Gas mole or vol% C_2H_6	Heat Load, Watts (Btu/hr) C_2H_6 Contribution	GH_2 Contribution	Heater Contribution	Total	LH_2 Boiloff Rate g/sec (lb/hr)
5	93.4 (319)	440 (1501)	300 (1024)	833 (2845)	1.88 (14.9)
10	157 (535)	349 (1193)	300 (1024)	806 (2753)	1.82 (14.5)
20	248 (845)	245 (835)	300 (1024)	792 (2705)	1.79 (14.2)

The pertinent operating parameters are summarized in Table 4. The gel production rate and the "efficiency" of the gelation process is presented in Figures 2-10 and 2-11, respectively.

In order to increase the gel production rate with a minimum of hardware modification, it is possible to increase the orifices in an injection tube such as shown in Figure 2-9 by drilling additional holes at divergent angles. In this manner, the gas plumes do not interact in the liquid hydrogen and such a tube with two orifices is shown in operation in Figure 2-12. From the plume pattern it is apparent that at least four orifices per tube can be used. This multi-orifice tube has the added advantage that heat load required to maintain the gas temperature high enough to prevent liquid condensation at the orifice exit is no greater for the multi-orifice tube than for the single orifice tube.

In order to establish that a gel of comparable quality can be obtained from either the single or multi-orifice tubes, the concentration of ethane particles in the settled volume was determined by chromatographic analysis. Using an injected gas mixture of 5 volume percent ethane in hydrogen, the ethane concentration was found to be 6 weight percent. This value is identical to that previously reported for a single orifice tube (Ref. 3).

2.2 GEL PRODUCTION FACILITY DEVELOPMENT

Based on the Aerojet evaluation of potential gelled liquid hydrogen production techniques and the results of the process design for a scaled-up system, Convair Aerospace has assembled a large-scale gel production facility at the liquid hydrogen test site "B" in Sycamore Canyon near San Diego. The gel production apparatus is located on a covered high bay pad which has sufficient additional room for the PPO foam/gelled LH_2 interfacial effects investigation apparatus (WBS 1320), discussed in Section 4, and the subscale tankage system required for Phases II and III (WBS 2000 and 3000). This pad also houses a vibration exciter which would have been used for gel and LH_2 sloshing and vibration during Phase III.

Table 4. Summary of Gel Preparation Parameters

Ethane Content of Injected Gas, mole or vol% C_2H_6	Injected Gas Flow Rate g/sec(1)			H_2 Off-Gas Flow Rate g/sec			Preparation of LH_2 Gel* (95% Wt LH_2 + 5% Wt C_2H_6)				Preparation of LH_2 Gel (90% Wt LH_2 + 10% Wt C_2H_6)				Preparation of LH_2 Gel (85% Wt LH_2 + 15% Wt C_2H_6)			
	C_2H_6	H_2	Total	Gelling Agent Carrier H_2	LH_2 Boil-off (3)	Total (3)	LH_2 Use Rate(3) g/sec	Gel Production Rate g/sec	Gel Production Rate $\mu(m)^3$/sec	Efficiency of LH_2 Use(2)	LH_2 Use Rate(3) g/sec	Gel Production Rate g/sec	Gel Production Rate $\mu(m)^3$/sec	Efficiency of LH_2 Use(2)	LH_2 Use Rate(3) g/sec	Gel Production Rate g/sec	Gel Production Rate $\mu(m)^3$/sec	Efficiency of LH_2 Use(2)
5	0.088	0.112	0.200	0.112	1.88	1.99	3.55	1.76	23.7	47	2.67	0.88	11.3	30	2.38	0.59	7.2	21
10	0.148	0.089	0.237	0.089	1.82	1.91	4.62	2.95	39.8	61	3.15	1.48	18.9	42	2.66	0.98	12.0	31
20	0.233	0.062	0.295	0.062	1.79	1.85	6.21	4.65	62.8	71	3.88	2.33	28.4	54	3.11	1.55	18.9	42

* See Footnote (1): If gelling agent inlet pressure is different from 791 kN/m^2 (100 psig) but greater than 205 kN/m^2 (15 psig), multiply all tabulated rates by $P_{(psia)}/791$ and if inlet temperature is different from 294K (70F) (but > saturation temperature at inlet pressure), multiply all tabulated rates by $(294/T(K))^{1/2}$. If more than one injection tube is used, multiply all tabulated rates by the number of injection tubes used.

(1) Assumes the use of a single injection tube having one 635 μm (0.025-in) diameter orifice operating with a gelling agent supply at 791 kN/m^2 and 294K (100 psig and 70F).

(2) Percentage of the LH_2 that is recovered in the form of gelled LH_2.

(3) Neglect the amounts of LH_2 added and boiled off necessary to achieve chilldown of the system and to overcome normal system heat leak.

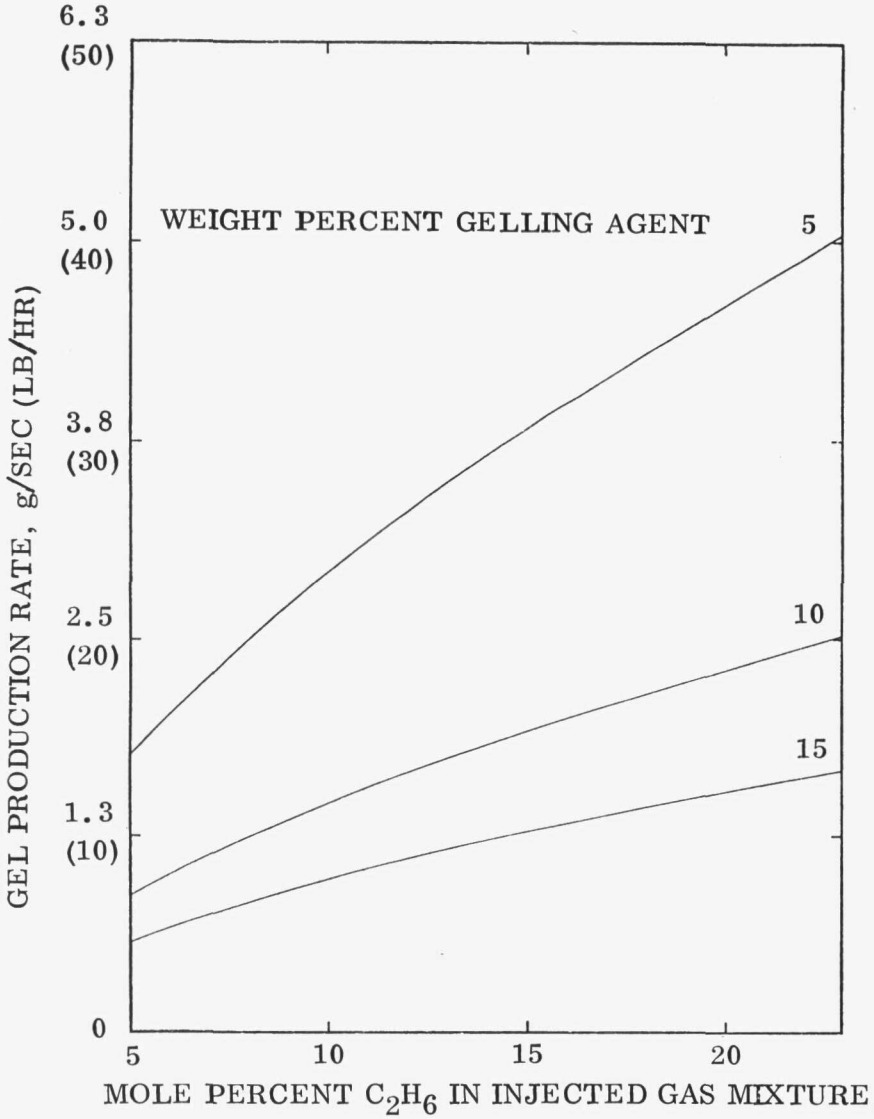

Figure 2-10. Gel Production Rate Versus Composition of Injected Gas Mixture

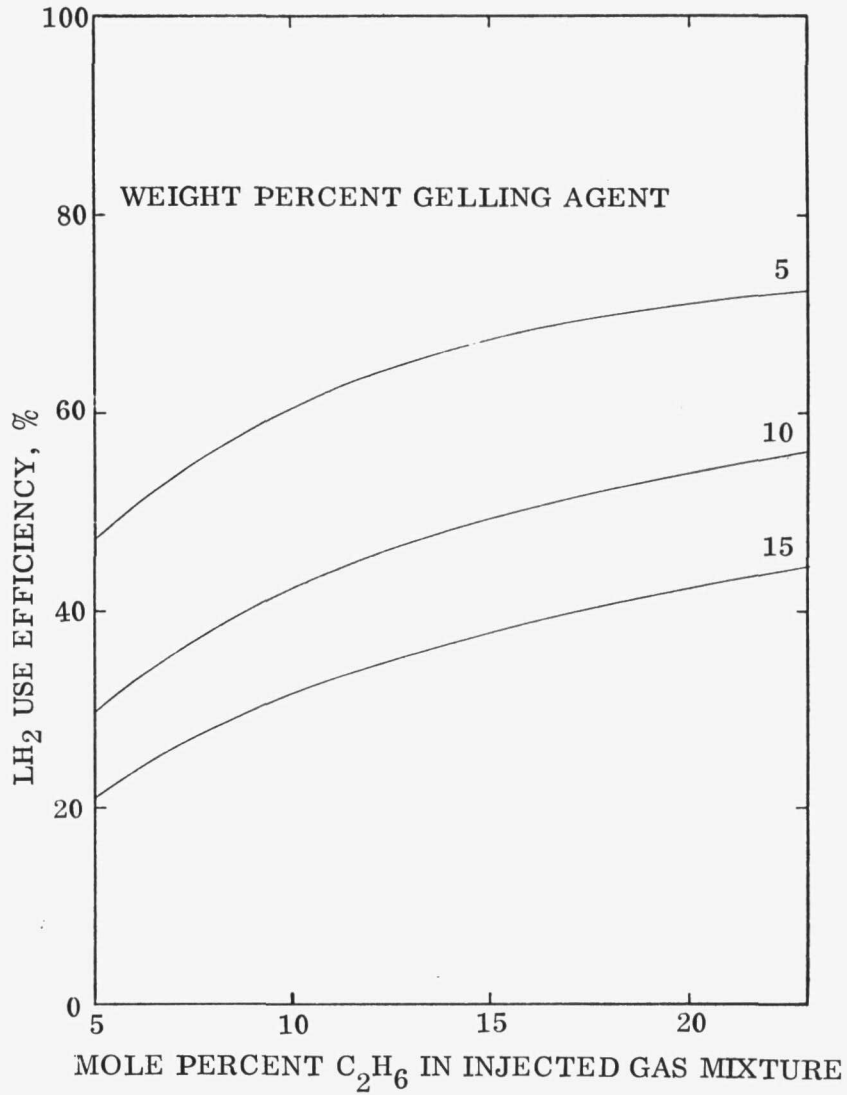

Figure 2-11. LH_2 Use Efficiency Versus Composition of Injected Gas Mixture

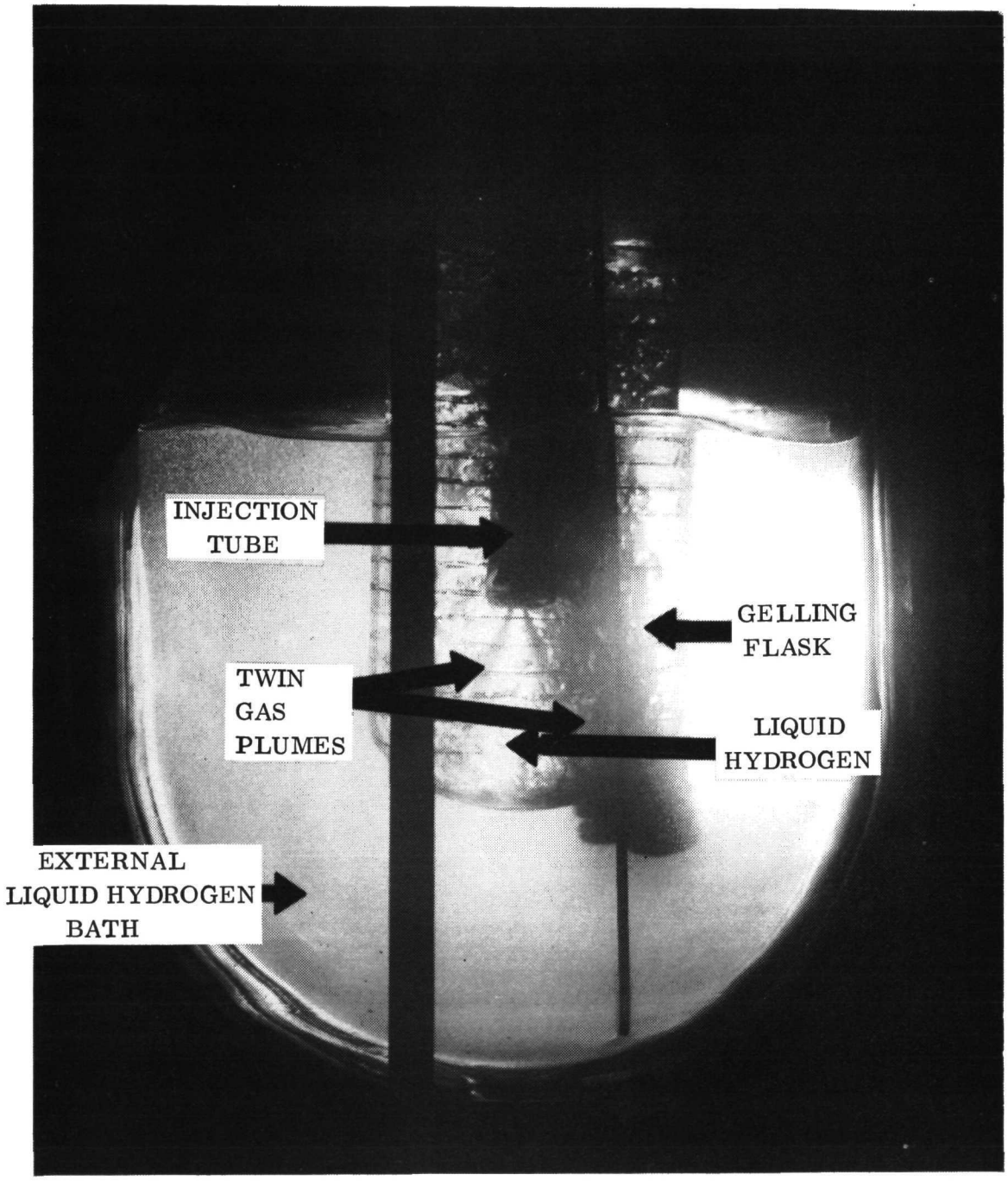

Figure 2-12. Twin-Orifice Injection Tube Operating in Liquid Hydrogen

A schematic diagram of the facility is shown in Figure 2-13 and a photograph in Figure 2-14. Liquid hydrogen is gravity fed from an elevated tank to the gel production tank. The ethane and hydrogen gases are mixed and stored at a high pressure and flowed through a filter and flowmeter into the injection tubes mounted in the tank. The large number of valves, sensors, and auxiliary systems required for safe operation of the facility is indicated in Figure 2-13. Gelled liquid hydrogen is produced and stored in a triple-walled, 1.90 m^3 (500 gal) tank designed for use up to 3.10 MN/m^2 (450 psia). The innermost tank is guarded by a liquid hydrogen jacket which in turn is surrounded by a vacuum jacket. Consequently, heat flow into the storage tank is minimal, coming mainly through the unguarded cover on the tank (Figure 2-15). The gel production tank is 1.90 m (43 in) in diameter with oblate spheroid heads and a 1.47 m (58 in) cylindrical section. A "hat section" on top is 40.6 cm (16 in) in diameter and 33.0 cm (13 in) tall. Tank fill and drain lines are protected by a vacuum guard. As shown in Figure 2-13, the fluid lines are arranged concentrically (drain-fill-vent-vacuum guard). Liquid hydrogen is pumped from the tank farm into a vacuum jacketed, 3.79 m^3 (1000 gal) "supply tank" which is elevated to allow gravity flow into the gel production tank (Figure 2-14). A deflection plate is mounted immediately downstream of the fill line to minimize surface disturbance of the LH_2 in the tank during top-off.

A small Pesco liquid hydrogen pump, shown in Figure 2-16, was installed on the drain line at the centerline of the tank, located 46 cm (18 in) up from the bottom, and pointed downward. The pump is operated by a 17 volt, 60 Hz, single phase input with a 40 μf external capacitor. At 3200 rpm the LH_2 throughput is 2.27 m (m^3)/sec (4.8 cfm) (Ref. 16). The pump was installed to sweep ethane particles off the bottom of the tank and provide bulk agitation during gelant mix flow. However, it was found to have insufficient capacity to provide continuous bulk motion and was subsequently used only to disturb the surface of settled ethane particles.

The gel production tank cover, shown in Figure 2-15, contains three 10 cm (4 in) ports and a number of smaller passthroughs. One of the large ports is used for the LH_2 lines and a second as a viewport. The third large port was used temporarily to mount the gelant injection tube during the development phase. Later a second tube will be manufactured and both will be mounted directly on the cover, thus freeing the large port for other uses. Another passthrough contains a clear Lucite acrylic rod, 1.9 cm (0.75 in) in diameter and approximately 2.3 m (9 ft) long. A small 28v light bulb is attached to the top of the rod and the system illuminates the entire tank interior permitting visual observation of gelant injection, pump operation, particle circulation, and sampling cup movement and contents. The sampling cup is mounted on a lateral arm at the end of a long tube which is fed through another fitting on the tank cover. The cup can be maneuvered underneath the injection plug or positioned at various locations within the liquid or gel bulk. It is used to make paths and depressions in the gel and to transport gel samples to the viewport for close visual inspection. The cup volume is approximately 300 cm^3 (18.4 in^3).

The gelant supply system is configured so that gaseous helium, gaseous hydrogen, or the gelant/carrier gas mixture can be flowed through the injection tubes. Helium is used

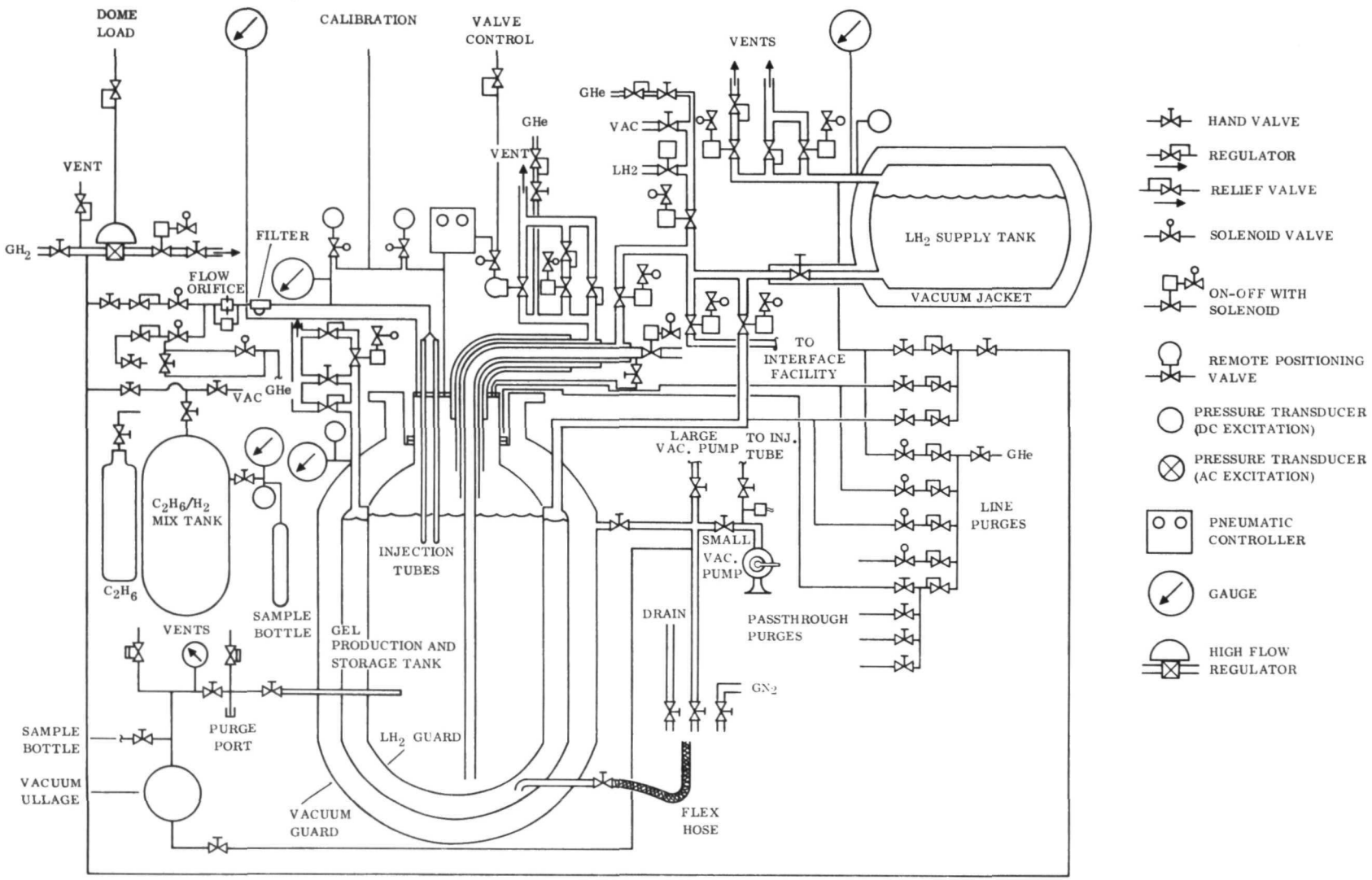

Figure 2-13. Large Scale Gel Production Facility Schematic

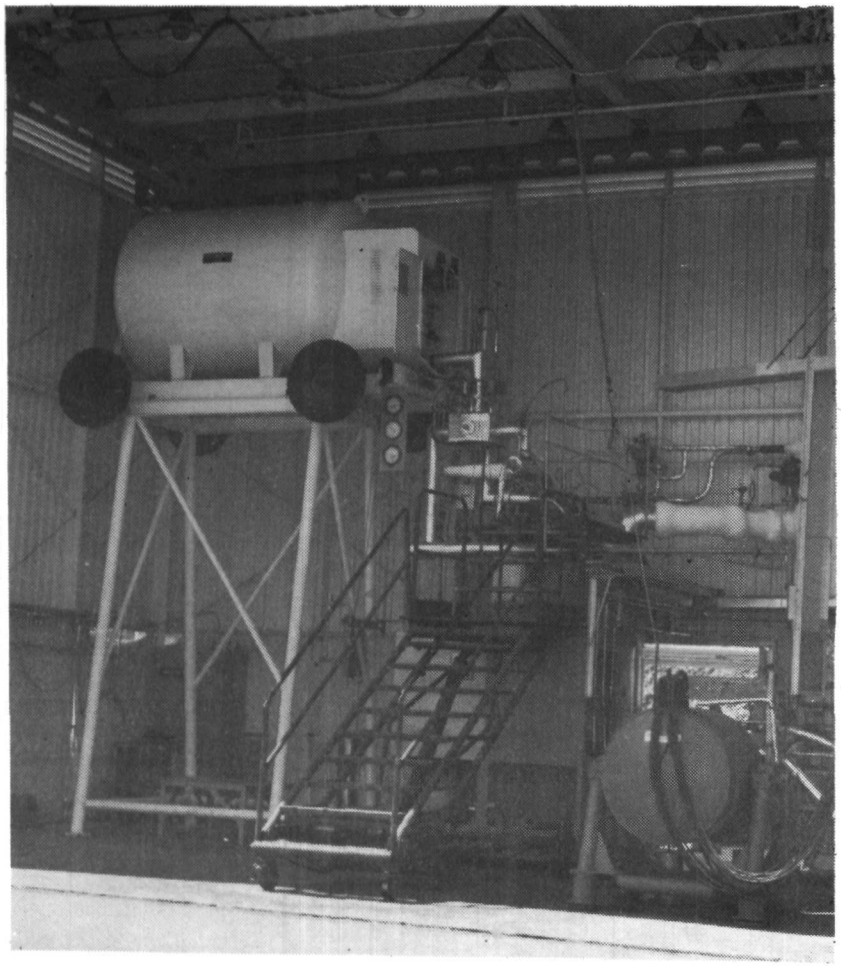

Figure 2-14. Large Scale Gel Production Facility

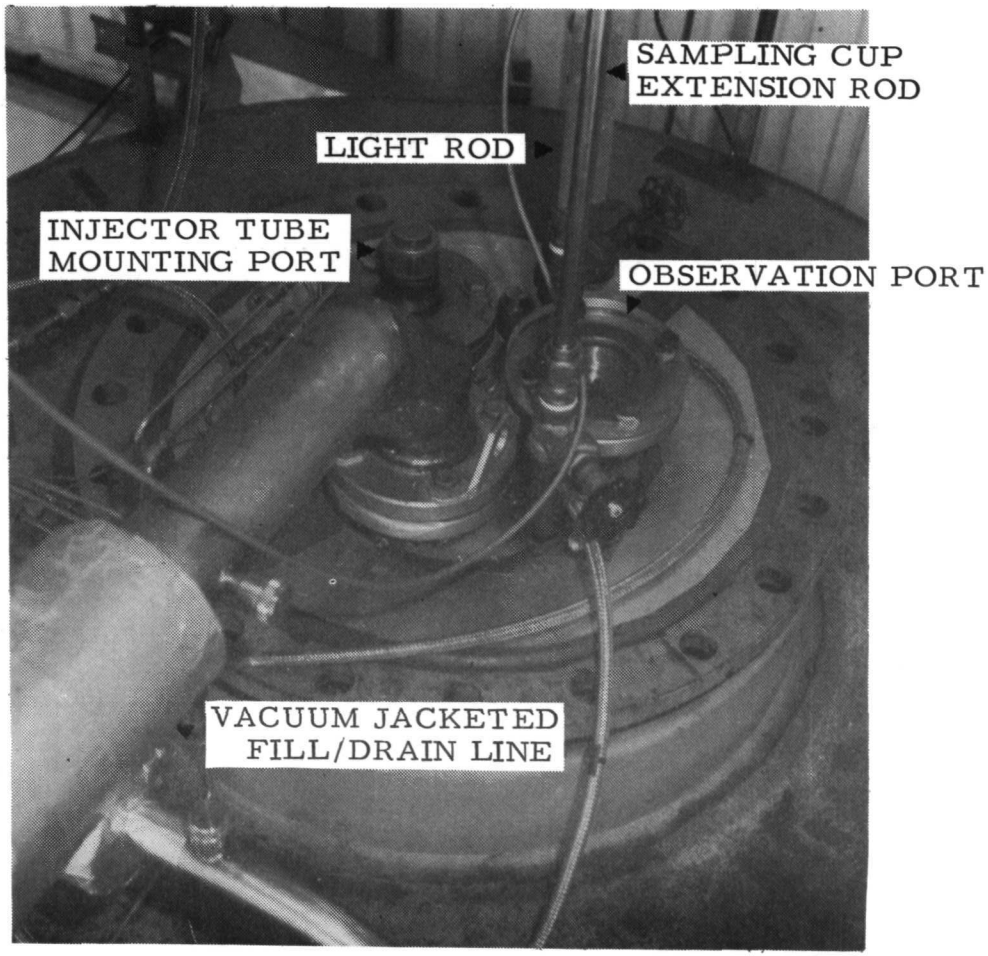

Figure 2-15. Cover of Gel Production and Storage Tank

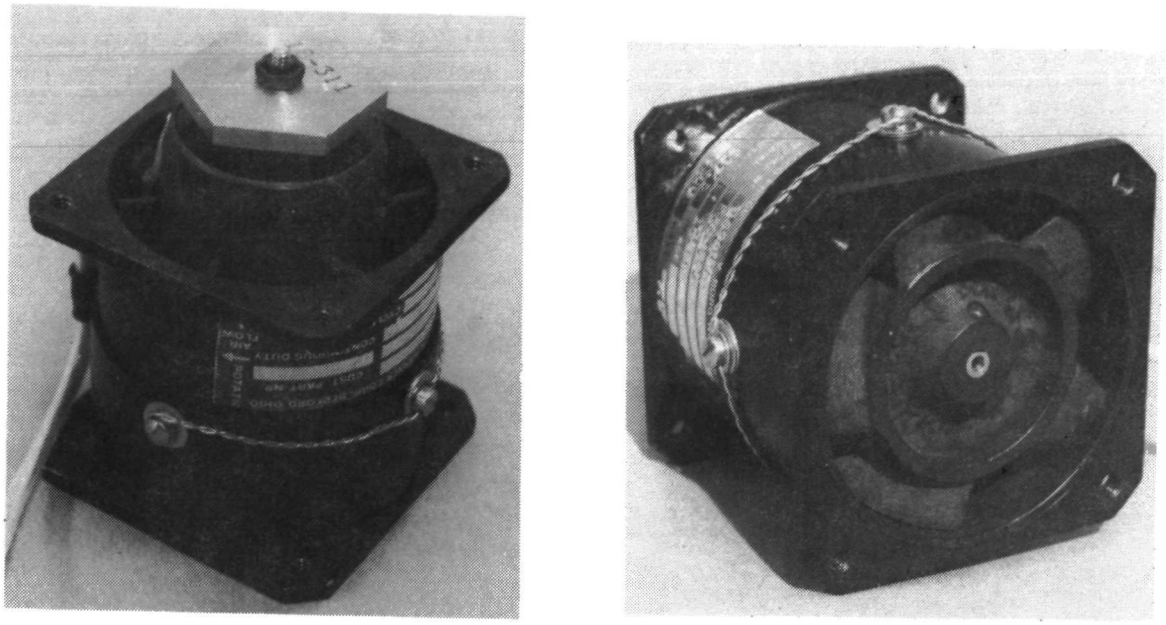

Figure 2-16. Pesco Liquid Hydrogen Pump

initially to purge the system and hydrogen to stabilize the flow rate and system temperatures prior to the initiation of gelant mix flow. The gaseous ethane gelant and the hydrogen carrier gas are mixed in a 1.22 m^3 (43 ft^3) tank located immediately behind the test pad. The tank was initially pressurized to 689 kN/m^2 (100 psia) with gaseous ethane and then to a total pressure of approximately 12.4 MN/m^2 (1800 psia) with gaseous hydrogen. Chemical analysis indicated an ethane concentration of 5.65 mole percent in the mixture, and the total pressure was subsequently raised to 13.8 MN/m^2 (2000 psia) with gaseous hydrogen to reduce the concentration to five percent. No further additions to the mix tank were made. Subsequent analyses of the chemical composition yielded ethane mole percents of 6.87 percent on 25 July and 7.06 percent on 9 October. This indicates that the hydrogen gas leaks more readily than does the ethane gas as would be expected from the 15-to-1 ratio of molecular weights.

The gel production apparatus contains two gelant injection tubes each having four 381-μm (0.015-in) diameter orifices (Figure 2-17). Operated at a differential pressure of 689 kN/m^2 (100 psi) a gel production rate of approximately 0.121 m^3/hr (32 gal/hr) can be achieved. A procedure identical to that outlined in the process design analysis (Section 2.1.2) was used to calculate this rate. A total time of 11 hours would then be required to produce a 1.33 m^3 (350 gal) batch of gelled liquid hydrogen containing ten weight percent ethane. A number of injection tube/orifice configurations were evaluated during the development of the facility. Initially too little heat was supplied to the injection system and the orifices would clog after 20 to 30 minutes of operation. Some problems associated with solid contamination were uncovered and subsequently eliminated by redesigning the components inside the injection tube. The primary cause of the flow stoppage, however, appeared to be a gradual buildup of ethane particles on the exterior surface of the orifice plug due to recirculation of the flow from the injection plumes. This large-scale system does not have the benefit of vigorous fluid scrubbing action present in a small-scale system due to the highly agitated motion of the liquid hydrogen.

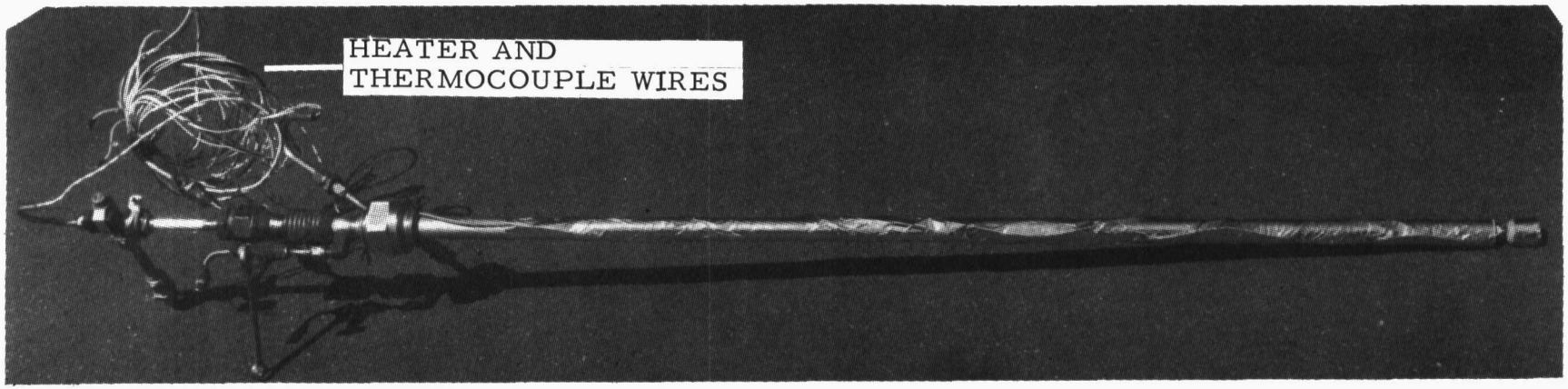

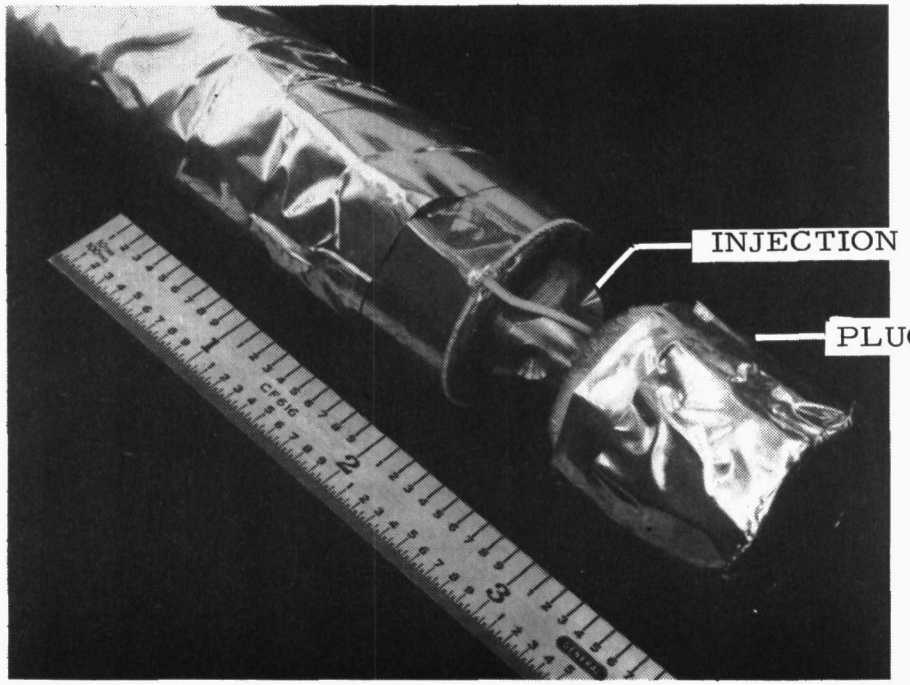

Figure 2-17. Gelant Injection Tube

Buildup slowly blocks the flow passages and occasionally a portion of the solid matter breaks off causing the passage to temporarily enlarge. The resulting flow pattern resembles a declining sawtooth eventually falling to zero.

A new injection orifice plug was designed to eliminate this problem. This plug, shown schematically in Figure 2-18, incorporates an extension below the four flow orifices to permit the application of an external plug heater. This heater, together with the internal heated alumina rod and an external wrapped sleeve heater, effectively prevents condensation within the tube or plug cavity. The plug heater also causes LH_2 vaporization at the surface, providing additional agitation near the flow orifices, which tends to inhibit the attachment of particles in the vicinity of the orifices.

Using this injector configuration, a 6.9 mole percent ethane in gaseous hydrogen mix was flowed into the production tank for two six-hour periods. In each period, once the injection system temperatures were stabilized the mix flowrate remained essentially constant, varying slightly about a mean value. Stability was achieved by supplying a total of 196 watts to the three heaters. At this power setting the temperature of the gas mixture upstream of the filter element (Figure 2-18) stabilized at 439K (330F) while the external surface of the injection plug in the vicinity of the four flow orifices remained at 122K (-240F). A total of 6.6 kg (14.6 lbs) of C_2H_6/H_2 mix, or 3.5 kg (7.7 lb) of ethane, was flowed into the tank during the twelve hour period. The ethane particles occupied a "settled volume" of 0.30 m^3 (80 gal) on the bottom of the tank. This volume is the initial volume formed by the particles in a hydrogen-rich mixture. The resulting volume of the hydrogen gel would be somewhat lower. Assuming that all of the injected ethane was in the settled volume, the resulting concentration of ethane was fourteen weight percent. This value is, however, an upper limit in that the wall of the tank and all horizontal surfaces below the liquid hydrogen surface were coated with ethane particles which had adhered to the surfaces. Attempts to withdraw a sample for chemical analysis were unsuccessful. A sampling system utilizing an evacuated sample bottle, similar to that employed by Aerojet, but on a much larger scale was tried, but an analysis of the contents of two sample bottles yielded ethane weight percents less than three percent. A new sampling system was subsequently developed with the valve seat physically submerged in the gel to eliminate the long flow path. This new system was to have been evaluated during Phase III.

Figure 2-19 is a photograph taken through the viewport showing the 0.30 m^3 (80 gal) settled volume of ethane particles in liquid hydrogen. The Pesco mixing pump, the sampling cup, and the light rod are also shown. A qualitative examination of the mixture was conducted. The sampling cup was submerged in the mixture and a cylindrical cavity some 15 cm (6 in) tall was created. By moving the cup laterally and slowly withdrawing it from the mixture, a cone of particles was observed protruding from the top of the cup. The sample was then raised out of the liquid hydrogen to the viewport for close visual inspection. This examination led to the conclusion that the mixture possessed significant, gel-like structure and did not appear to be merely a collection of solid particles.

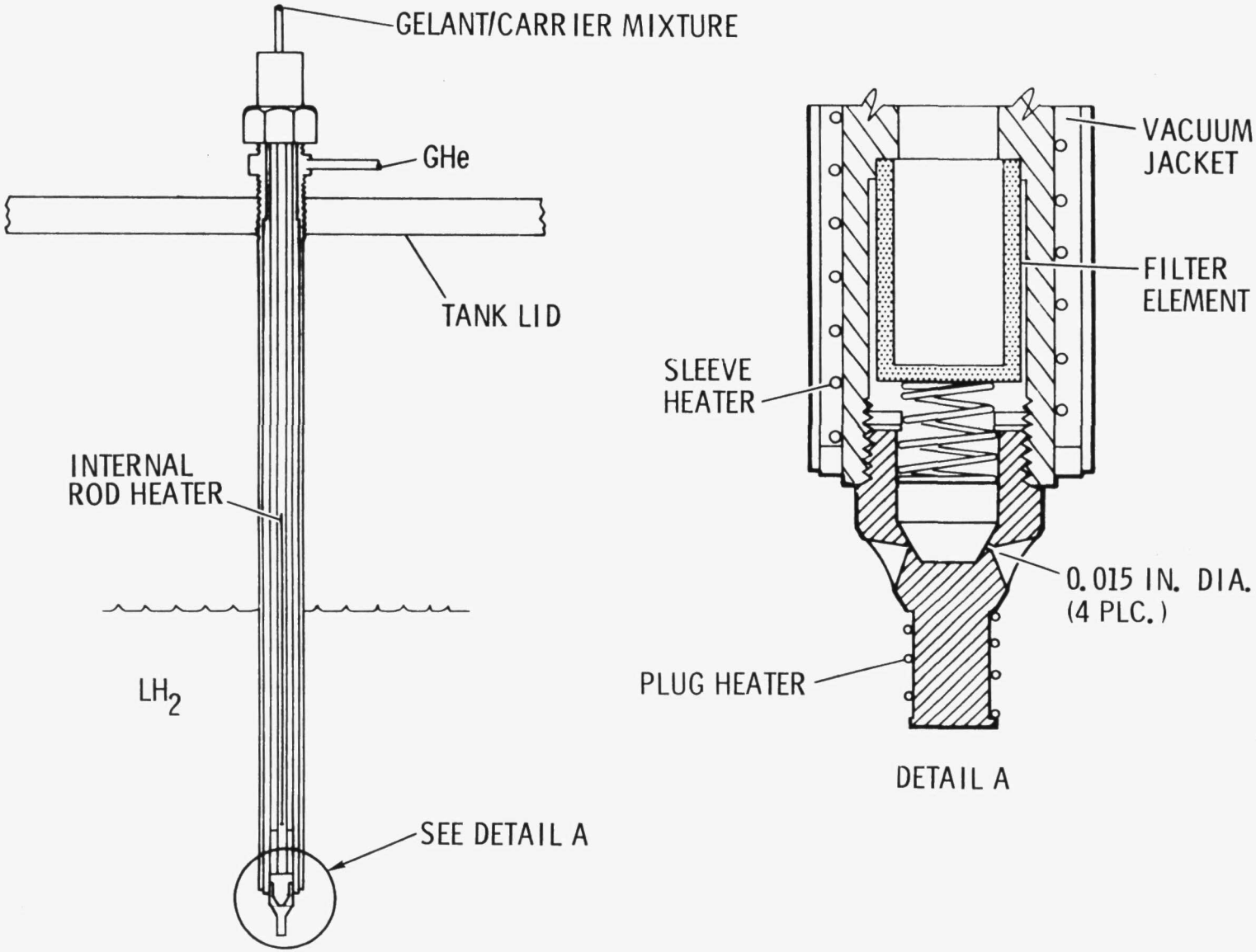

Figure 2-18. Schematic of Gelant Injection Tube

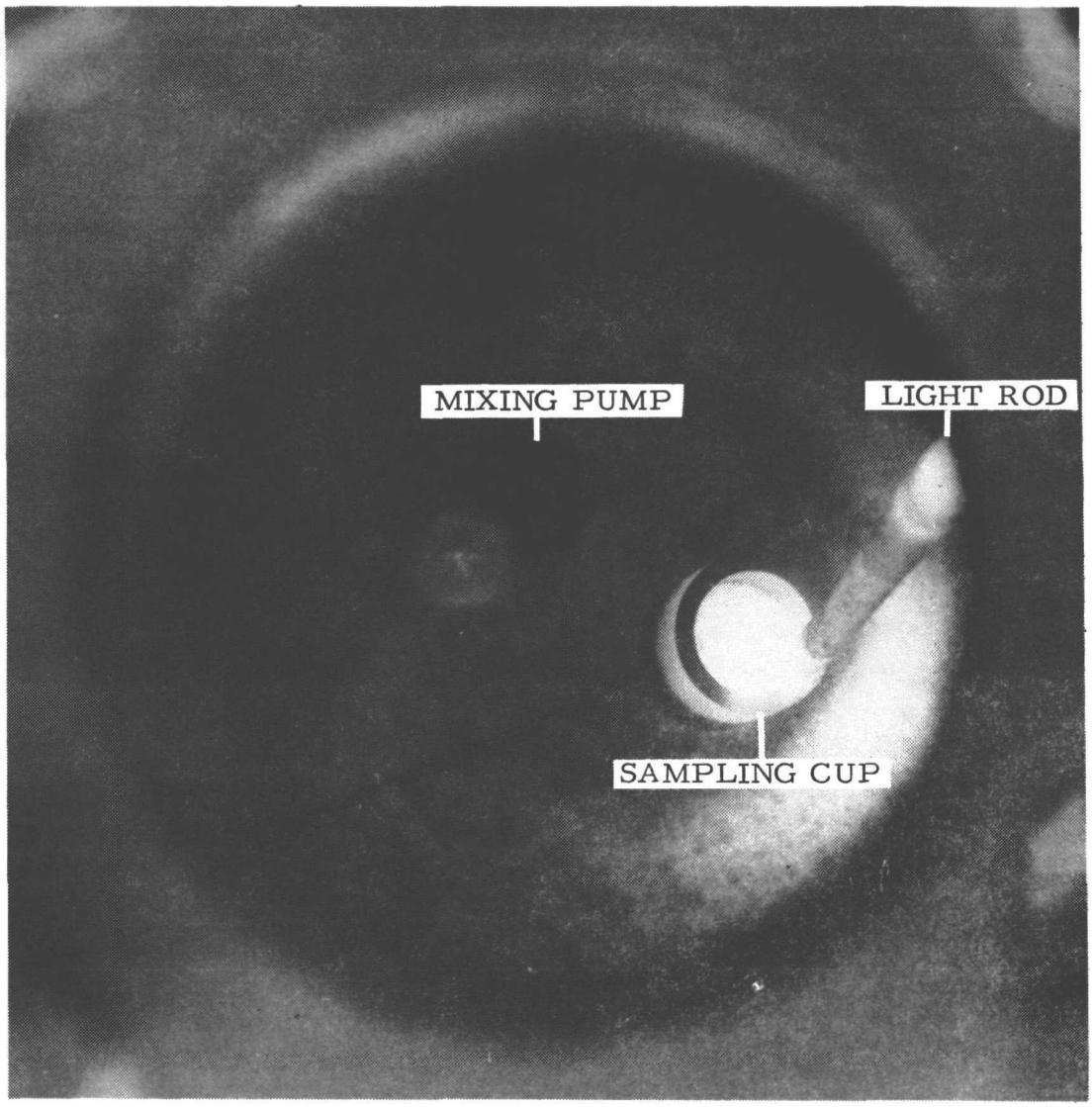

Figure 2-19. View Into Gel Tank Through Viewport

SECTION 3

TRANSFER AND SOLUBILITY

The transfer characteristics of gelled liquid hydrogen were investigated by Aerojet. The extent of gel structural degradation due to repeated shearing, the viscosity of flowing gelled hydrogen, and the effect of varying incident heat flux levels on gel transfer were determined. In addition the rate of dissolution of helium in both gelled and neat liquid hydrogen were measured.

3.1 GEL TRANSFER

Although gelled liquids exhibit the characteristics of semi-solids when at rest, they assume the flow characteristics of the ungelled liquids as the shear rate is increased. This phenomenon is referred to as "shear thinning," and the gel as "thixotropic," if the viscosity decreases with increasing shear rate and is considered to be non-Newtonian behavior. Both the extent of shear thinning during transfer and the effect of repeated transfer on the "at rest" structure of the gel have been investigated.

3.1.1 SHEAR DEGRADATION TESTS. Gels prepared with particulate gelants normally shear thin rapidly when exposed to stress, that is, the apparent viscosity value decreases with increasing shear rate. However, when the stress is removed, the gel structure immediately returns and the gelled liquid assumes its semi-solid characteristic. In some instances, the gel structure does not completely return after the stress is removed, and with each subsequent application of stress the degree of gel structure decreases, until finally the structure is completely destroyed.

In order to demonstrate that the gelled liquid hydrogen is a suitable fuel, the effect of repeated shearing on the gel structure was evaluated. The evaluation was conducted in the following manner. A batch of gel was prepared in a 1.2 liter flask which was immersed in a liquid hydrogen bath. After preparation of the gel, a sample was withdrawn for analysis of the ethane content. Then the gelled liquid hydrogen was passed through a 4.83-mm (0.19-in.) I.D. flow coil with an equivalent length of 14.02 m (46 ft) into the gel receiver flask. The driving pressure and the flow rate were measured during the transfer. The gel was then returned to the preparation flask through the same coil, and the driving pressure and flow rate were again measured. The basic apparatus is shown in Figure 3-1,and Figure 3-2 shows the apparatus installed in the test purge box.

The first batch of gelled liquid hydrogen was prepared using an injection tube similar to that shown in Figure 2-9. The diameter of the orifice was 635 μm (0.020 in) in order to enhance the formation of ethane particles with greater gelant capacity. In all

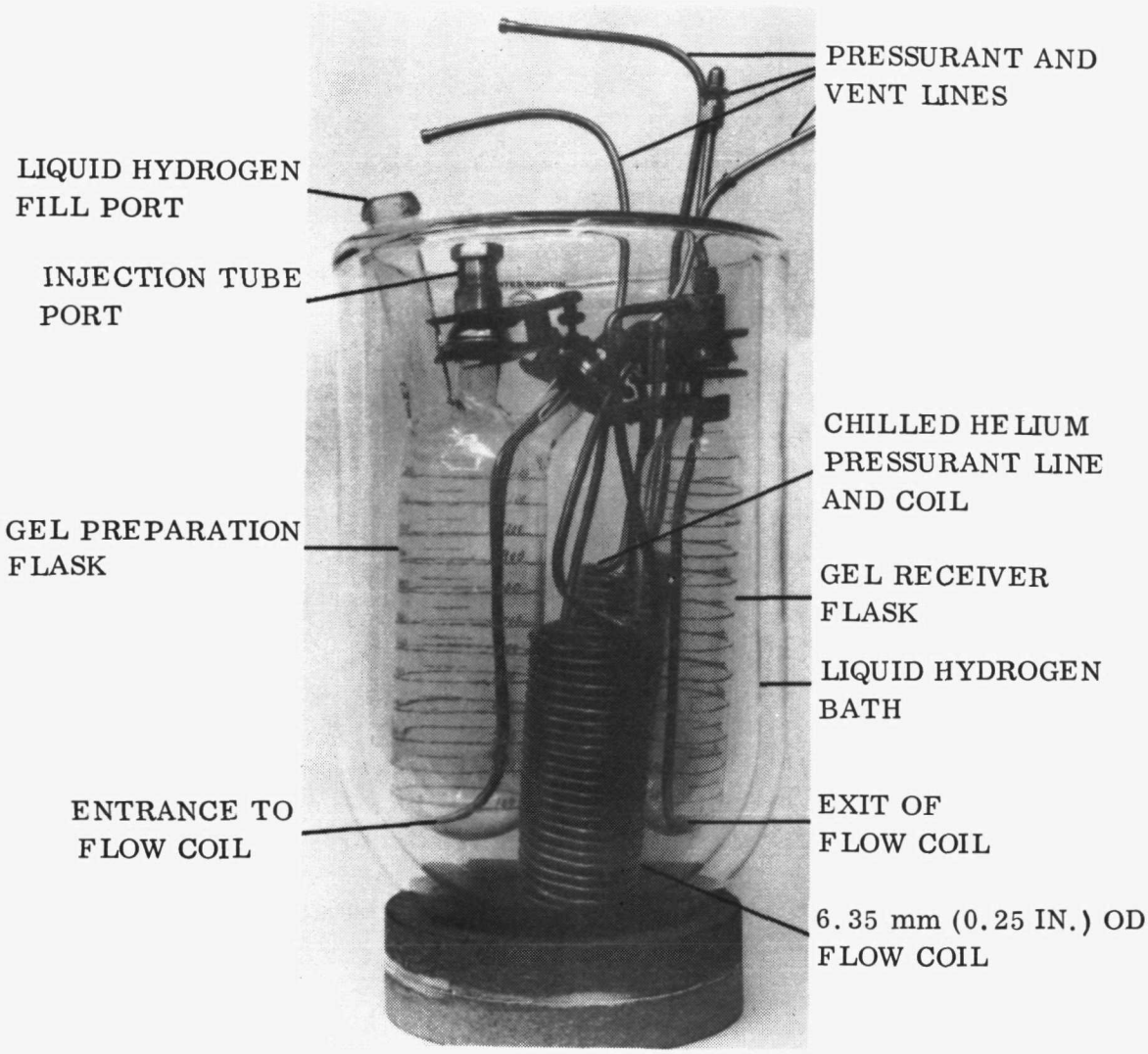

Figure 3-1. Gel Shear Degradation Test Apparatus

the experiments, the electrical power supplied to the injection tube heater was 225 watts. Seven batches of gel were prepared and flowed in a cyclic manner.

Data from representative experiments are presented in the form of characteristic flow curves. A baseline curve for neat (ungelled) liquid hydrogen passing through the apparatus is shown in Figure 3-3 for comparison purposes. The ratio of the shear stress to the shear rate is the apparent viscosity of the fluid. The data in Figure 3-3 demonstrate that the liquid hydrogen is flowing in the turbulent regime because the slope of the curve is greater than one. A slope with the value of one corresponds to a Newtonian fluid flowing in the laminar regime.

The gelled liquid hydrogen for which the data are shown in Figure 3-4 was prepared by using a gas mixture of 10 volume percent ethane in hydrogen to prepare the ethane particles. The resultant concentration of ethane in the gel was found to be 12.75 weight percent. The data presented in Figure 3-4 demonstrate that the gel was not of uniform

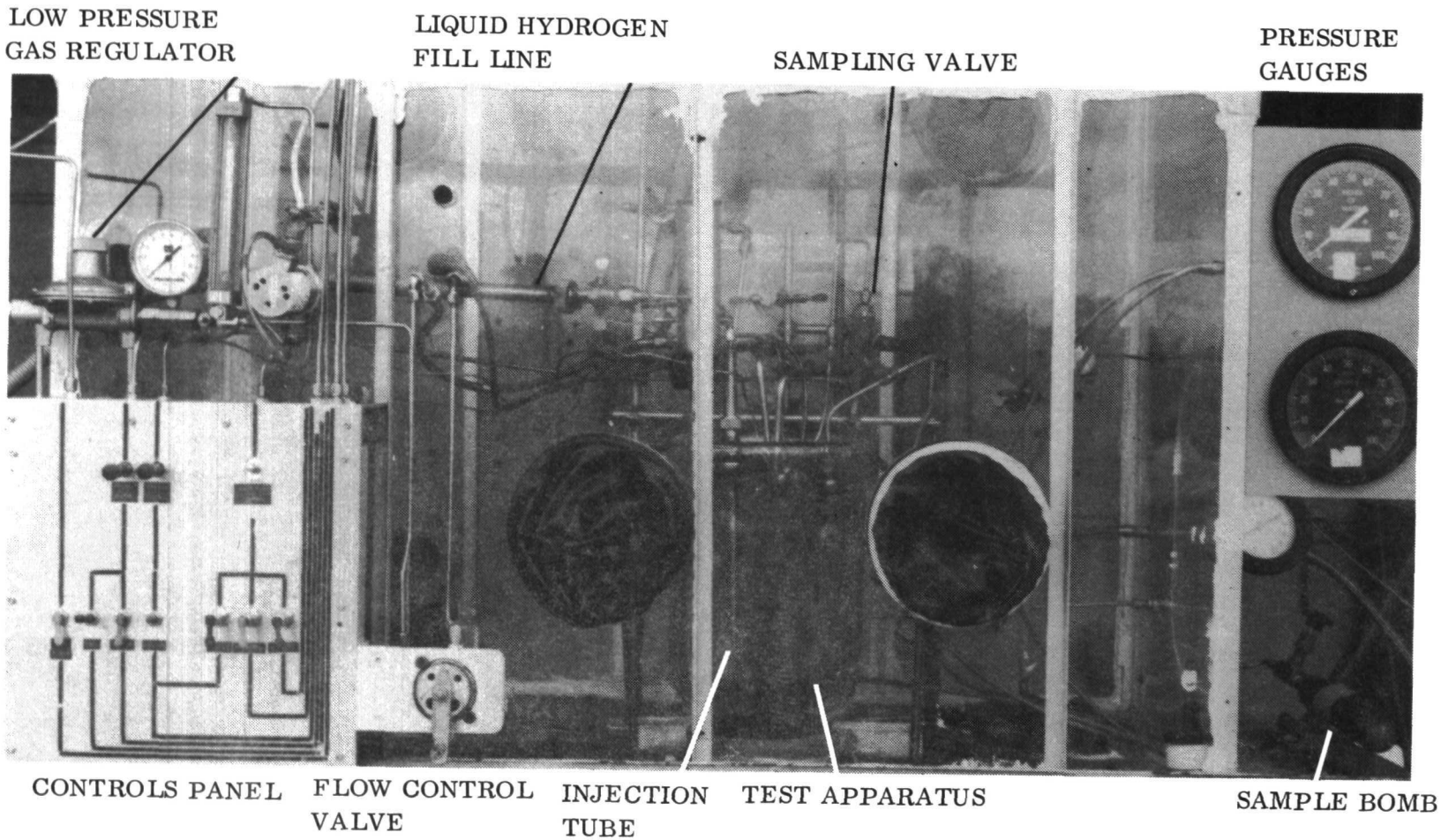

Figure 3-2. Test Apparatus in Test Box

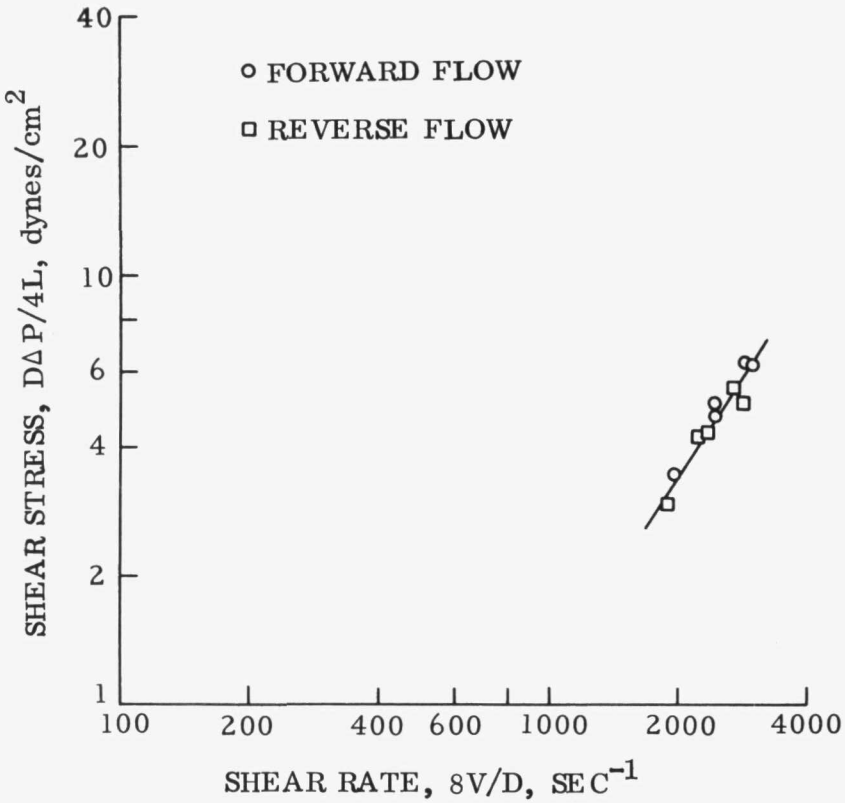

Figure 3-3. Characteristic Flow Curve, Neat Liquid Hydrogen

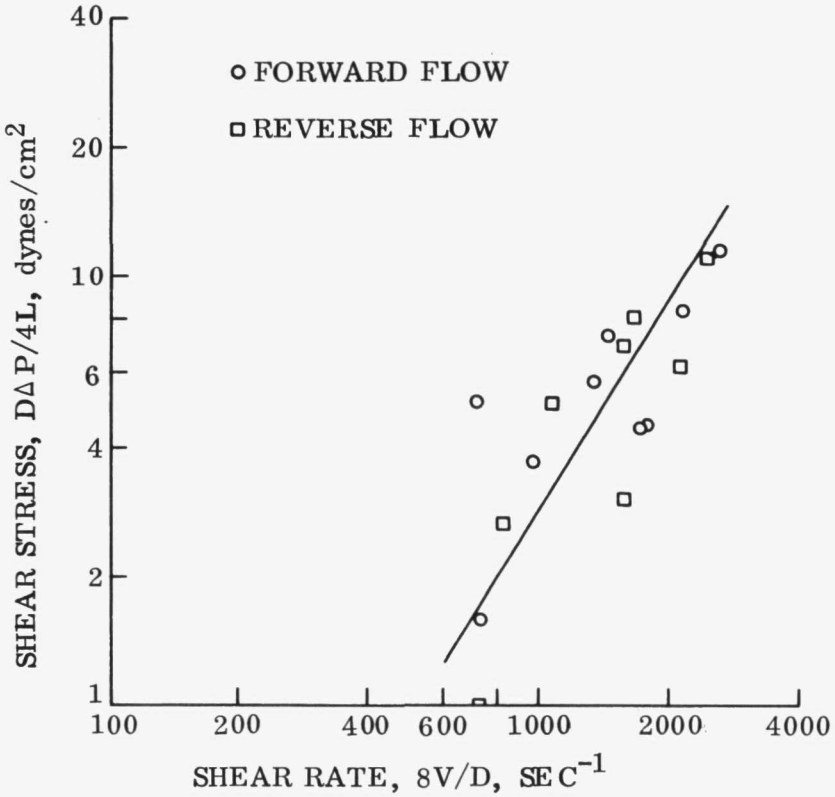

Figure 3-4. Characteristic Flow Curve, Gelled Liquid Hydrogen (12.75% Ethane)

texture because the data exhibit a significant amount of scatter. If shear degradation were to occur, a point for forward flow would be displaced to the left from the subsequent reverse flow datum point at the equivalent driving pressure. In general, this did not happen and shear degradation is not apparently significant. It was observed, however, that liquid hydrogen did separate from the mixture during transfer. This is attributable to insufficient gel structure in this batch.

Subsequent batches of gelled liquid hydrogen were prepared with a gas mixture consisting of 3 volume percent ethane in the hydrogen for preparation of the gelant particles. The data obtained with a batch of this gel is shown in Figure 3-5. The batch of gel had a uniform texture and the uniformity is reflected by the diminished scatter in the data as compared with that in Figure 3-4. The gelant concentration was found to be 9.5 weight percent ethane. No significant shear degradation is apparent from the data.

Another batch of gel containing 8.4 weight percent ethane was prepared in the manner described above and the characteristic flow data are presented in Figure 3-6. The driving pressure was maintained at a constant value during the experiment. The data again demonstrate the shear degradation of the gel is not significant, but they do reflect that less gel structure is present than in the previous gel. The data exhibit greater scatter and are displaced toward the right as compared with the previous experiment indicating a lower apparent viscosity.

In summation, shear degradation of the gel structure due to repeated transfer does not appear to be prohibitive within the conditions under which tests were conducted. The implication of the tests is that gelled liquid hydrogen can be subjected to several transfers prior to use and the gel structure will maintain its integrity.

3.1.2 VISCOSITY OF GELLED LIQUID HYDROGEN. Because a gelled liquid in the absence of an applied stress has the characteristics of a semi-solid, it exhibits a higher apparent viscosity value at low shear rates than does the neat liquid. As the shear rates increase, the apparent viscosity value of the gelled liquid approaches that of the neat liquid and this phenomenon is referred to as "shear-thinning." The apparent viscosity value is directly proportional to the pressure drop required to transfer a liquid through a line, and so the item of interest is the apparent viscosity of gelled liquid hydrogen versus that of the neat liquid hydrogen. Due to the inherent low viscosity value of liquid hydrogen, its flow in propellant transfer lines occurs in the turbulent regime; consequently, the viscosity measurements were made in the turbulent regime. The tests were conducted with three sizes of tubing and the results are discussed below.

The viscosities were determined in the following manner. A batch of gelled liquid hydrogen was prepared in a flask which contained a coil of 7.87 mm (0.31 in) tubing with an effective length of 3.17 m (125 in), calculated from standard formulas (Ref. 17). The flask was immersed in liquid hydrogen bath. Prior to passing the gel through the coil, the gel was sampled to determine the ethane concentration in the gel. The gel was

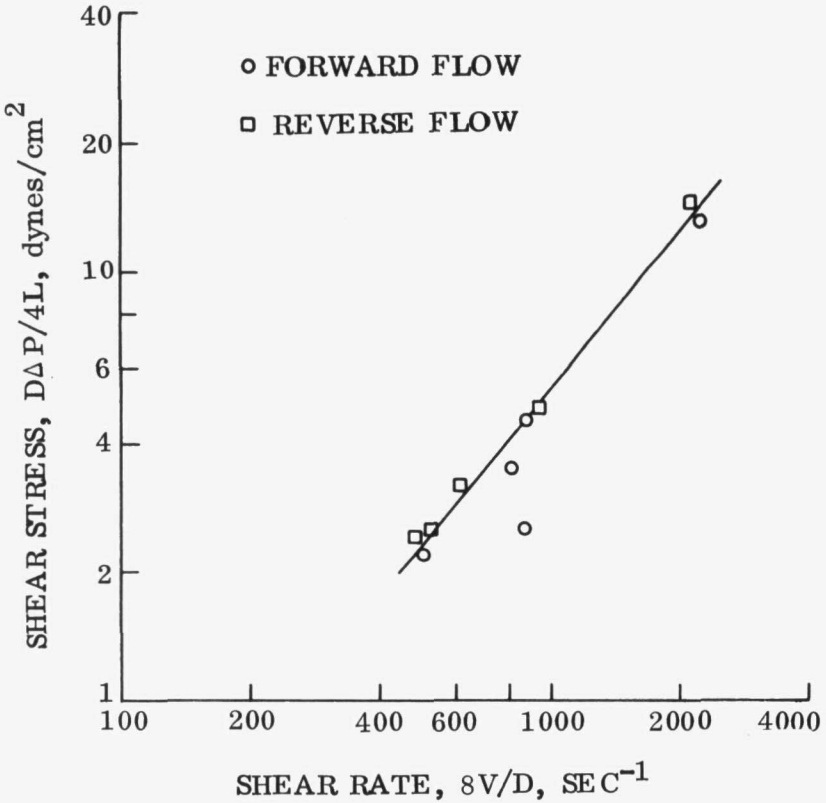

Figure 3-5. Characteristic Flow Curve, Gelled Liquid Hydrogen (9.5% Ethane)

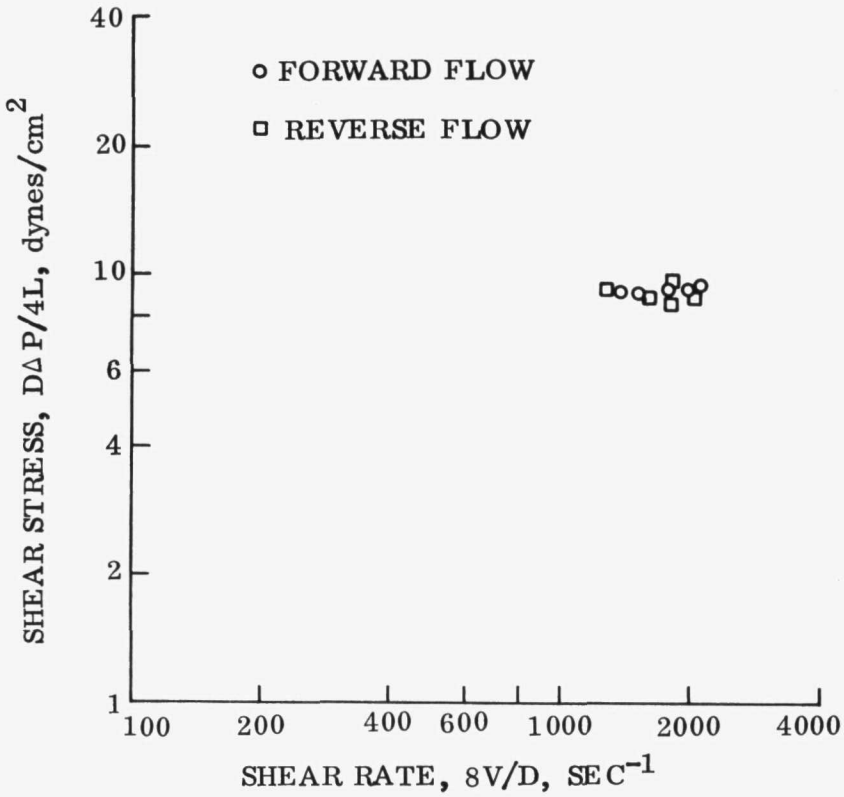

Figure 3-6. Segment of Flow Curve for Gelled Liquid Hydrogen (8.4% Ethane)

then pressurized to a preselected value and a measured quantity of gel was expelled through the coil which was immersed in the liquid hydrogen. The pressure used to expel the gel through the coil was measured using a sensitive differential transducer. The time of flow was measured by a manual timer and verified by the pressure trace obtained using a recording oscillograph. The volume of gel which passed through the coil was noted by means of fiduciary marks on the external flask into which the gel was expelled. A series of tests was also conducted with neat liquid hydrogen to provide a basis for comparison. The data are presented in Figure 3-7 in a characteristic flow curve format. The numbers associated with the data points indicate the gelant concentration as identified in the legend. The apparent viscosity value in the unit of poise is obtained by dividing the shear stress value (dynes/cm^2) by the shear rate value (sec^{-1}). Representative data are also presented in tabular form in Table 5.

The significant items to be noted from the data are that the gelant concentration in the LH_2 has only a secondary effect on the viscosity value, and that as the shear rate increases, the apparent viscosity of the gels approaches that of the neat liquid. It should be noted that in a rocket injector the shear rate values are in the range of 10^4 to 10^6 sec^{-1}, whereas the range investigated here was 10^2 to 10^4 sec^{-1}. Because of this, the pressure drop through an injector may be independent of whether gelled or neat liquid hydrogen is used.

Viscosity measurements in 3.25 mm (0.128 in) tubing were determined in the following manner. The apparatus used was the same as that described for use in the shear degradation tests. The 4.83 mm (0.19 in) internal diameter tubing used for the shear degradation test was replaced with a coil with an effective length of 16.92 m (55.5 ft) of 3.25 mm (0.128 in) internal diameter tubing. The gel was prepared in the gel preparation flask, sampled to determine the ethane concentration, and then transferred into the calibrated gel receiver flask. The pressure, time of flow, and quantity of gel flowed were measured as described in the previous experiments. The data are presented in Figure 3-8 along with data obtained with neat liquid hydrogen. The data indicate that the gel does shear thin rapidly and that the gel viscosity values approach that of the ungelled liquid hydrogen at the higher shear rates. The apparent viscosity values of the gel in 3.25 mm (0.128 in) internal tubing were calculated and representative data are presented in Table 6.

The data indicate that the viscosity of the gelled liquid hydrogen ranges from 2 to 3 fold greater than that of the neat liquid hydrogen in the same apparatus under comparable conditions. On comparison of the apparent viscosities in the three tube sizes, it appears that the viscosity values decrease as the tube sizes decrease under comparable driving pressures. This is as expected in that as the tube diameter decreases, the flow becomes less turbulent.

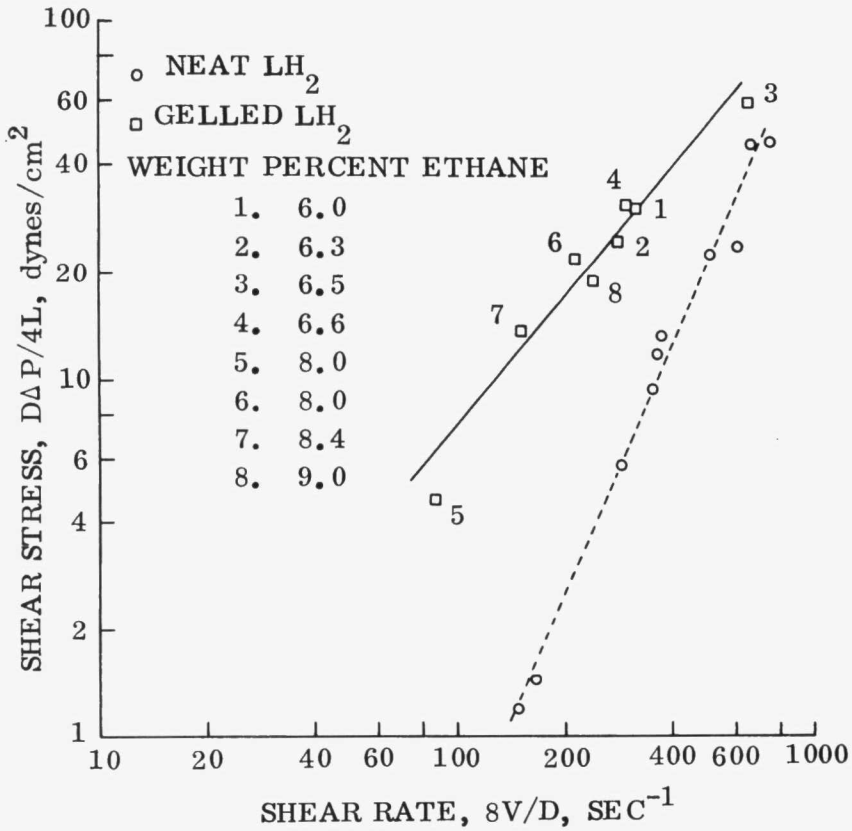

Figure 3-7. Characteristic Flow Curves for Gelled and Neat Liquid Hydrogen, 7.87 mm Tubing

Table 5. Apparent Viscosity of Gelled and Neat Liquid Hydrogen, 7.87 mm Tubing

Gelant Concentration wt % Ethane	Pressure Drop Across Coil kN/m^2 (psi)	Gel Flow Rate cc/sec	Calculated Apparent Viscosity $mN\text{-}s/m^2$ (cp)
6.0	3.86 (0.56)	44	2.23
6.0	4.48 (0.65)	133	0.86
6.3	3.59 (0.52)	110	0.84
8.0	8.76 (1.27)	258	0.87
6.6	4.48 (0.65)	117	0.98
6.5	0.69 (0.10)	34	0.52
8.4	3.24 (0.47)	83	0.99
8.0	2.00 (0.29)	58	0.87
9.0	2.76 (0.40)	93	0.75
None	1.93 (0.28)	148	0.34
None	0.18 (0.03)	57	0.08
None	6.83 (0.99)	294	0.68
None	3.31 (0.48)	200	0.42

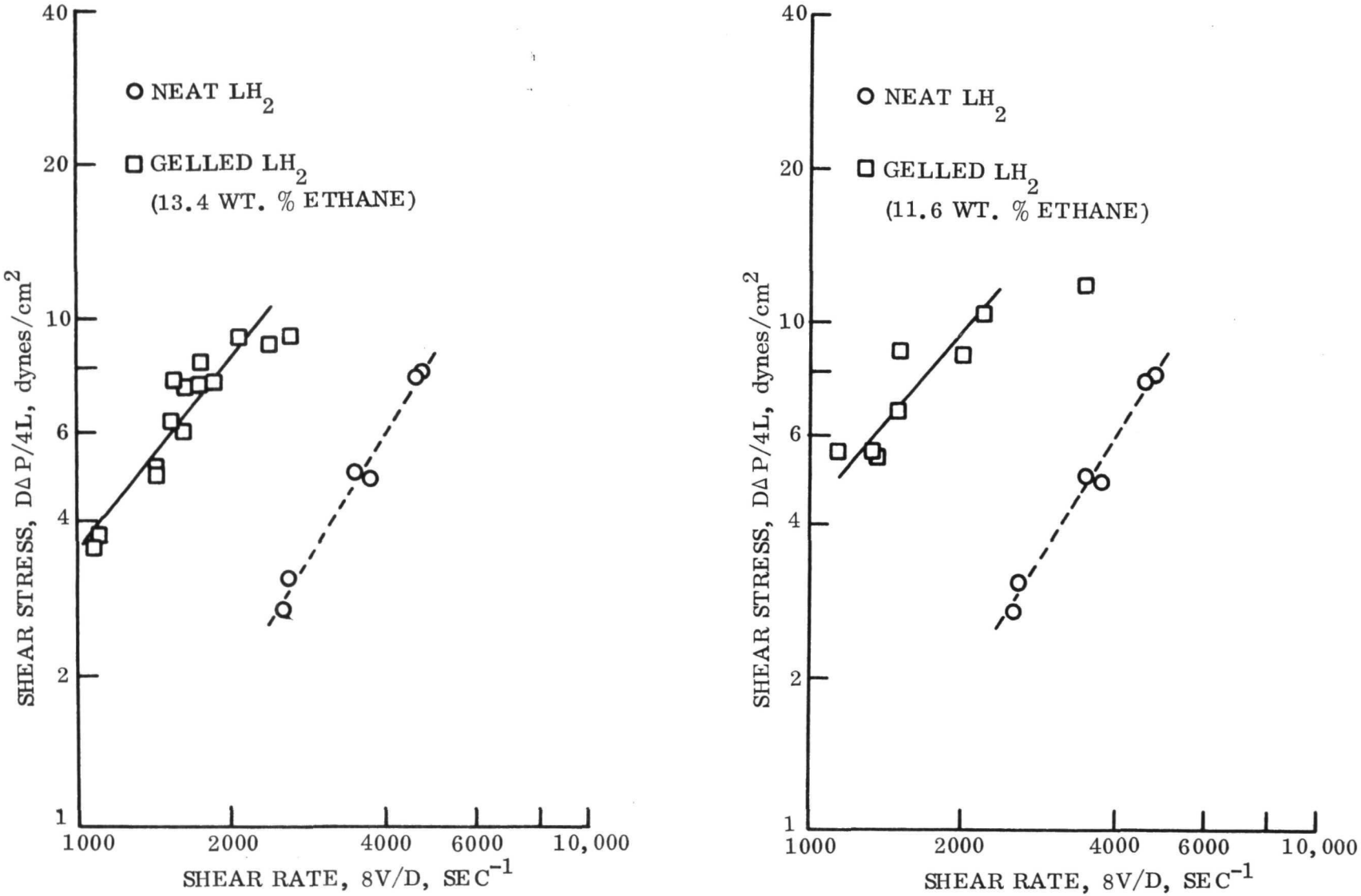

Figure 3-8. Characteristic Flow Curves for Gelled and Neat Liquid Hydrogen, 3.25 mm Tubing

Table 6. Apparent Viscosity of Gelled and Neat Liquid Hydrogen, 3.25 mm Tubing

Gelant Concentration wt % Ethane	Pressure Drop Across Coil kN/m^2	(psi)	Gel Flow Rate cc/sec	Calculated Apparent Viscosity $mN\text{-}s/m^2$ (cp)
13.35	18.6	(2.70)	7.98	0.37
13.35	19.1	(2.77)	8.79	0.34
13.35	15.4	(2.24)	5.79	0.42
13.35	15.2	(2.21)	5.47	0.44
13.35	13.1	(1.90)	5.14	0.40
13.35	10.5	(1.52)	4.81	0.34
13.35	7.8	(1.13)	3.72	0.33
11.55	24.6	(3.57)	11.70	0.33
11.55	21.2	(3.08)	7.50	0.45
11.55	17.9	(2.60)	6.69	0.42
11.55	13.8	(2.00)	5.00	0.44
11.55	11.4	(1.65)	3.79	0.48
None	16.5	(2.40)	15.60	0.17
None	10.1	(1.47)	12.59	0.13
None	6.4	(0.93)	8.63	0.12
None	5.6	(0.81)	8.41	0.11

Table 7. Apparent Viscosity of Gelled and Neat Liquid Hydrogen, 4.83 mm Tubing

Gelant Concentration wt % Ethane	Pressure Drop Across Coil kN/m^2	(psi)	Gel Flow Rate cc/sec	Calculated Apparent Viscosity $mN\text{-}s/m^2$ (cp)
12.75	6.69	(0.97)	14.8	0.43
12.75	5.79	(0.84)	12.0	0.46
9.4	15.17	(2.20)	25.3	0.57
9.4	16.55	(2.40)	23.8	0.67
9.4	2.83	(0.41)	5.9	0.46
9.4	2.55	(0.37)	5.6	0.43
8.4	10.69	(1.55)	19.7	0.51
8.4	10.41	(1.51)	17.7	0.56
None	7.31	(1.06)	31.3	0.22
None	5.58	(0.81)	26.9	0.20
None	3.45	(0.50)	21.0	0.16

3.1.3 EFFECT OF VARYING HEAT FLUXES ON GEL TRANSFER. The flow characteristics of gelled liquid hydrogen presented above were evaluated with the entire apparatus immersed in a bath of liquid hydrogen at its normal boiling point. The experiments presented in this section were conducted with the gelled liquid hydrogen being transferred through lines which were either surrounded by liquid nitrogen or warm gaseous nitrogen. The purpose of these experiments was to establish that gelled liquid hydrogen can be expelled through warm transfer lines as could be encountered during the startup or restart of a rocket engine. In addition, the experiments were to investigate possible clogging of the transfer lines due to the accumulation of the gelant.

The gelled liquid hydrogen was prepared in the gel preparation flask shown in Figure 3-1. However, the flow coil and gel receiver flask were eliminated and replaced by the transfer tubes depicted in Figure 3-9. One of the transfer tubes was a 4.6 mm (0.18 in) I.D. tube 45.7 cm (18 in) long; the other was a 7.0 mm (0.277 in) I.D. tube 45.7 cm (18 in) long. Both tubes were fitted with an external jacket through which the nitrogen was passed. The transfer tubes were instrumented with chromel-alumel thermocouples. At the entrance one thermocouple was attached to the outer surface of the tube; one thermocouple was inserted into the wall of the tube in order to measure the inner wall temperature; and one thermocouple was inserted through the wall of the tube to measure the temperature of the flowing hydrogen. These thermocouples are designated TO-1, TI-1, and TF-1, respectively. At the midpoint of the tube, one thermocouple (TI-2) was inserted into the wall to measure the inner wall temperature, and another (TF-2) was inserted through the wall to measure the flowing hydrogen temperature. Near the exit of the tube three thermocouples were installed: one to measure outer wall temperature (TO-3), one to measure inner wall temperature (TI-3), and one to measure the hydrogen temperature (TF-3). A schematic diagram depicting the thermocouple locations is shown in Figure 3-10. Prior to the transfer tests with the tubes described above, a few scoping experiments were conducted. It was found that liquid hydrogen could not be expelled through a 3.91 m (154 in) length of coiled tubing with an internal diameter of 4.6 mm (0.18 in) while immersed in a liquid nitrogen bath, when a driving force of 27.6 kN/m^2 (4 psid) was applied. In addition, it was found that a 30.5 cm (12 in) length of 3.0 mm (0.118 in) internal diameter tubing at ambient temperature would not allow expulsion of liquid hydrogen with a driving force of 41.4 kN/m^2 (6 psid). In both cases, the transfers were hampered by insufficient driving pressure. Because glass vessels were used in the experiments, it was decided not to exceed the 41.4 kN/m^2 driving pressure, but to reduce the length of the transfer tubes.

Chromel-alumel thermocouples were installed in the transfer tubes and calibrated using liquid nitrogen and liquid hydrogen baths with an ice reference junction. The temperatures of the couples after calibration were found to agree within plus or minus two Centigrade degrees.

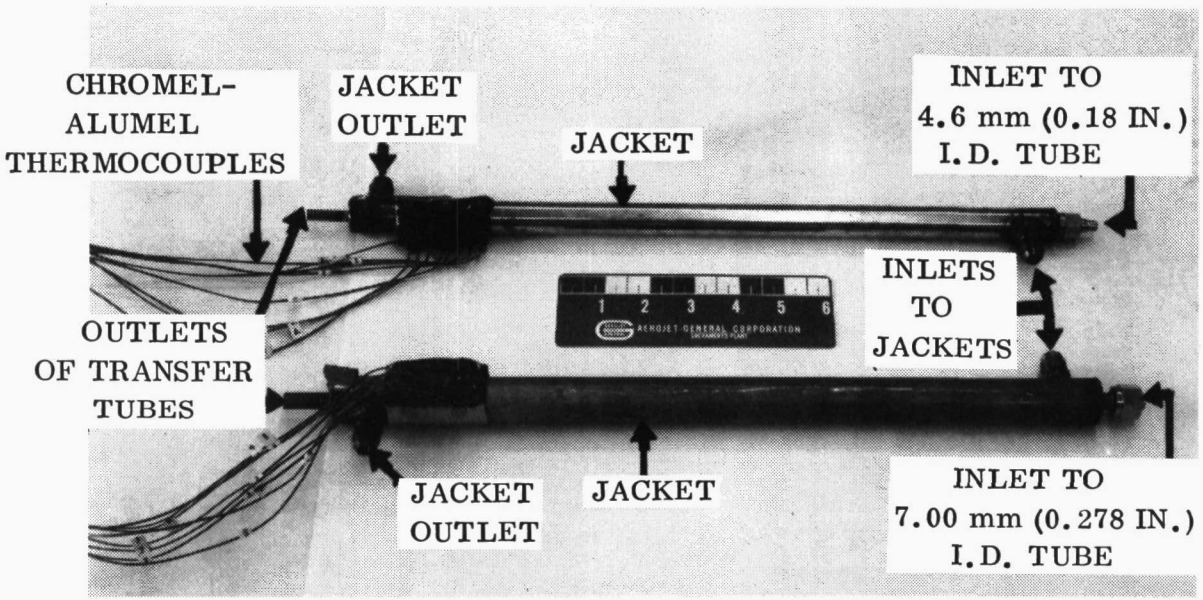

Figure 3-9. Gel Transfer Tubes

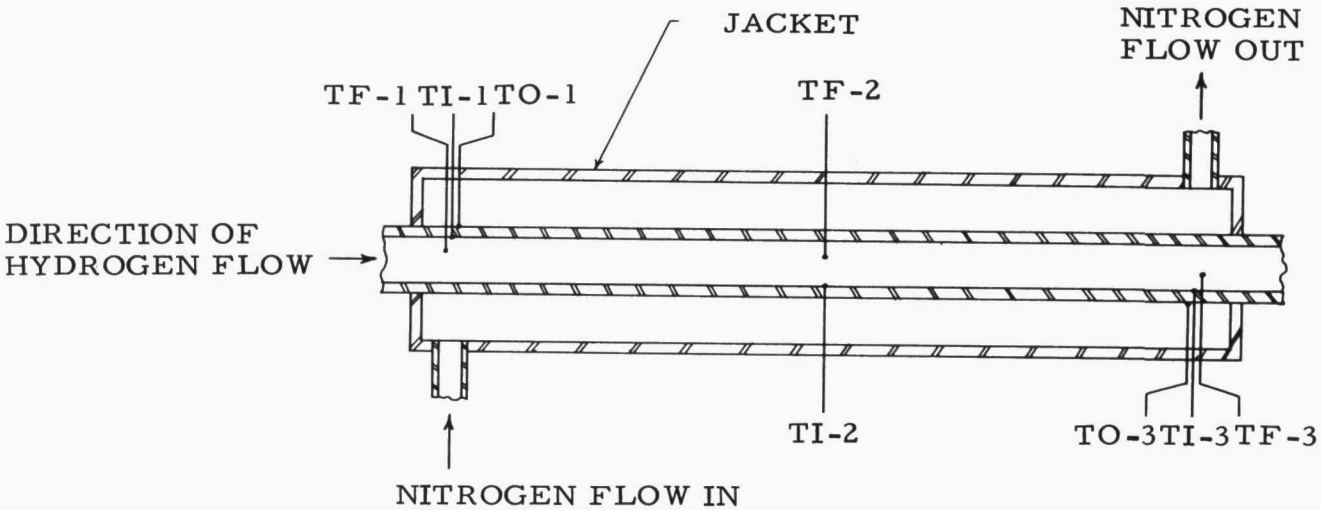

Figure 3-10. Schematic Diagram of Thermocouple Locations In Transfer Tubes

The results for eleven separate flow tests are presented in Table 8. The first seven tests were performed using the 4.6 mm (0.18 in) I.D. flow tube and the other four with the 7.0 mm (0.28 in) tube. Test 101 involved the expulsion of neat liquid hydrogen through the 4.6 mm (0.180 in) internal diameter tube with gaseous nitrogen flowing through the external jacket. The temperature profiles are shown in Figure 3-11. Plot A is the record of the temperature profiles at the entrance to the tube and Plot B is a record of the temperature profiles at the midpoint and exit of the tube. The temperature traces defined in the legend correspond to the thermocouple locations designated in Figure 3-10. The data indicate that with the gaseous nitrogen as the heat source and with a liquid hydrogen flow rate of 41.5 cm^3/sec utilizing a driving pressure of 17.7 kN/m^2 (2.56 psi), liquid hydrogen is expelled at the exit of the tube because the fluid temperature is 20K.

Test 103 involved the expulsion of liquid hydrogen gelled with 9.6 weight percent ethane through the 4.6 mm (0.180 in) internal diameter tube with gaseous nitrogen flowing through the external jacket. The temperature profiles are presented in Figure 3-12. The data indicate that with gaseous nitrogen as the heat source and with a gelled liquid hydrogen flow rate of 28.0 cm^3/sec utilizing a driving pressure of 16.2 kN/m^2 (2.35 psi), the gelled liquid hydrogen is expelled in the liquid phase as indicated by the internal temperature of 20K. A comparison of the data from Tests 101 and 103 indicates that gelled liquid hydrogen flow is approximately 50 percent of that of neat liquid hydrogen for expulsion through tubing under comparable pressure drop and heat flux conditions.

Test 102 involved the expulsion of neat liquid hydrogen through the 4.6 mm (0.180 in) internal diameter tube with liquid nitrogen flowing through the external jacket. The temperature profiles are shown in Figure 3-13 with Plot A again exhibiting the inlet condition and Plot B the midpoint and exit conditions. The data indicate that with liquid nitrogen as the heat source and with a liquid hydrogen flow rate of 54.4 cm^3/sec utilizing a driving pressure of 13.7 kN/m^2 (1.98 psi), the liquid hydrogen is converted to the gaseous state with a temperature of approximately 25K which remains essentially constant throughout the tube.

Table 8. Flow Test Parameters

Test No.	Tube Dia (mm)	Bath Environ.	Wt % C_2H_6	Press. Drop (kN/m^2)	Flow Rate (cm^3/sec)
101	4.6	GN_2	0	17.7	41.5
103	4.6	GN_2	9.6	16.2	28.0
102	4.6	LN_2	0	13.7	54.4
105	4.6	LN_2	5.6	17.4	36.7
106	4.6	LN_2	24.0	17.4	20.3
107	4.6	LN_2	17.4	17.4	30.8
108	4.6	LN_2	17.4	16.5	27.0
109	7.0	GN_2	0	11.4	59.0
112	7.0	GN2	10.2	11.2	51.3
110	7.0	LN_2	0	7.4	70.0
114	7.0	LN_2	10.2	7.7	58.5

Test 105 replaced the neat LH_2 with liquid hydrogen gelled with 5.6 weight percent ethane. The temperature profiles are shown in Figure 3-14.

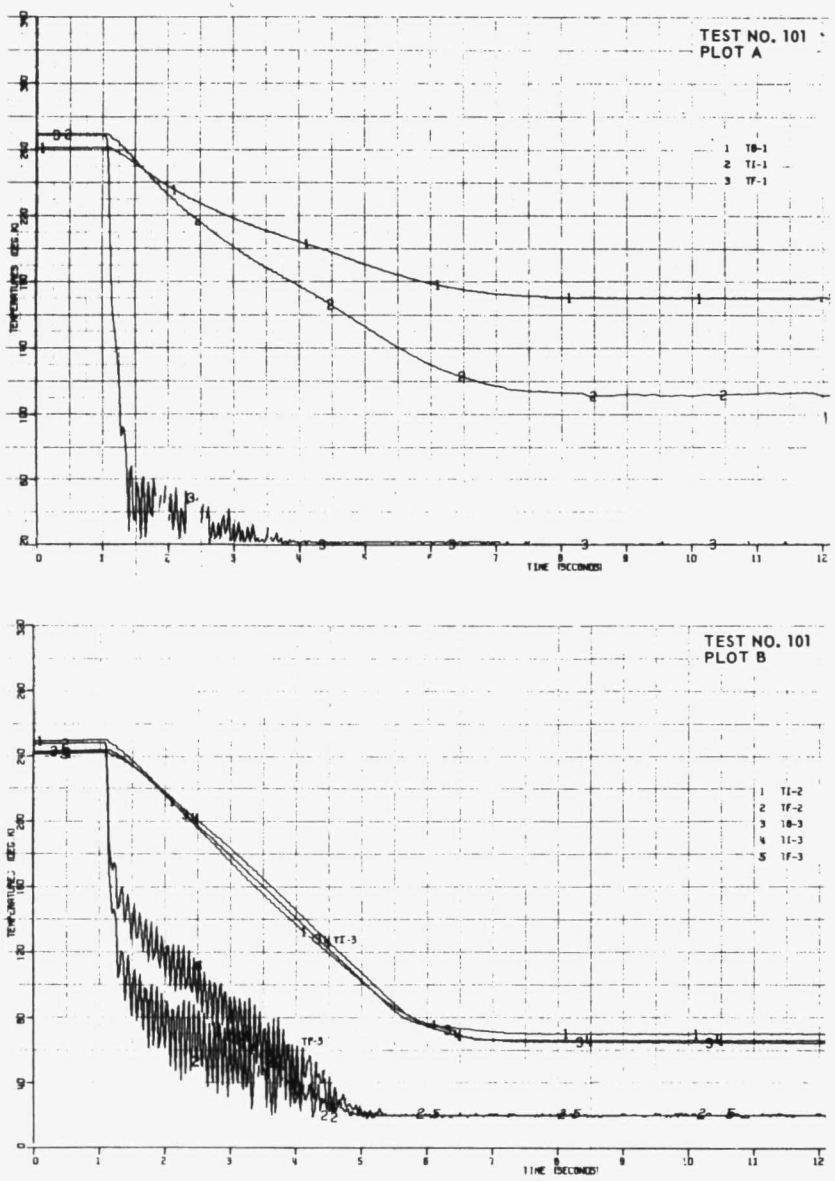

Figure 3-11. Transfer of Neat Liquid Hydrogen Through a 4.6 mm I.D. Tube Surrounded by Gaseous Nitrogen

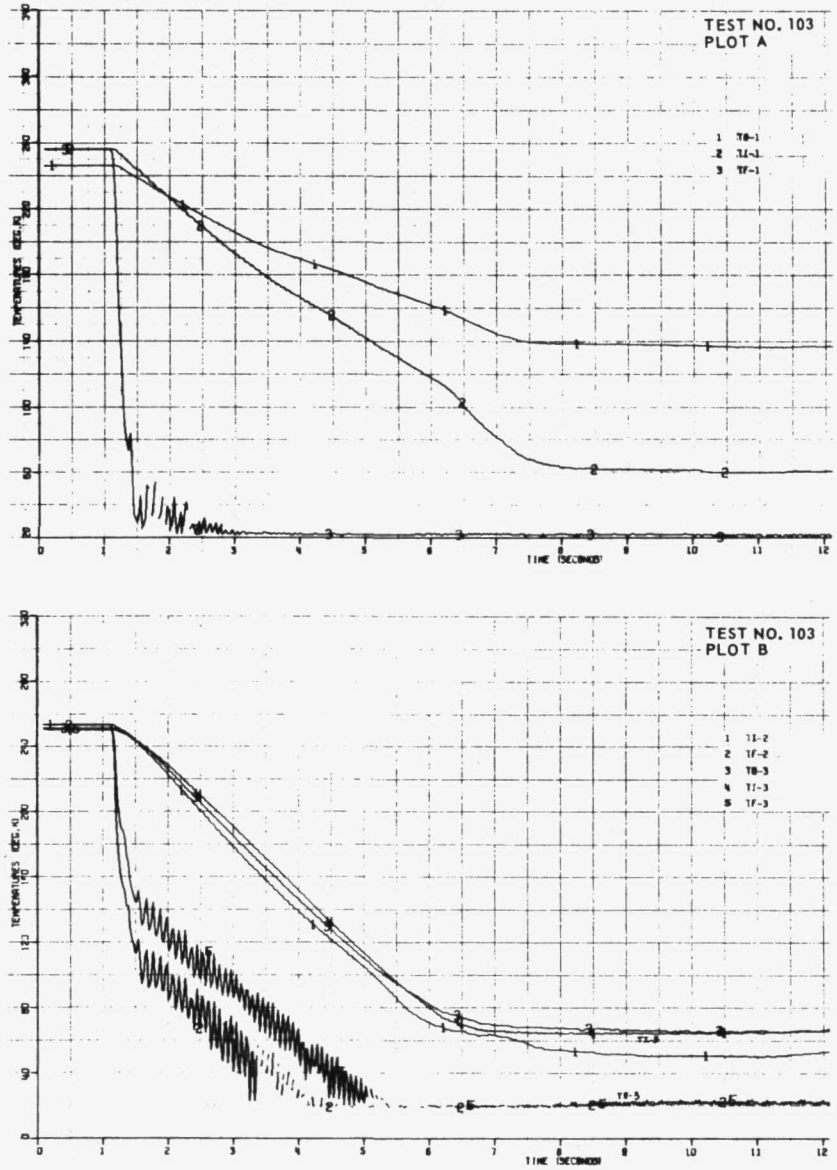

Figure 3-12. Transfer of Liquid Hydrogen Gelled With 9.6 Weight Percent Ethane Through a 4.6 mm I.D. Tube Surrounded by Gaseous Nitrogen

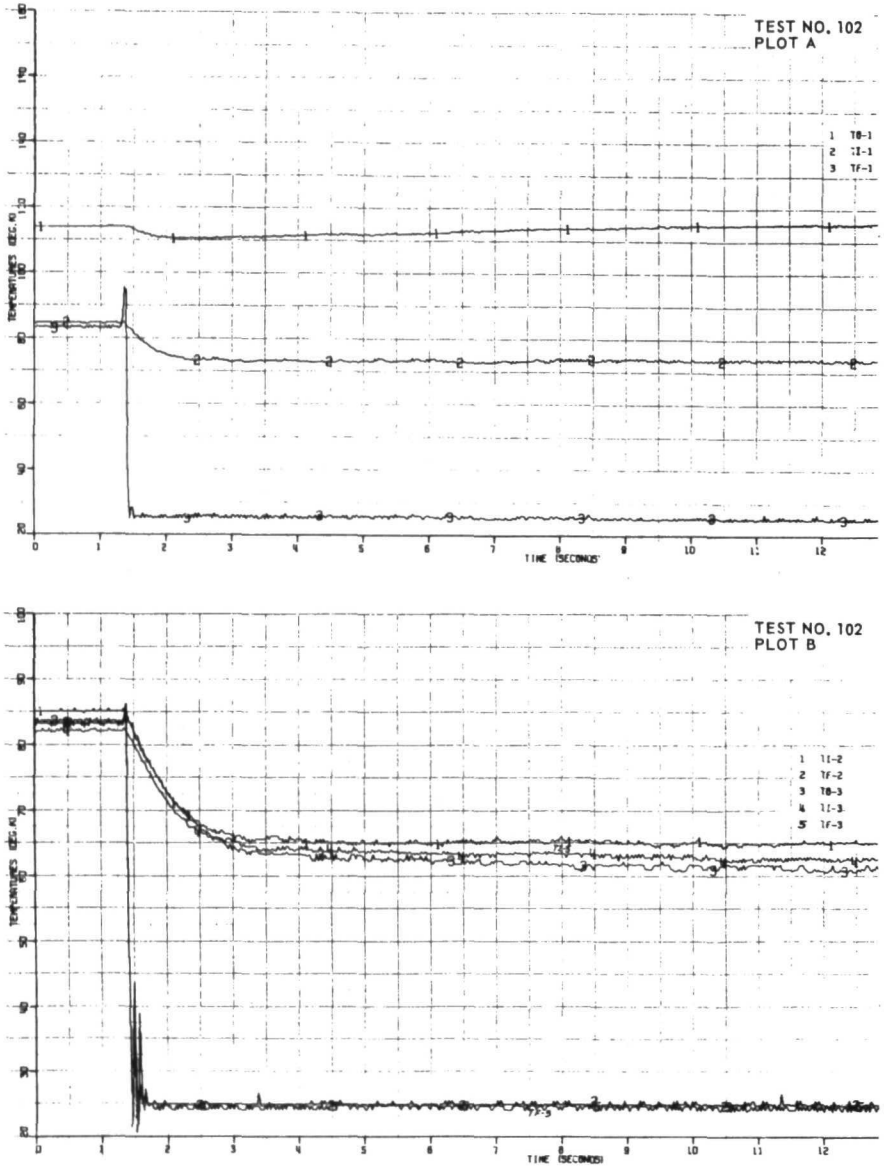

Figure 3-13. Transfer of Neat Liquid Hydrogen Through a 4.6 mm I.D. Tube Surrounded by Liquid Nitrogen

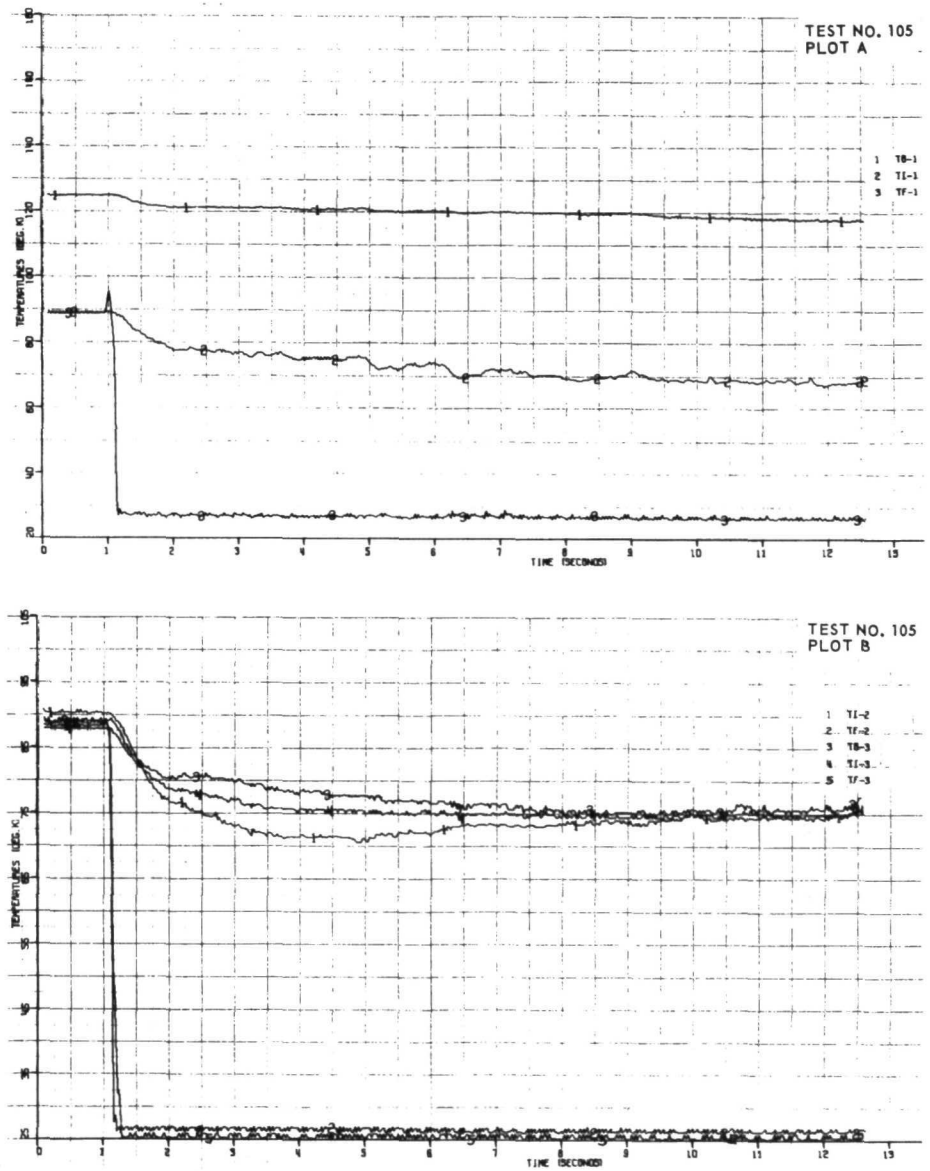

Figure 3-14. Transfer of Liquid Hydrogen Gelled With 5.6 Weight Percent Ethane Through a 4.6 mm I.D. Tube Surrounded by Liquid Nitrogen

The data indicate that with liquid nitrogen as the heat source and with a gelled liquid hydrogen flow rate of 36.7 cm^3/sec utilizing a driving pressure of 17.4 kN/m^2 (2.53 psi), the gelled liquid hydrogen is converted to gaseous hydrogen and solid ethane at a temperature of approximately 26-27K. A comparison of the data from Tests 102 and 105 indicates that gelled liquid hydrogen requires approximately a 100 percent greater driving pressure than liquid hydrogen itself for expulsion through tubing under these conditions. No problems were encountered during the transfer, so the expulsion was terminated and a significant quantity of hydrogen was evaporated from the gel in the flask. A gel sample was removed and analysis indicated an ethane content of 24 weight percent. This gel was then expelled through the same tube under similar conditions. The test is designated by Number 106 and the temperature profiles are shown in Figure 3-15. After six seconds, the gel supply was exhausted as indicated by the temperature increases. The data indicate that with liquid nitrogen as the heat source and with a gelled liquid hydrogen flowrate of 20.3 cm^3/sec utilizing a driving pressure of 17.4 kN/m^2 (2.53 psi), the gelled hydrogen is converted to gaseous hydrogen and solid ethane at a temperature of approximately 26K. The items of significance to note are (1) as the gelant concentration increased from 5.6 to 24 weight percent the flow rate decreased from 36.7 to 20.3 cm^3/sec, (2) although the flowrate was decreased 45 percent while the heat flux was the same as in Test 105, the temperature of the products expelled in Test 105 and 106 was essentially the same, and (3) no difficulty was experienced in restarting the flow even though the gelant concentration was quadrupled between Tests 105 and 106.

Tests 107 and 108 involved the expulsion of liquid hydrogen gelled with 17.4 weight percent ethane through the 4.6 mm (0.180 in) internal diameter tube with liquid nitrogen flowing through the external jacket. The conditions are comparable to Tests 102, 105 and 106. The temperature profiles for Tests 107 and 108 are presented in Figures 3-16 and 3-17. Test 108 was a restart of flow at the termination of No. 107. The data from Test 107 indicate that the gelled liquid hydrogen with a flow rate of 30.8 cm^3/sec utilizing a driving pressure of 17.4 kN/m^2 (2.53 psi) is converted to gaseous hydrogen and solid ethane at a temperature of 26-27K during passage through the tube. In Test 108 the flowrate of 27.0 cm^3/sec utilizing a driving pressure of 16.5 kN/m^2 (2.39 psi) produces similar results. In Test 108, the gel supply was exhausted after seven seconds as indicated by the rise in temperatures. The items of significance to be noted are that (1) restart in Test 108 was not impaired by the possible presence of deposits from previous Test 107, and (2) the flowrates with comparable driving pressures are very similar.

Test 109 involved the expulsion of neat liquid hydrogen through the 7.0 mm (0.277 in) internal diameter tube with gaseous nitrogen flowing through the external jacket. The temperature profiles are shown in Figure 3-18. The data indicates that with gaseous nitrogen as the heat source and with a liquid hydrogen flow rate of 59.0 cm^3/sec utilizing a driving pressure of 11.4 kN/m^2 (1.66 psi), the liquid hydrogen is expelled in the liquid phase as indicated by the external temperature of approximately 20K at the exit.

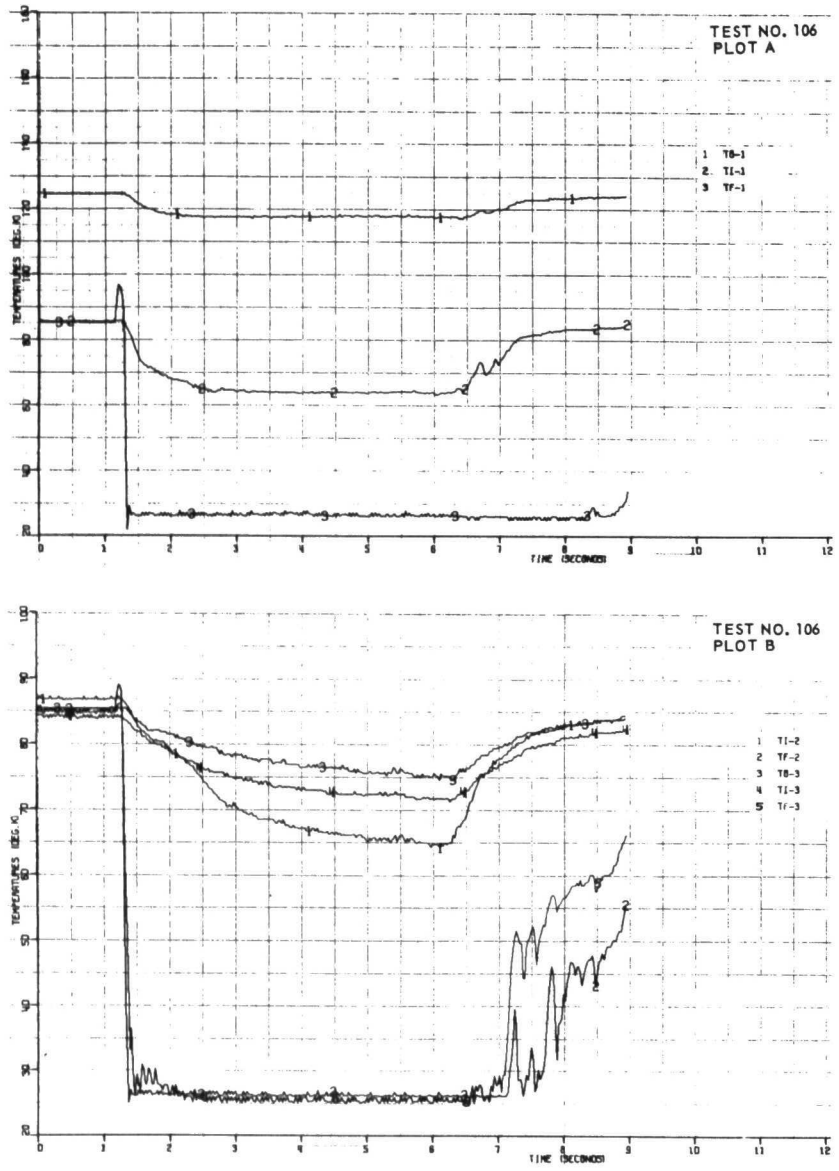

Figure 3-15. Transfer of Liquid Hydrogen Gelled With 24 Weight Percent Ethane Through 4.6 mm I.D. Tube Surrounded by Liquid Nitrogen

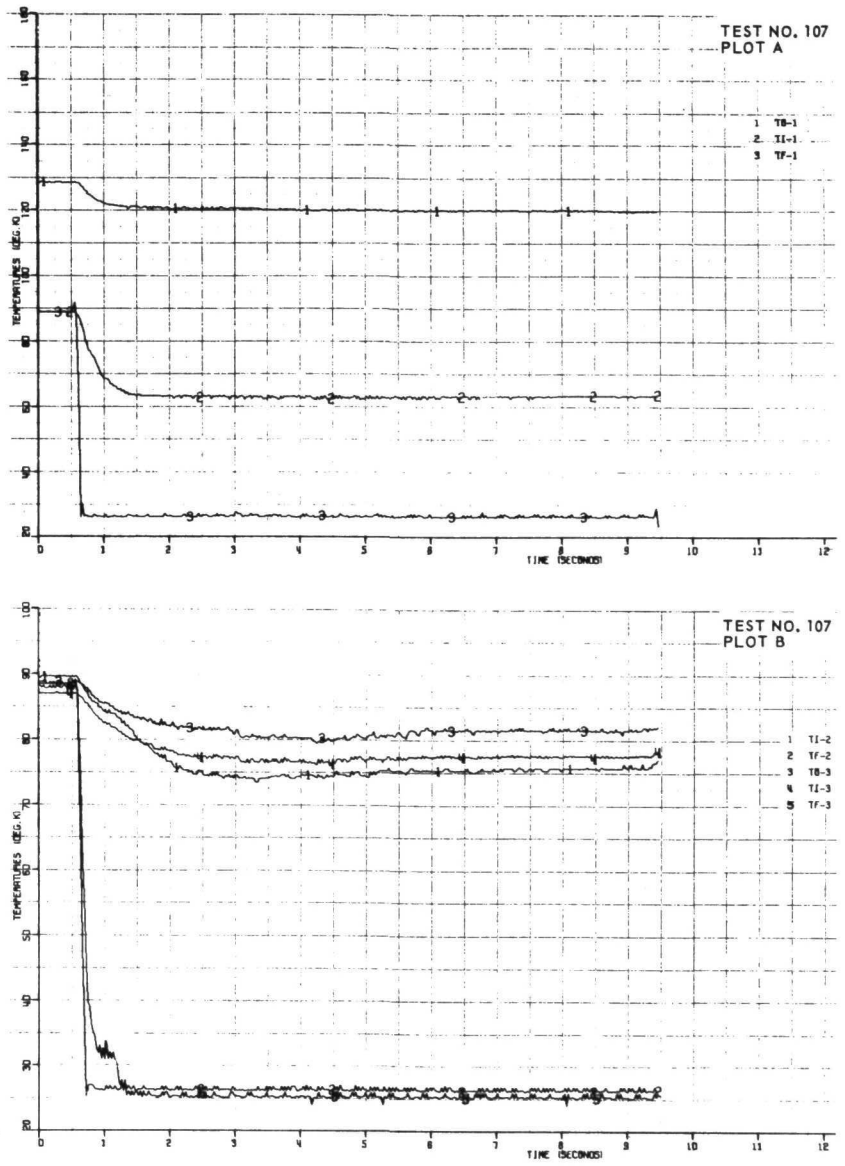

Figure 3-16. Transfer of Liquid Hydrogen Gelled With 17.4 Weight Percent Ethane Through a 4.6 mm I.D. Tube Surrounded by Liquid Nitrogen

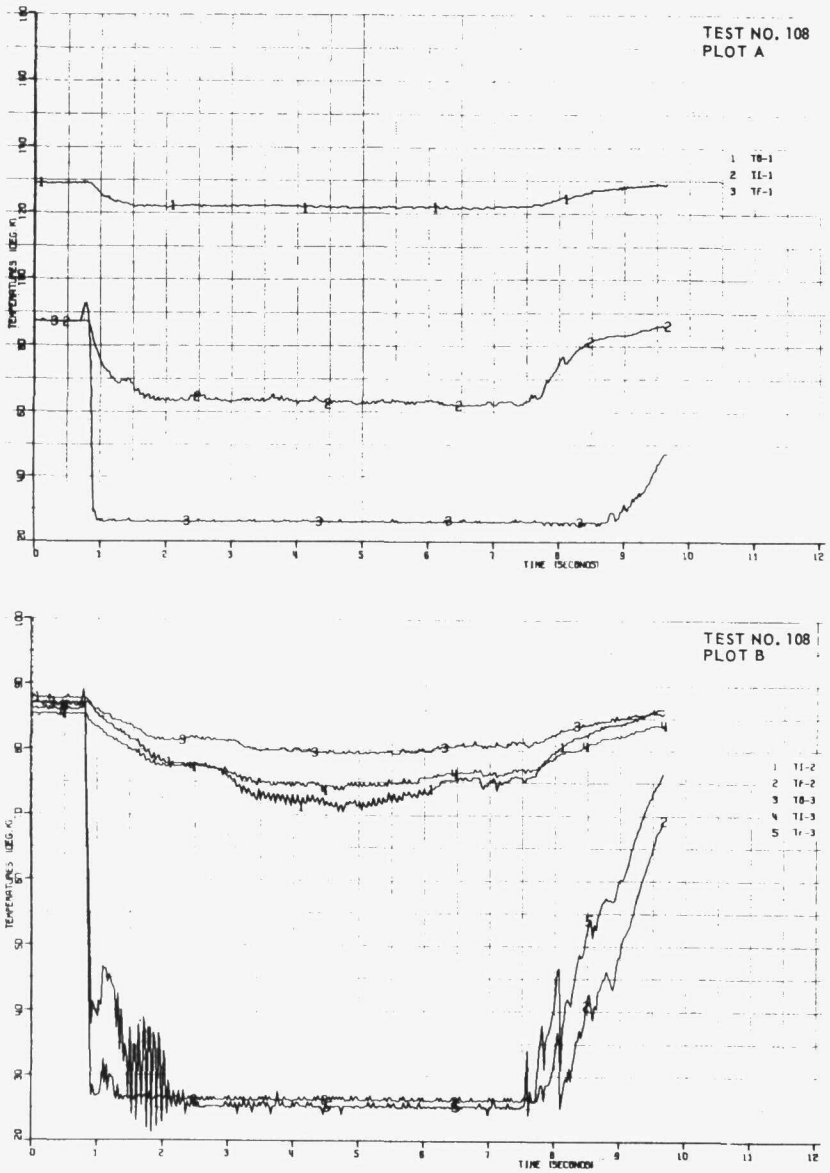

Figure 3-17. Restart of Transfer of Liquid Hydrogen Gelled With 17.4 Weight Percent Ethane Through a 4.6 mm I.D. Tube Surrounded by Liquid Nitrogen

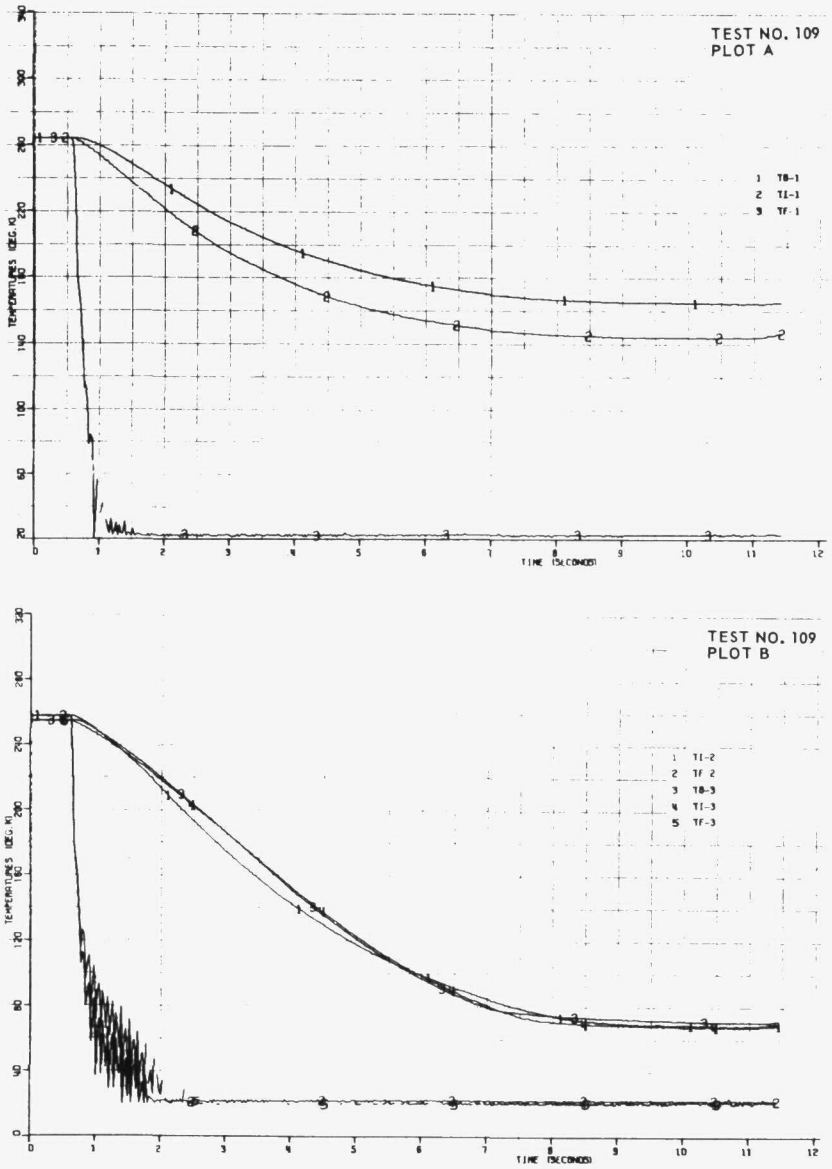

Figure 3-18. Transfer of Neat Liquid Hydrogen Through a 7.0 mm I.D. Tube Surrounded by Gaseous Nitrogen

Test 112 replaced the neat LH_2 with liquid hydrogen gelled with 10.2 weight percent ethane. The temperature profiles are presented in Figure 3-19. The data indicate that with the liquid nitrogen as the heat source and with a gelled liquid hydrogen flowrate of 51.3 cm^3/sec utilizing a driving pressure of 11.2 kN/m^2 (1.63 psi), the gelled liquid hydrogen is expelled with the liquid phase still present. A comparison of the results from Tests 109 and 112 indicates that at a similar driving pressure in the larger tube, the flowrate of the gelled hydrogen is decreased only 13 percent as compared with the neat liquid.

Test 110 involved the expulsion of neat liquid hydrogen through the 7.0 (0.277 in) internal diameter tube with liquid nitrogen flowing through the external jacket. The temperature profiles are shown in Figure 3-20. The data indicate that with liquid nitrogen as the heat source and with a liquid hydrogen flowrate of 70 cm^3/sec utilizing pressure of 7.4 kN/m^2 (1.08 psi), the liquid hydrogen is expelled in the vapor phase at a temperature of 25-26K at the exit. The supply of liquid hydrogen was exhausted after 9.5 seconds as indicated by the temperature increases occurring at that time.

Test 114 was similar to No. 110 except that the neat LH_2 was replaced with liquid hydrogen gelled with 10.2 weight percent ethane. The temperature profiles are shown in Figure 3-21. The data indicate that with liquid nitrogen as the heat source and with a gelled liquid hydrogen flowrate of 58.5 cm^3/sec utilizing a driving pressure of 7.7 kN/m^2 (1.12 psi), the gelled liquid hydrogen is converted to a mixture of gaseous hydrogen and solid ethane with a temperature of approximately 25K at the exit. A comparison of the results from Tests 110 and 114 indicates that at similar driving pressures, the flowrate of gelled liquid hydrogen is decreased only 16 percent as compared to the next liquid.

In summation, the tests demonstrated no difficulty in transferring the gelled material through relatively warm transfer lines. Although the flowrate of the gelled liquid hydrogen is less than that of the neat liquid at the same test conditions, the decrease does not appear to be prohibitive. For liquid hydrogen gelled with a nominal 10 weight percent ethane, the flowrate is decreased 33 percent using the 4.6 mm (0.18 in) tube and approximately 15 percent using the 7.0 mm (0.277 in) tube as compared to the neat liquid. It is also of interest to note that temperatures of the final products expelled from the transfer tubes were essentially the same with the gelled and neat liquids even though the flowrates of the gels were consistently less. This is indicative of less heat transferred to the gel matrix.

3.2 HELIUM SOLUBILITY

Although gelation does not change the solubility limit of a gas in a liquid, the rate of dissolution of the gas in the liquid is significantly reduced. The rate is decreased because the mass transfer within the liquid is limited to a diffusion mechanism. Experiments were conducted to determine the relative rates of dissolution of helium in neat and gelled liquid hydrogen at the normal boiling point of liquid hydrogen.

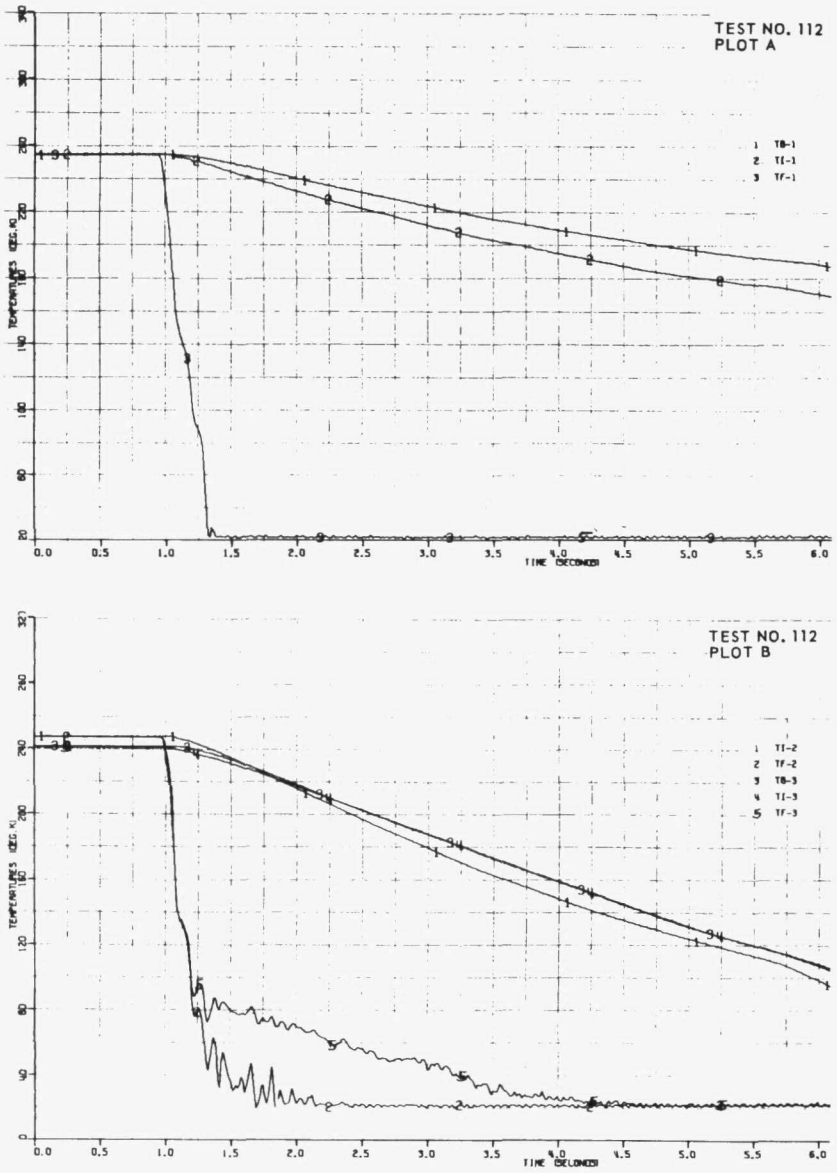

Figure 3-19. Transfer of Liquid Hydrogen Gelled With 10.2 Weight Percent Ethane Through a 7.0 mm I.D. Tube Surrounded by Gaseous Nitrogen

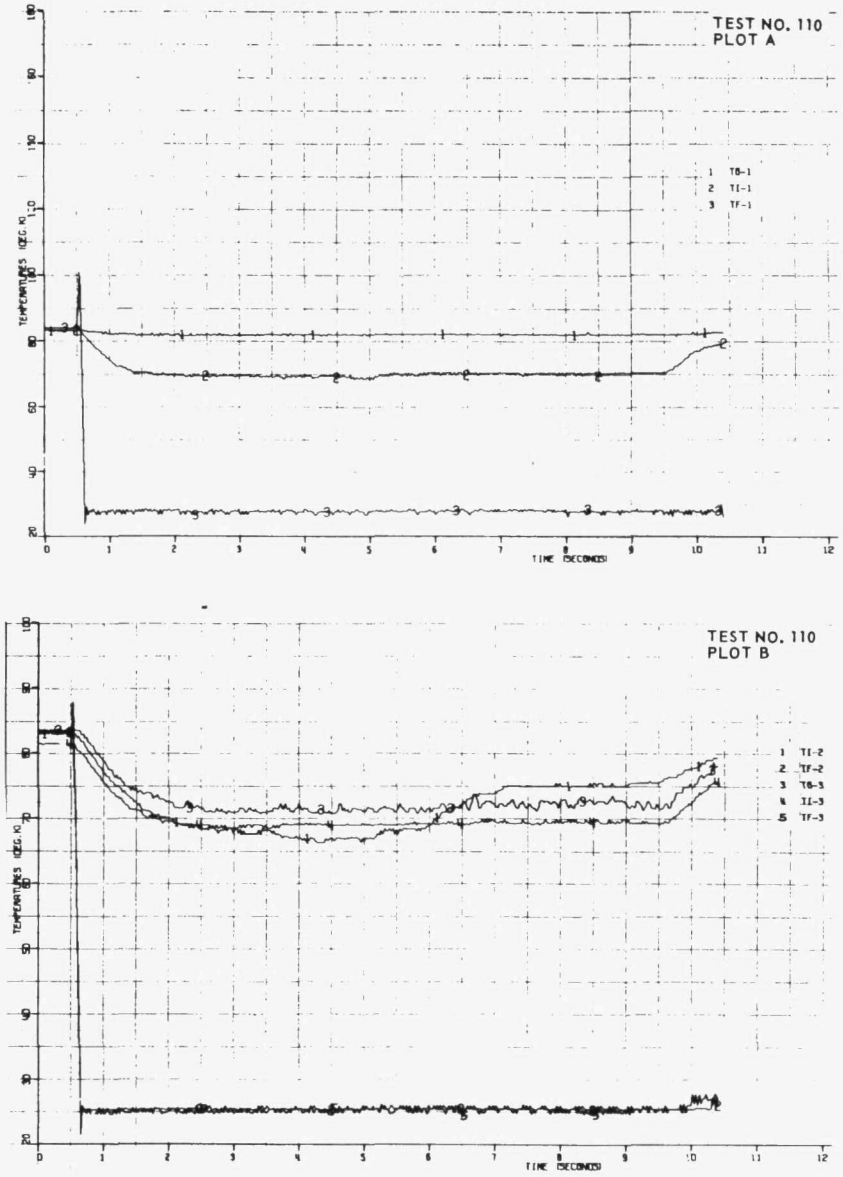

Figure 3-20. Transfer of Neat Liquid Hydrogen Through a 7.0 mm I.D. Tube Surrounded by Liquid Nitrogen

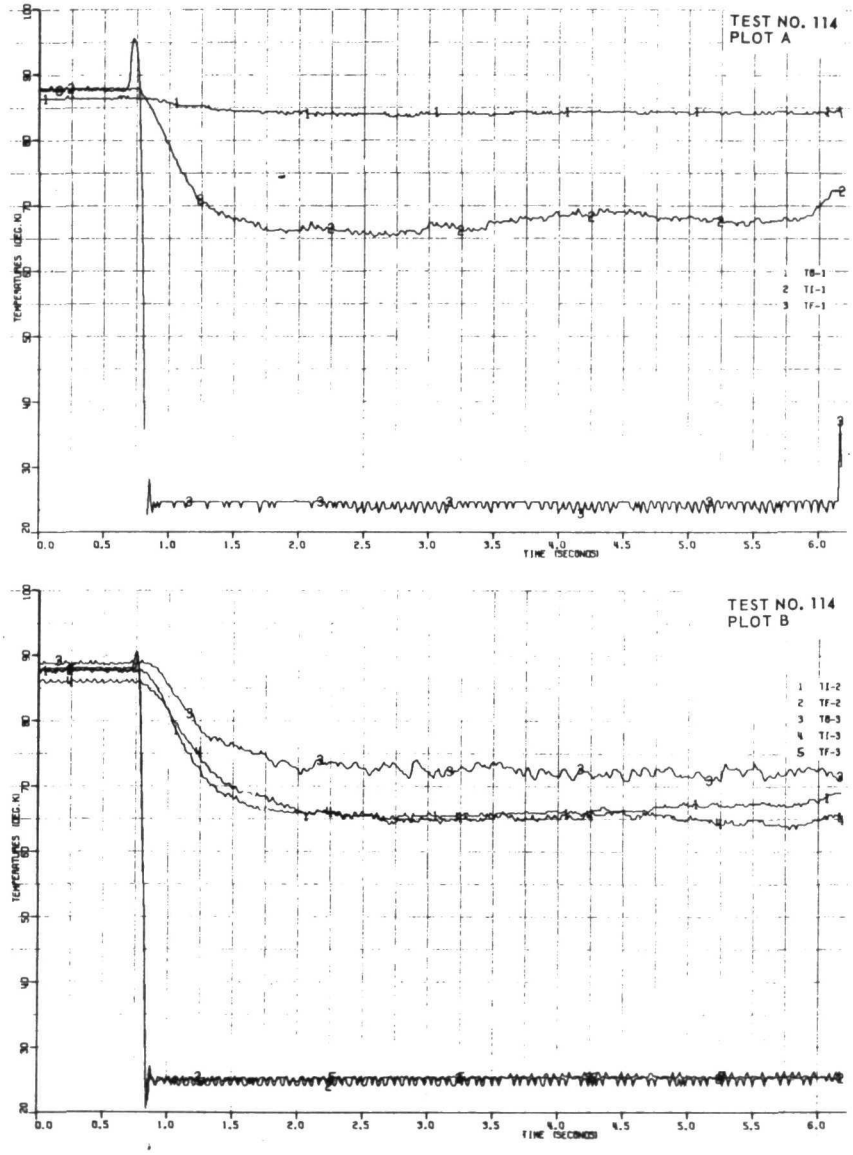

Figure 3-21. Transfer of Liquid Hydrogen Gelled With 10.2 Weight Percent Ethane Through a 7.0 mm I.D. Tube Surrounded by Liquid Hydrogen

The rate of dissolution of helium in liquid hydrogen was determined by measuring the pressure drop of helium in a reservoir connected to a flask which contained a liter of liquid hydrogen. The flask itself (shown in Figure 3-22) was immersed in a liquid hydrogen bath for temperature-conditioning purposes. The pressure was measured with a gauge accurate to within 68.9 N/m^2 (0.01 psi) which corresponded to 4 mg of helium in the reservoir. The partial pressure of helium applied to the liquid hydrogen in the flask was 32.4 kN/m^2 (4.7 psia); the surface area of liquid hydrogen was 62 cm^2 (9.6 in^2). After determining the dissolution rate of helium in the liquid hydrogen during the period of one hour, the same flask was filled with gelled liquid hydrogen and the experiment was repeated. The data are presented in Figure 3-23. The

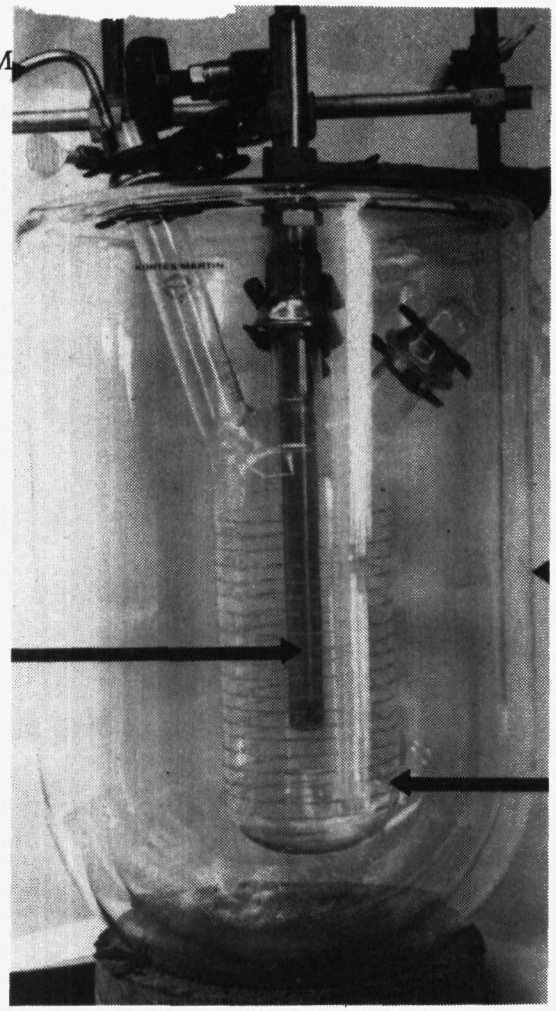

Figure 3-22. Flask Arrangement Used to Measure the Rate of Solubilization of Helium in Liquid Hydrogen

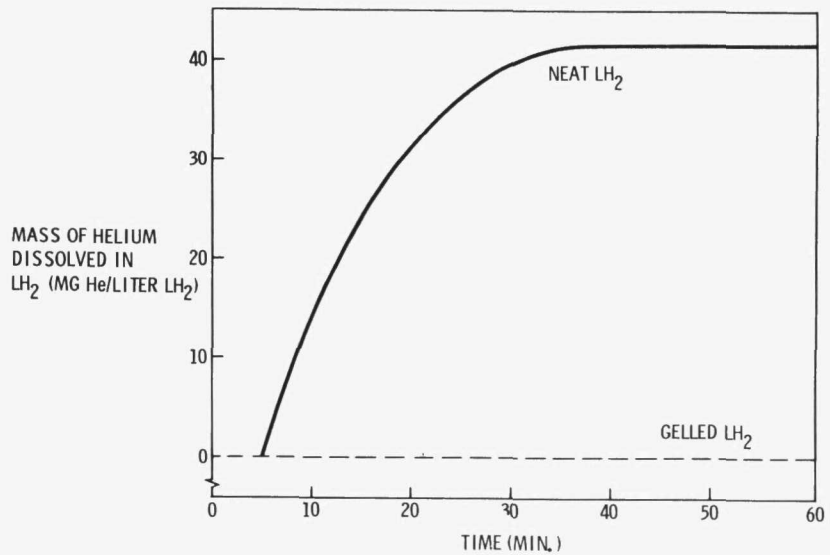

Figure 3-23. Relative Rate of Dissolution of Helium in Neat and Gelled LH_2

significant item to be noted from the data is that no measurable dissolution of helium occurred in the gelled liquid hydrogen, while the neat liquid hydrogen was saturated with helium within 30 minutes after exposure. The gelled liquid hydrogen contained approximately 20 weight percent ethane which produced a very thick gel. As long as the gel structure is present and the convective mechanism is inoperative, variations in the weight percent of ethane would have little effect on the helium dissolution rate.

The gelled liquid hydrogen was then sloshed at a frequency of 2 cycles per second for ten minutes and with sufficient amplitude to cause a ± 2.5 cm ($\pm$ 1.0 in) displacement of the neat liquid hydrogen at the surface. No detectable quantity of helium was absorbed by the gelled liquid hydrogen and the gel surface was not displaced significantly. During the sloshing of the neat liquid hydrogen, no helium absorption was detected. This was most likely due to the fact that the liquid hydrogen was splashing on the slightly warmer top of the flask and sufficient pressure was being generated by the vaporizing hydrogen to prevent helium from flowing through the regulator.

In summation, gelation of liquid hydrogen greatly inhibits the dissolution rate of gaseous helium and also significantly reduces the amplitude of sloshing.

SECTION 4

INTERFACIAL PHENOMENA

A small scale investigation of the relative interfacial phenomena which occur between PPO foam and both neat and gelled liquid hydrogen has been conducted. The compatibility of PPO foam with the ethane gelant and various gross interfacial effects were investigated by Aerojet. Convair Aerospace subsequently performed a detailed analysis and empirical investigation of the relative interfacial effects.

4.1 COMPATIBILITY AND GROSS EFFECTS

As the liquid hydrogen in the gel vaporizes, the ethane gelant remains as a solid residue. After the liquid hydrogen has been removed and as the tank temperature increases, the ethane liquifies before it evaporates. Because it is anticipated that the polyphenylene oxide (PPO) foam may be in contact with the gelled liquid hydrogen for long periods of time, it is essential that the PPO foam be compatible with liquid ethane.

Tests were conducted to demonstrate the compatibility of ethane and PPO foam. To accomplish this, a nominal 2.5 cm (1 in) cube of PPO foam was immersed in liquid ethane for a period of 3 hours at a temperature of approximately 175K (315R) in the apparatus shown in Figure 4-1. The ethane was then distilled off the sample, the sample weighed, and dimensions measured. This cycle was repeated six times. At the conclusion of the tests, there was no significant dimensional change in the PPO foam and no apparent change in the structural integrity of the foam. There was a weight increase of 35 mg but this is attributable to the presence of silicone grease used as a sealant for the glass apparatus in which the experiment was conducted. A photograph of the PPO foam used in the experiment is shown in Figure 4-2; a sample of PPO foam in the as-received condition is also shown in the photograph to facilitate comparison. Based on the experiment, it is apparent that liquid ethane causes no significant, observable alterations in the physical characteristics of PPO foam.

Additional tests were conducted to evaluate the behavior of gelled liquid hydrogen in conract with PPO foam and to obtain a relative indication of the boil-off rate of gelled and neat liquid hydrogen in the presence of the foam.

The vacuum-jacketed glass flask in which the tests were conducted is shown in Figure 4-3. The internal diameter of the flask is 73 mm (2.88 in) and the bottom of the flask was fitted with a 45 mm (1.8 in) thick disc of PPO foam which was bonded in place using Crest 7343 polyurethane adhesive.

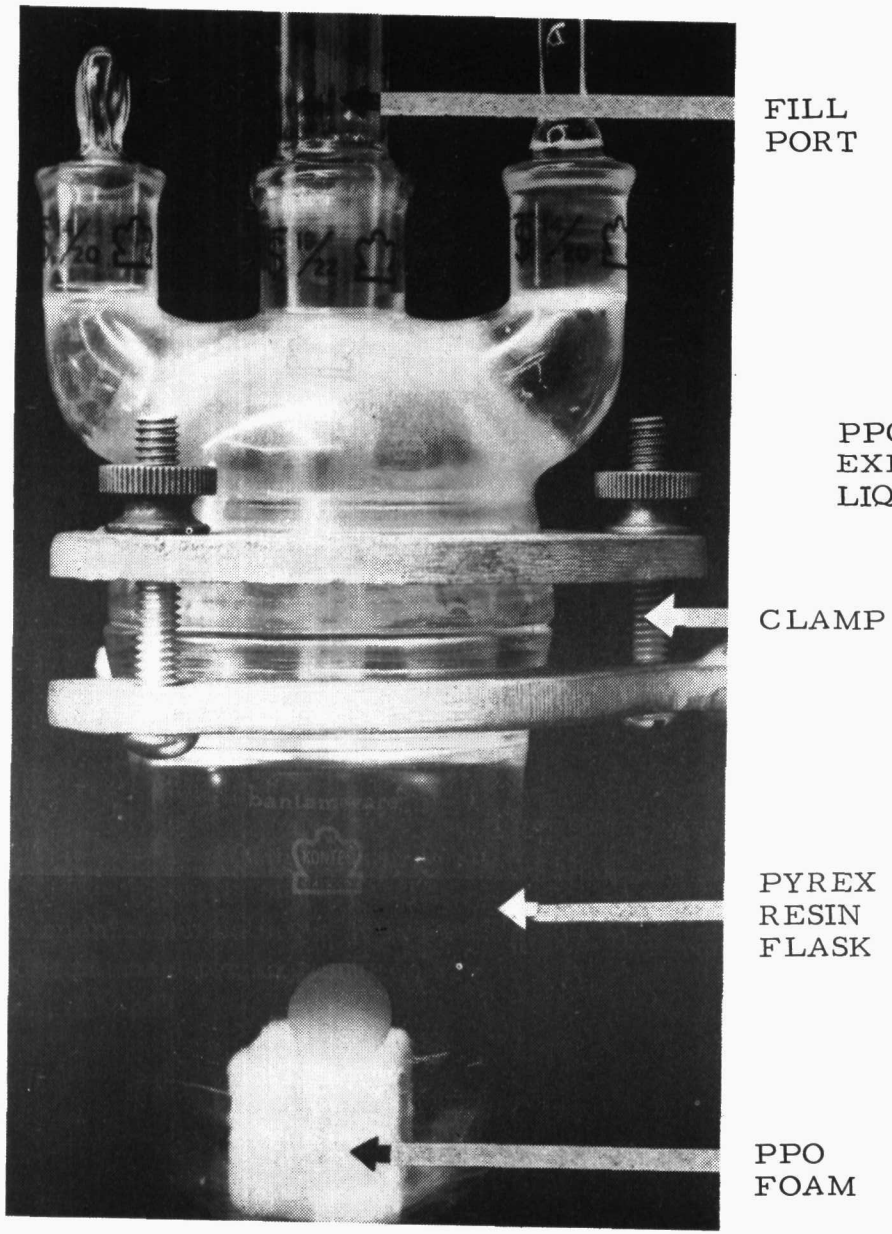

Figure 4-1. Apparatus Used for Immersion Testing of PPO Foam in Liquid Ethane

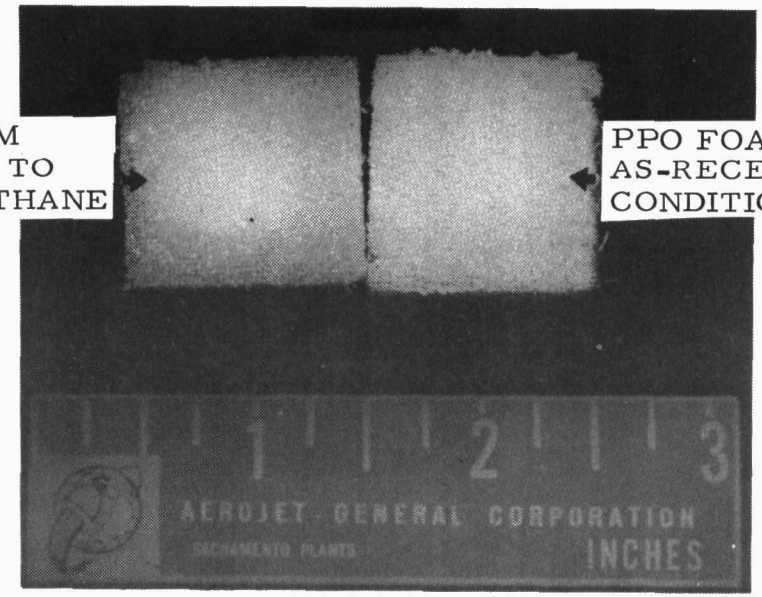

Figure 4-2. PPO Foam Samples in As-Received Condition and After Exposure to Liquid Ethane

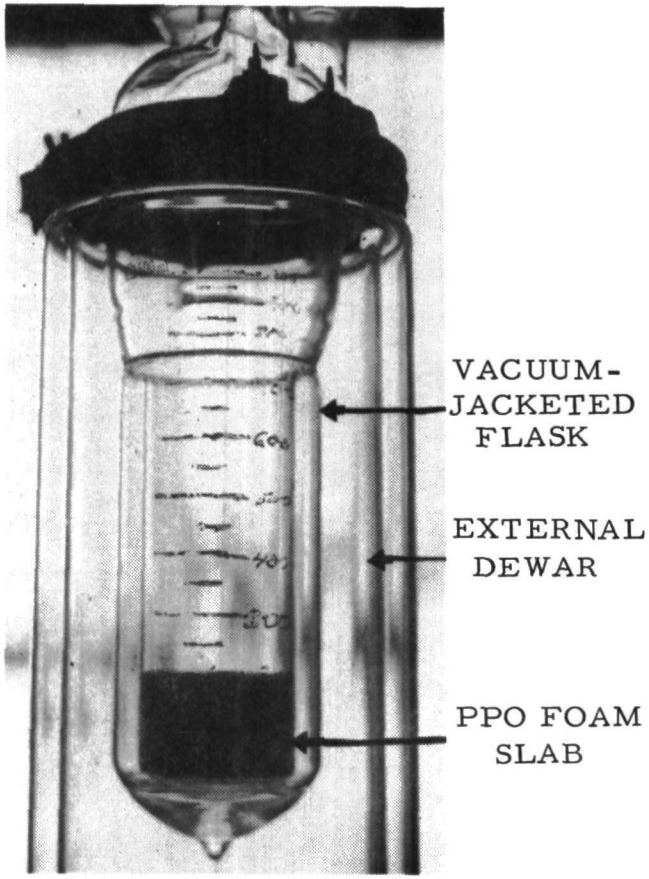

Figure 4-3. Flask for Boil-off Tests With PPO Foam Present

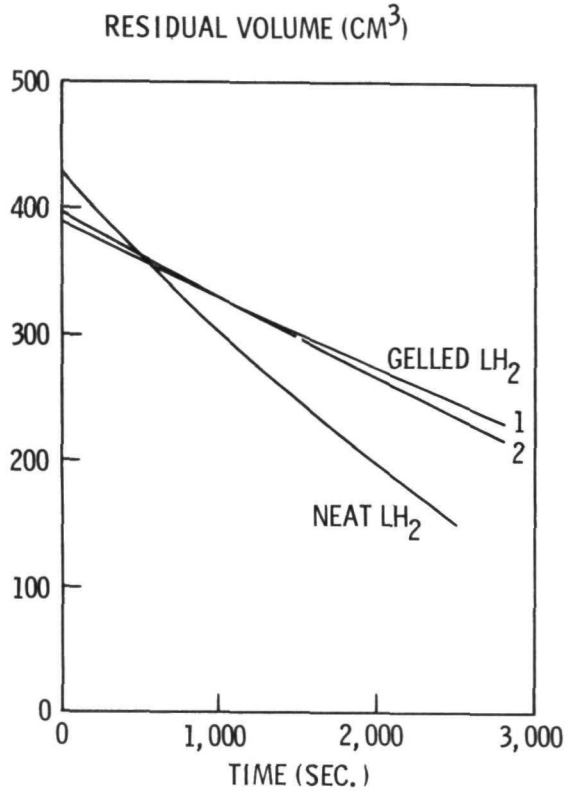

BOILOFF RATE (CM^3/MIN.)

LEVEL	350 CM^3	250 CM^3
NEAT LH_2	7.8	6.3
GELLED LH_2		
1	3.5	3.1
2	4.2	3.6

Figure 4-4. Comparative Boiloff Rates

Two series of tests were conducted in the flask to evaluate any gross effects which may occur at the interfaces. In addition to visual observations, the rates of hydrogen boiloff from the flask were measured and the data are plotted in Figure 4-4. The residual volume of liquid hydrogen in the flask is plotted as a function of time. A comparison of relative boiloff rates at the 350 and 250 cm^3 levels is tabulated. The rate values were obtained from the tangent to the curves at these points. The concentration of ethane in the gelled liquid hydrogen was approximately 13 weight percent. The boiloff rate values are compared at the same volume levels so that the surface areas are similar. The average boiloff rates of the gelled liquid hydrogen are approximately one-half of that of the neat liquid hydrogen under similar conditions.

The following visual observations were also made. With neat liquid hydrogen, the initiation of gas bubbles during boiling occurred primarily at the glass/PPO foam/liquid hydrogen interface. There were relatively few bubbles formed at the PPO foam/liquid hydrogen interface. With the gelled liquid hydrogen, the gas bubbles were again initiated at the glass/PPO foam/liquid hydrogen interface and eventually formed channels along the glass/gel interface. No bubbles were observed to move through the bulk of the gelled liquid hydrogen itself.

The relative boiloff rates of neat liquid hydrogen and gelled liquid hydrogen were also determined without the PPO foam in the apparatus. A vacuum-jacketed glass flask similar to that shown in Figure 4-3 without the PPO foam was used for the experiments. The flask was instrumented with three chromel-alumel thermocouples; one on the outer wall of the vacuum jacket at the 300 cm^3 fiduciary mark, one inside the flask at the 300 cm^3 fiduciary mark, and one positioned in the center of the flask at the 300 cm^3 level. A liquid hydrogen bath was used as the reference junction.

The data again demonstrate a decrease in the boil-off rate with gelation of the liquid hydrogen. At equivalent volumes, the surface areas exposed to the liquid hydrogen are equal and to facilitate comparison, the boiloff rates at the 400 cm^3 level are presented below. The wall surface area at this level is 260 cm^2 (40 in^2).

Wt % Ethane	Average ΔT C(F)	Boiloff Rate cm^3/min
0	170 (306)	0.36
0	190 (342)	0.40
7	150 (270)	0.22
14	170 (306)	0.26

With the same average temperature differential across the vacuum-jacketed flask, gelation decreased the boiloff rate by 28 percent. The quantity of gelant present does not appear to significantly change the boiloff rate as long as there is sufficient gelant to produce structure. An attempt was made to document the boiloff of hydrogen from gelled liquid hydrogen photographically. Unfortunately, a slight powdery residue of solid ethane adhering to the flask walls prevented a clear delineation of the gel level in the photographs.

4.2 INTERFACIAL EFFECTS

A facility for investigating the characteristics of the LH_2/PPO and gel/PPO interfaces was developed and tests were conducted. An analysis of the characteristics of the interfaces has been performed and correlated with test data.

4.2.1 INTERFACE TEST APPARATUS. The large facility used to produce gelled liquid hydrogen was modified to include a small scale setup to more conveniently investigate detailed LH_2/PPO and gel/PPO interfacial effects. For this investigation the emphasis was on visual observation of phenomena; thus a transparent apparatus was fabricated similar to that used by Aerojet. A schematic of the test facility is shown in Figure 4-5. A large purge box, approximately one cubic meter in volume, was fabricated with two opposing sides being large, bolt-on Plexiglas windows. The box was purged continuously with gaseous helium while testing was in progres to prevent air entry and water vapor condensation. A large, 0.020 m^3 (5.39 gal) dewar was mounted in the purge box and filled with LH_2 to thermally guard the test container. The latter was a 30.5 cm (12 in.) long, 17.8 cm (7 in.) diameter section of clear acrylic tubing which contained the test specimen (Figure 4-6). The test specimen assembly consisted of a heater assembly sandwiched between a 2.3 cm (0.9 in.) thick disk of test foam and a 6.9 cm (2.7 in.) thick guard foam disk. The heater assembly consisted of a circular, 10.2 cm (4 in.) diameter test heater surrounded by a 3.5 cm (1.375 in.) wide annular guard heater. The two heaters were independently powered, the function of the guard heater being to minimize radial heat losses from the test heater to the LH_2 in the guard dewar. A total of nine Chromel-Constantan thermocouples were installed at strategic locations within the specimen assembly to measure temperature profiles. The temperatures, heater volts and amps, and the container ullage pressure were recorded on tape by a Dymec data acquisition system. The location of the interface test apparatus with respect to the large gel production facility is shown in Figure 4-7.

Rather than produce gel using the large-scale facility and transfer it to the interface test facility, the gelant injection tube was mounted directly in the test container (Figure 4-8) and gel was produced over the test foam as needed. Flow parameters similar to those described in Section 2 were employed for gel production. In eight minutes time approximately 2 m(m^3) (0.6 gal) of gel was produced for evaluation (Figure 4-9). This apparatus was used to measure relative temperature profiles in the foam for the two propellants as a function of source heat flux, and to investigate relative gas layer stability, bubble formation, and bubble motion for the two systems. Attempts to measure LH_2 boiloff from the test container were unsuccessful due to gas leakage around the cryogenic seal isolating the test container from the guard dewar. Prior to testing a detailed analysis of the interfacial phenomena was performed.

4.2.2 INTERFACE ANALYSIS. PPO foam, as a open cell-gas layer insulation, must maintain a stable vapor barrier between the propellant and the tank wall under all likely heating and acceleration conditions. For this to occur, a stable interface must exist in each cell. Stability means that forces contributing to a stable interface are

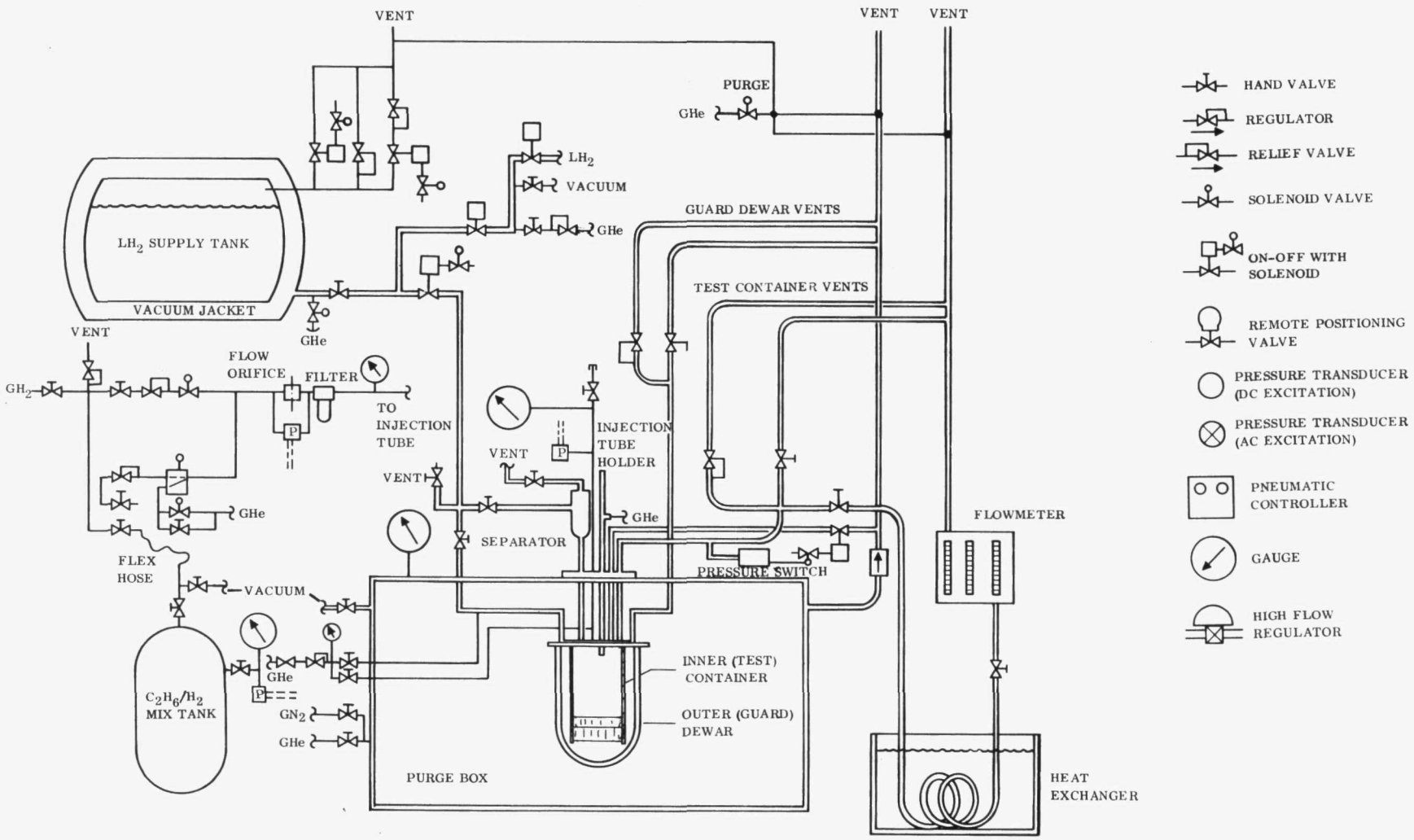

Figure 4-5 Interface Test Facility Schematic

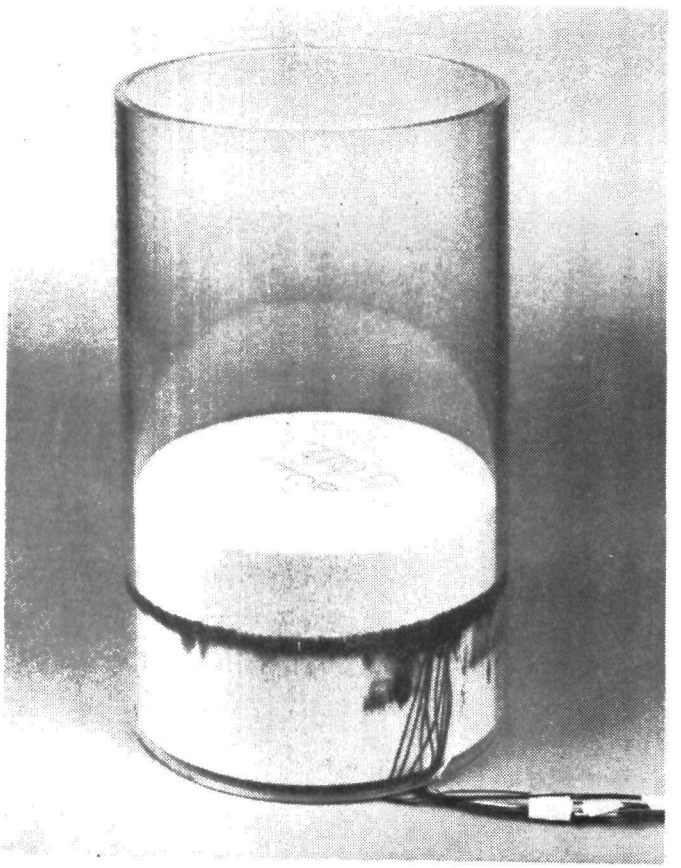

Figure 4-6. Interface Test Apparatus

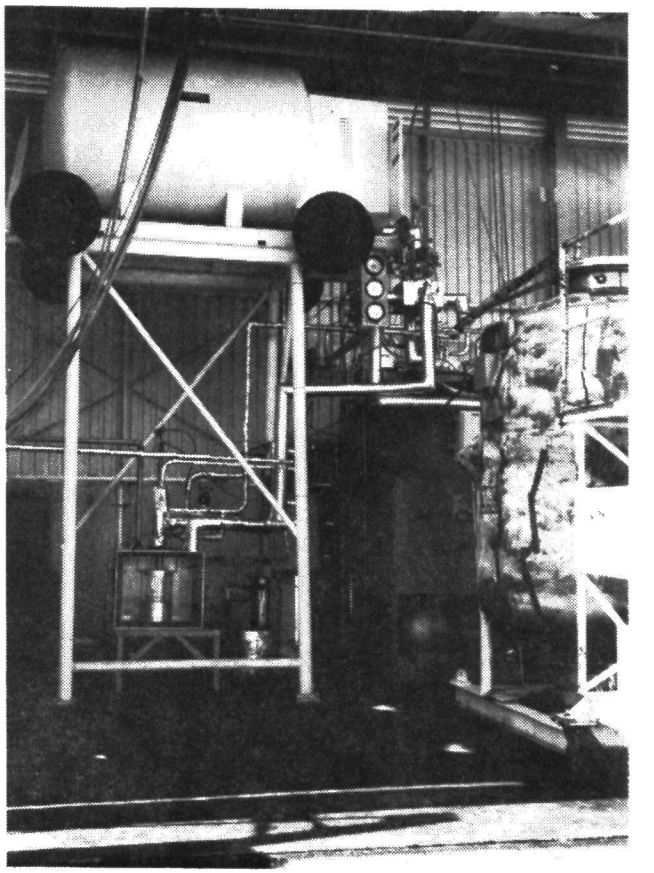

Figure 4-7. Interface Test Facility

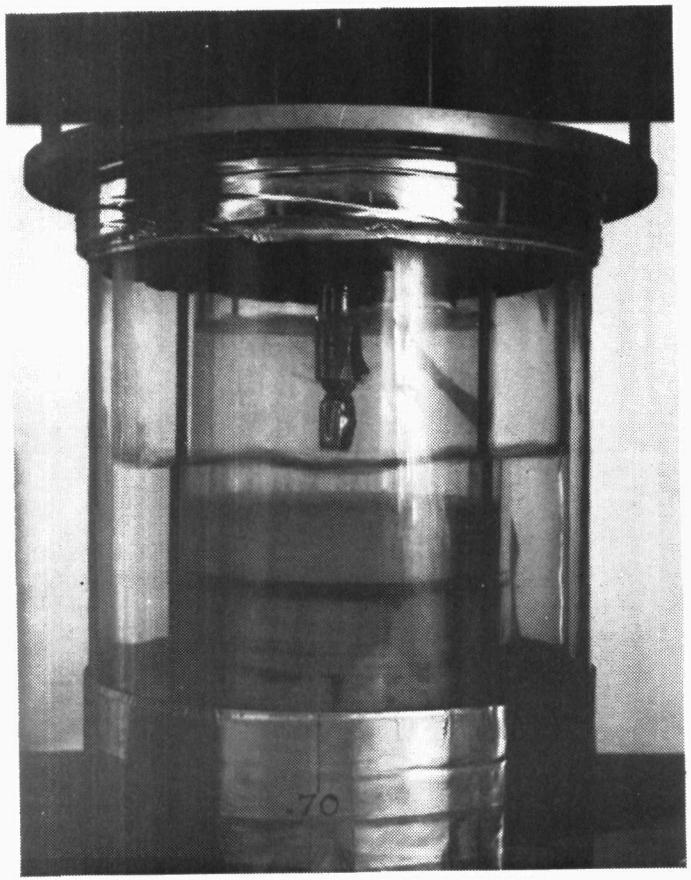

Figure 4-8. Liquid Hydrogen in Test Container

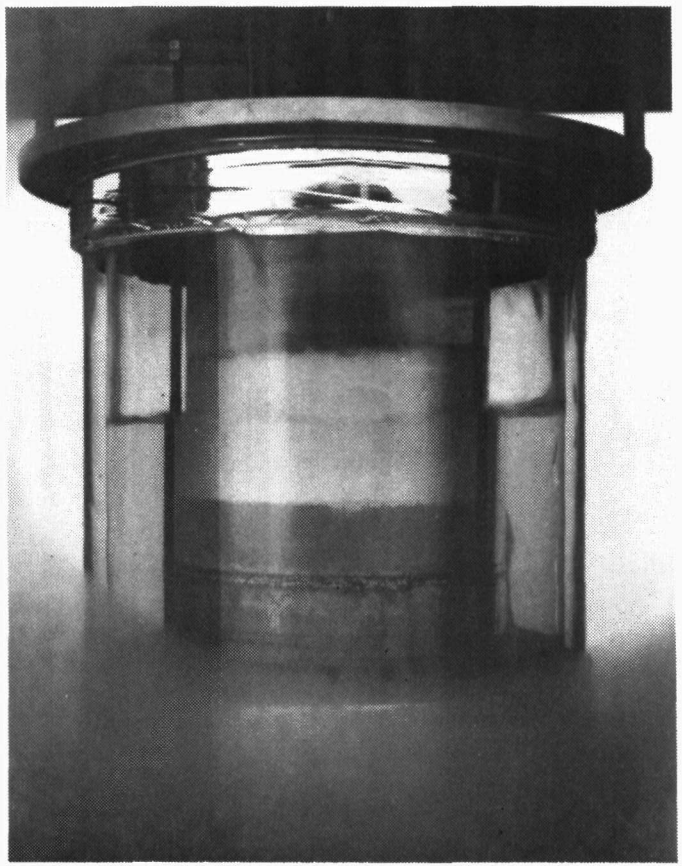

Figure 4-9. Gel in Test Container

sufficient to overcome the forces tending to make the interface unstable. For an open cell insulation,the cohesive force is a result of surface energy while the destabilizing force is characteristically caused by gravitational acceleration. The non-dimensional Bond number, the ratio of acceleration forces to surface tension forces, may be used to differentiate between stable and unstable liquid vapor interfaces. Figure 4-10 illustrates a liquid/vapor interface in an idealized right circular cylindrical cell. The Bond number (Bo) = $\rho g R^2/\sigma$ is less than the critical value of 0.84 (Ref. 18), thus the interface is surface tension stabilized. Here ρ is the liquid density, R is the cell radius, and σ is the liquid surface tension. Vapor pressure supports the interface. This condition is expressed as

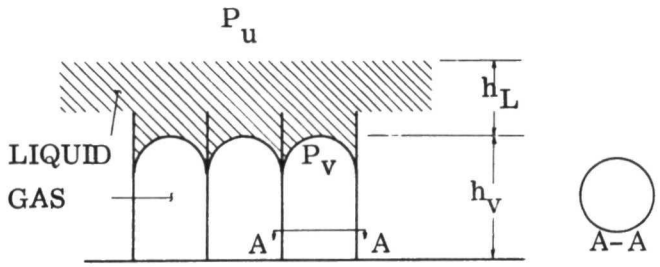

Figure 4-10. Interface Stability in a Circular Cylindrical Cell

$$P_v = P_u + \rho g h_L + 2\sigma/R \qquad (1)$$

where P_v is the vapor pressure in the cell, P_u the ullage pressure and h_L the liquid head.

Bubble point testing was used in a Convair IRAD program (Ref. 19) to determine PPO foam cell size and frequency distribution. This determination indicated that the largest cell size was 172 to 205 μm (0.0068 to 0.0081 in.) for the samples tested. These cell sizes are well below the anticipated diameter needed for surface tension stability. For example, for cells of this size the Bond number for LH_2 will be approximately 0.01 which is well below the anticipated stability limit for PPO foam. To evaluate the stability limit of PPO foam, high "g" testing is required since fluids with ρ/σ high enough to give an unstable Bond number at normal gravity do not exist. For a Bond number stability limit of 0.10, LH_2 will have a stable liquid/vapor interface in PPO foam at approximately 40 g's. Since this stability limit is well in excess of anticipated vehicle requirements, plans have not been made to determine the exact stability limits of PPO foam.

The liquid/vapor interface in each cell is pressure supported and surface tension stabilized. If a condition occurs which will not allow the cell to hold pressure, such as a leak, the interface will no longer be supported by pressure and liquid will reach the bottom of the cell since both surface tension (for a wetting fluid) and hydrostatic forces are acting in the same direction. The liquid penetration to the tank wall will cause a large increase in heat transfer directly to the boiling LH_2. With a stable vapor barrier, heat transfer in a cell depends upon convection within the cell. Convection depends upon cell size, insulation and vapor barrier thickness and flow patterns within the insulation. From the standpoint of convection as well as interface stability and support it is desirable not to have interconnections between adjacent

PPO foam cells. Uniform minimum density consistent with no cell interconnections will yield the minimum thermal conductivity possible with PPO foam.

Referring again to Figure 4-10 and Equation 1, the distance h_V, determined by the vapor volume needed to produce a pressure P_V in the cell, is a function of the liquid head and the cell size. As the tank wall is heated, liquid is evaporated at the interface and mass is added to the vapor barrier. To retain the pressure balance, with simultaneous addition of heat and mass, it is necessary to expand the vapor volume. Since h_L has been slightly reduced, a corresponding reduction in cell pressure will occur. When the liquid is forced to the top of the cell the vapor in the cell continues to expand as shown in Figure 4-11 due to evaporation and temperature rise. In Equation 1 the terms $\rho g h_L$, $2\sigma/R$, and P_V decrease as the vapor expands until the bubble breaks off. After the bubble departs P_V should rise due to the smaller R and the larger h_L.

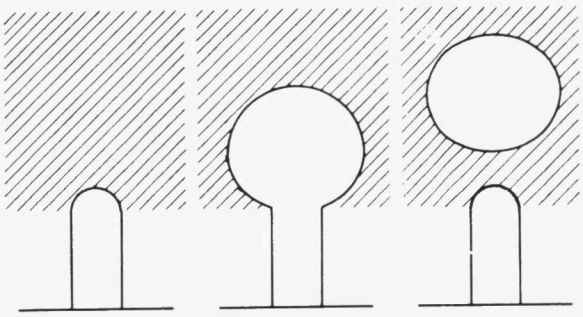

Figure 4-11. Stages of Growth of Bubble in a Stable Gas Layer

Bubbles break off when the buoyancy and pressure forces exceed the surface forces holding the bubble to the cell. For bubbles growing at a rapid rate, inertial forces are also important. The only force opposing bubble departure is the surface force.

Bubble growth and detachment flows of interest fall into two general regimes determined by the flow rate. The low flow regime is characterized by a constant bubble volume leaving the surface. The bubble size is determined by the balance between surface and buoyancy forces;

$$(\rho_L - \rho_V)\, V_b = \pi D_o \sigma \qquad (2)$$

where ρ_L is the liquid density, ρ_V is the vapor density, V_b is the bubble volume acted on by buoyancy forces (i.e., the bubble volume which has liquid below it), and D_o is the orifice or cell diameter. At higher flows the dynamic forces become significant with a maximum bubble departure frequency being reached. Beyond this point, the bubble volume increases linearly with flow rate. There are other regimes of flow as the flow rate is increased, but these are of no interest for this application.

The initial determination which must be made is the regime of operation. Hughes, et. al. (Ref. 20) suggests that a Reynolds number (Re) of 1 is the transition point where

$$Re = \bar{q}\, \rho_L / (\pi D_B \mu_L)$$

where $\bar{q}$ is the average volumetric flow of vapor, μ_L the liquid viscosity, and D_B the diameter of a spherical bubble volume at departure. For relatively inviscid fluids,

L'Ecuyer and Murthy (Ref. 21) indicate that a volumetric flow rate corresponding to

$$\bar{q} \geq 28\, a^{1/2}\, R_o^{5/2} \tag{3}$$

represents the transition flow rate, where a is the acceleration and R_o is the orifice radius, or in this case, the cell radius.

In order to apply three transition criteria, the mass rate of vapor generated in the insulation was approximated as $\dot{m} = \dot{m}_{vapor\ generated} = (\dot{Q}/A\ A_{cell})/h_{fg}$. Under relatively constant pressure and temperature conditions the equation becomes $\dot{m} = (\dot{Q}/A\ \pi\ R_o^2)/h_{fg}$, where $\dot{Q}/A$ is the heat flux per unit area at the cell of interest, R_o is the cell radius and h_{fg} is the heat of vaporization of the fluid. The volume generated is given by

$$q = \dot{m}/\rho_v = (\dot{Q}/A\ A_{cell})/(\rho_v\ h_{fg})$$

The cell area, A_{cell}, is related to the bubble diameter at breakoff by Equation 2, where for a spherical bubble

$$V_B = \frac{\pi D_b^3}{6} = \frac{\pi D_o\ \sigma}{\rho_L - \rho_v} + \frac{\pi D_o^2\ D_b}{4} \tag{4}$$

where D_o is the cell diameter assuming a circular cell, and D_b is the bubble diameter. The term $(\pi D_o^2\ D_b)/4$ is the bubble volume directly over the cell and thus does not contribute to the buoyancy force. Equation 4 may be solved for the cell diameter D_o yielding the surface area subjected to heating, $(\pi D_o^2)/4$. The applicable flow equation for a circular cell with impervious side walls is

$$q = \frac{\frac{\dot{Q}}{A}\ \frac{\pi D_o^2}{4}}{\rho_v\ \lambda} \tag{5}$$

Since cell walls are not impervious, some modification must be made to this equation. As can be seen from Equation 1, small cells will have higher internal pressures than large cells. As shown in a previous study (Ref. 19) interconnections exist which allow circulation to occur between cells. This will cause flow to occur between cells, with larger cells having a greater tendency to eject bubbles than small cells. Since the heat flux generating departing bubbles in a large cell is dependent upon the vapor being generated in small cells as well, Equation 5 must be modified. Since knowledge of cell size variation and interconnections is not available, this will be expressed as

$$q = \frac{C_1\ (\dot{Q}/A\ \pi\ D_o^2)^N}{4\ \rho_v\ \lambda}$$

where C_1 and N are constants to be evaluated from the data.

This equation can be made more useful for data correlation purposes by substituting $q = fV_b$ where f is the frequency of bubbles departing in bubbles/sec and V_b is bubble volume

$$V_b = \frac{\pi D_b^3}{6}$$

and

$$f = \frac{C_1 (\dot{Q}/A \ \pi D_o^2)^N}{4\rho_v \lambda \pi (D_b^3/6)} \tag{6}$$

After departure the bubble rises through the fluid. The flow and heat transfer during bubble rise will affect temperature stratification in the liquid. The flow of bubbles rising in a liquid is characterized by four flow regions (Ref. 22), discussed in order of increasing Reynolds number. In Region 1, spherical bubbles rise under the influence of buoyancy and viscous forces, according to the equation $U = 2R_B^2 (\rho_L - \rho_v) g/9\mu_L$, where U is the rise velocity. At Re > 2 the drag forces predominate over the viscous forces, bubbles become flattened spheroids, and $U = 0.33 g^{0.76} (\rho_L/\mu_L)^{0.52} R_B^{1.28}$ in Region 2 up to a Reynolds number limit which is a function of the fluid properties. For Region 3 the bubbles become deformed ellipsoids flattened horizontally rising spirally through the liquid, and $U = 1.35 [\sigma g_c/(\rho_L R_B)]^{1/2}$ with Reynolds number limits determined by fluid and geometric properties. For Region 4 in which mushroom-like bubbles occur; $U = 1.18 (\sigma g g_c/\rho_L)^{0.25}$. Ref. 23 indicates that bubble rise terminal velocity will be reached in less than 2.5 cm (1.0 in.). Peebles and Garber, Ref. 22, assumed transients would be eliminated after 15 cm (6 in.).

Gelled Liquid Hydrogen

Gels are colloids having two distinct phases with a definite separation between each liquid and solid particle (Ref. 24). Gels generally behave as elastic solids and retain their shape whereas sols behave as liquids by possessing the shape of the container. LH_2 gels display the "thixotropic" characteristic evidenced by transformation into sols upon being agitated or subjected to shear stress sufficient to produce motion. The sol sets into the gel form if allowed to stand. One theory of gelation is that solid particles unite to form chains or fibrils which become interlocked, increasing system viscosity and forming a semi-solid. More important perhaps are the high capillary forces holding the liquid between the fibrils. It has been estimated from vapor pressure measurements that small pools of liquid between the fibrils have diameters on the order of 5 nm. This would be more than sufficient to cause capillary effects to control the liquid. Gels may also be categorized as elastic or inelastic. The elastic gels retain their solid structure upon drying while the inelastic gels become glassy, fall to a powder and lose their elasticity. This property can have considerable importance in the maintenance of a stable liquid/vapor interface with LH_2 gel and PPO foam and will be considered in more detail in the following paragraphs.

Initially it was assumed that the solid matrix would breakdown, and the resulting fluid mechanics and heat transfer were evaluated on this basis. With the solid matrix breaking down, all the ethane above the cell could collapse into it. Based on the gelant concentration and vapor generation rates anticipated, the solid buildup for the largest cell was computed as a function of time. These calculations indicated that the ethane would quickly predominate as the major constituent in the foam and an ethane liquid/vapor interface could form at the top of the foam with solid ethane just above the liquid. The relative heat transfer of this configuration compared to a neat LH_2 vapor barrier is too difficult to predict without a thermal network being set up to determine evaporation/liquefaction, melting/freezing, gas conductivity and LH_2/ethane heat transfer. It appears, however, that boiloff would be lower with the gel than with the neat LH_2 due mainly to the much lower conductivity of ethane vapor compared to that of hydrogen vapor.

If the solid matrix does not break down, the ethane will remain intact and the LH_2 will vaporize causing a liquid/vapor interface to form. Some small ethane concentration may initially be present in the cell, however, this will tend to affect only the initial transient behavior. Considering the bubbles forming at the foam with the stable solid matrix, bubble breakoff in Region 1 is determined by the balance of surface forces and buoyancy forces. Since the medium is more dense, the buoyancy force, $F_b = V_B (\rho_L - \rho_v)$ will be larger for the gelled LH_2 than it will be for the neat LH_2. This will be approximately a 10 percent increase in the force tending to detach the bubble from the foam. The increase of surface forces holding the bubble on the foam will be much greater. This is caused by the additional solid surface present in the form of the solid ethane matrix. The surface force is $F_S = \Sigma \sigma L$ where L is the length of the liquid/solid interface. The length of the liquid hydrogen/solid ethane interface must be added to the length of the liquid/PPO foam interface to determine the total surface force. The surface force may actually be increasing faster than the buoyancy force as the bubble size increases. This would tend to capture vapor near the foam by not permitting the bubbles to rise. Examination of test results should give an indication of the relative increase between surface forces and buoyancy forces by measuring the size of any bubbles which do escape from the foam.

The vapor forming at the surface of the foam may tend to spread over the surface causing a vapor layer to form under the gel bulk. This could occur due to the vapor being trapped by the high surface forces and could be accentuated by the possibility of a lower ethane concentration occurring near the foam surface than at a short distance away due to incomplete mixing during the gelation process. This would tend to produce a coarser solid matrix near the foam with correspondingly lower surface forces. The vapor could thus move more freely through the large pores near the foam than it could some distance away from it. If a vapor barrier forms over the foam, buoyancy forces will be negligible since no liquid exists under the vapor buoying it upward. The vapor generated, for a given heat flux level, will be similar to that generated for the neat LH_2. If vapor does leave the surface, the bubble departure should be in the constant volume regime, as with LH_2, since the growth Reynolds number will decrease, if

anything, due to higher viscosity. If bubbles do break off they will be larger than bubbles leaving the neat LH_2/foam surface. The rise velocity will be relatively lower since the increase in viscous forces (by a factor of 2 to 4) and drag forces is likely to exceed the small increase in buoyancy forces.

As indicated, the relative heat transfer with gel and neat LH_2 is dependent, among other things, on whether a stable structure of ethane gelant can be maintained when LH_2 is evaporated from the matrix. In any case, however, the heat transfer will be reduced. For the stable matrix, for example, reduced departure rates will produce less convective flow in the cells with heat transfer approaching that due to gas conduction. If vapor is trapped by the gel structure, heat transfer will be reduced further by the additional vapor barrier distance between the gel and tank wall. For the nonstable structure, the reduced conductivity of the ethane in the cells, compared to that of GH_2 should be sufficient to counteract the reduced temperature difference producing a net reduction in heat transfer. Thus a net reduction in boiloff with gelled LH_2 compared to neat LH_2 would be expected.

4.2.3 EXPERIMENTAL RESULTS. Motion pictures of bubble growth, departure and rise in neat and gelled LH_2 were taken at several camera speeds. The photographs were analyzed frame by frame using a Vanguard Motion Analyzer. Data were obtained in terms of bubble departure diameter vs interval between departures at a given site, and bubble rise velocity vs bubble diameter for both neat and gelled liquid hydrogen. Reduced data are shown in Table 9.

Initial inspection of the data shows that bubble diameters at breakoff from the foam were significantly greater in gelled LH_2 than in neat LH_2. Assuming that the bubbles tabulated represent an average cross section of bubbles, bubble diameter in the gel system averaged 3.45 mm (0.136 in.) while bubbles in the neat system had an average diameter of 1.25 mm (0.494 in.) at breakoff. Using the neat system bubble diameter in Equation 4, an average diameter of cells ejecting bubbles of 101 μm (0.00396 in.) is obtained, a value less than a tenth of the bubble diameter. Using this cell diameter and the average gel system bubble diameter, and solving Equation 4 for the surface force indicates that the surface forces are approximately 25 times greater in the gelled LH_2 system than they are in the neat LH_2 system. It should be noted here that bubbles in the gel could only be observed at the wall of the container because of the opacity of the gel. Since bubble sites at the foam surface could not be seen in the gel, no direct comparison is possible between individual gel sites and LH_2 sites. Bubbles in the gel were generally observed to appear several centimeters above the foam surface, apparently travelling laterally as well as vertically through the gel. Another point to note is that the few gel bubble sites observed appeared immediately with no additional sites occurring once gelation had occurred. This indicates bubble paths are formed during gelation. For the neat system, bubbles had a spherical shape and uniform volume at a given site with a $Re < 1$ which is in the constant volume regime, as assumed in Equation 2.

Bubble departure interval is plotted vs bubble diameter in Figure 4-12 for both gelled and neat LH_2. Nucleate boiling correlations are plotted to indicate the lack of correlation between the data and these models. Considerable scatter exists in the data

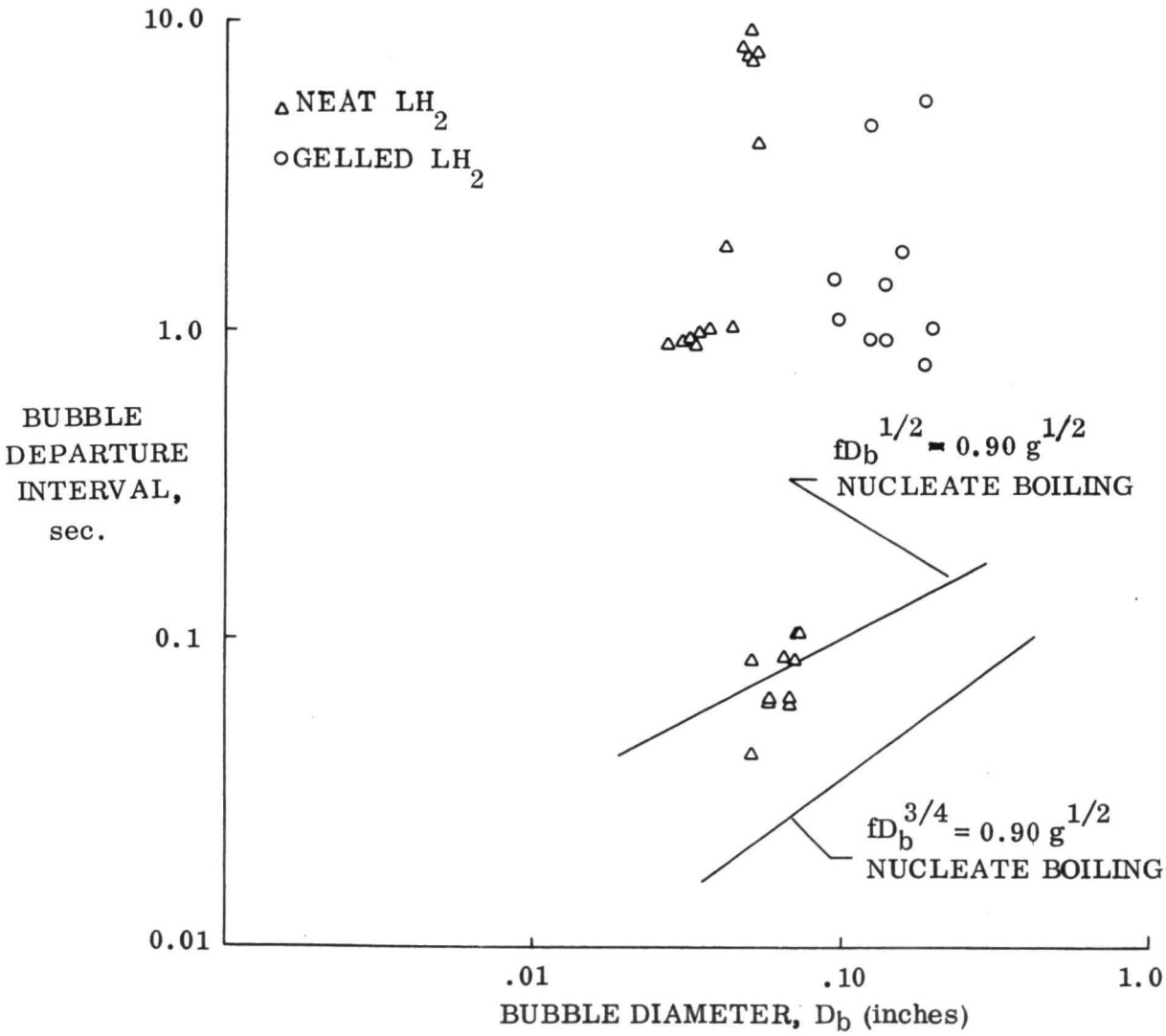

Figure 4-12. Neat and Gelled LH_2 Bubble Departure Time and Departure Diameter

Table 9. Interface Effects Test Bubble Data

	Bubble Dia. mm (in.)		Frequency (bubbles per sec)	Bubble Dia. mm (in.)		Rise Velocity cm/sec (ft/sec)	
Neat Liquid Hydrogen	1.3	(.051)	12.0	1.47	(0.058)	16.15	(0.53)
	1.5	(.058)	16.0	1.47	(0.058)	20.21	(0.663)
	1.07	(.042)	0.55	1.47	(0.058)	15.70	(0.515)
	0.86	(.034)	1.04	1.35	(0.053)	39.62	(1.30)
	0.81	(.032)	1.09	1.12	(0.044)	46.33	(1.52)
	0.84	(.033)	1.12	1.07	(0.042)	13.72	(0.45)
	0.97	(.038)	1.02	1.07	(0.042)	20.42	(0.67)
	0.76	(.030)	1.09				
	0.94	(0.37)	1.00				
	0.69	(.027)	1.12				
	1.12	(.044)	1.00				
	1.73	(.068)	15.87				
	1.85	(.073)	9.62				
	1.78	(.070)	11.76				
	1.80	(.071)	9.62				
	1.65	(.065)	11.76				
	1.30	(.051)	23.81				
	1.47	(.058)	15.87				
	1.73	(.068)	15.87				
	1.19	(.047)	0.25				
	1.35	(.053)	0.24				
	1.27	(.050)	0.23				
	1.30	(.051)	0.109				
	1.24	(.049)	0.135				
	1.35	(.053)	0.129				
	1.30	(.051)	0.128				
	1.20	(.047)	0.124				
Gel LH_2	4.7	(.185)	0.1296	4.19	(0.165)	10.61	(.348)
	3.5	(.138)	1.09	4.19	(0.165	13.26	(.435)
	5.2	(.206)	0.184	5.08	(0.20)	8.35	(.274)
	5.0	(.197)	1.0	5.08	(0.20)	27.43	(.90)
	3.1	(.122)	1.09	5.08	(0.20)	13.96	(.458)
	2.36	(.093)	0.695	5.08	(0.20)	30.48	(1.0)
	2.44	(.096)	0.943	5.08	(0.20)	18.50	(.607)
	3.51	(.138)	0.716	4.83	(0.19)	21.95	(.72)
	3.84	(0.151)	0.571	4.45	(0.115)	33.22	(1.09)
	3.12	(0.123)	0.872	4.45	(0.175)	7.13	(.234)
	3.20	(0.126)	0.218	4.45	(0.175)	15.09	(.495)
				4.45	(0.175)	13.045	(.428)
				4.4	(.173)	10.88	(.357)

Table 9. Continued

	Bubble Dia. mm (in.)	Frequency (bubbles per sec)	Bubble Dia mm (in.)		Rise Velocity cm/sec ft/sec)	
Gel LH_2 (continued)			4.04	(.159)	14.20	(.466)
			4.57	(.180)	14.42	(.473)
			4.95	(.195)	13.11	(.43)
			5.23	(.206)	5.30	(.174)
			3.12	(.123)	19.20	(.63)
			2.69	(.106)	10.24	(.336)
			3.048	(.120)	10.24	(.336)
			2.82	(.111)	26.21	(.86)

due perhaps to the nonuniformity in PPO foam geometry. It was noted that the bubbles leaving the PPO foam in neat LH_2 were separated sufficiently so that agglomeration did not appear to occur on the surface of the foam. A comparison of Equation 5 results with the data, indicated that bubble departure times were three orders of magnitude greater than predicted. Bubble diameters are greater than ten times the cell diameters on the average, and bubbles are separated on the surface. These observations indicate that the surface area producing the vapor for each bubble is much greater than the cell area causing a wide discrepancy between Equation 5 and the data to be physically possible. The observed bubble pattern was consistent with the above discussion of cell diameter variation and interconnections, and with the bubble point tests of Ref. 19 which indicated that the preponderence of cells were below 40 microns in diameter. These cells would feed the larger cells to produce the bubble departure data observed.

Comparing the trend of the neat LH_2 data with that of the gel LH_2 data indicates that for the same size bubbles, gel LH_2 bubbles will have greater departure intervals. This is due mainly to the fact that the heat flux is lowest at the edge of the foam and that the neat bubbles were observed several centimeters from the edge. Also, for a given foam cell size, the bubble diameter at departure will be greater in the gel/LH_2 PPO system than it would be in the neat LH_2/PPO system. Thus the direct heat flow path feeding the bubble is proportionally smaller in the gel PPO system.

Figure 4-13 shows data plotted in the format of Equation 6 with a correlating line found by a linear least squares regression analysis. For Equation 6, N was found to be 0.473 and C_1 was found to be 2.36×10^{-2}. A similar equation could be obtained for gelled LH_2 by utilizing the approximate surface force increase factor of 25 and heat flux data for the edge of the foam. Based on these assumptions an equation in the form of Equation 6 was plotted to the data with N found to be 0.551 and $C_1 = 2.281$. This is also plotted in this figure. The comparison of correlation equations confirms the observation that bubble frequency will be greater for neat LH_2 compared to gel LH_2 for a given bubble diameter. Both data plots have limited usefulness other than for comparison purposes due to the large variance between the data and correlating equations.

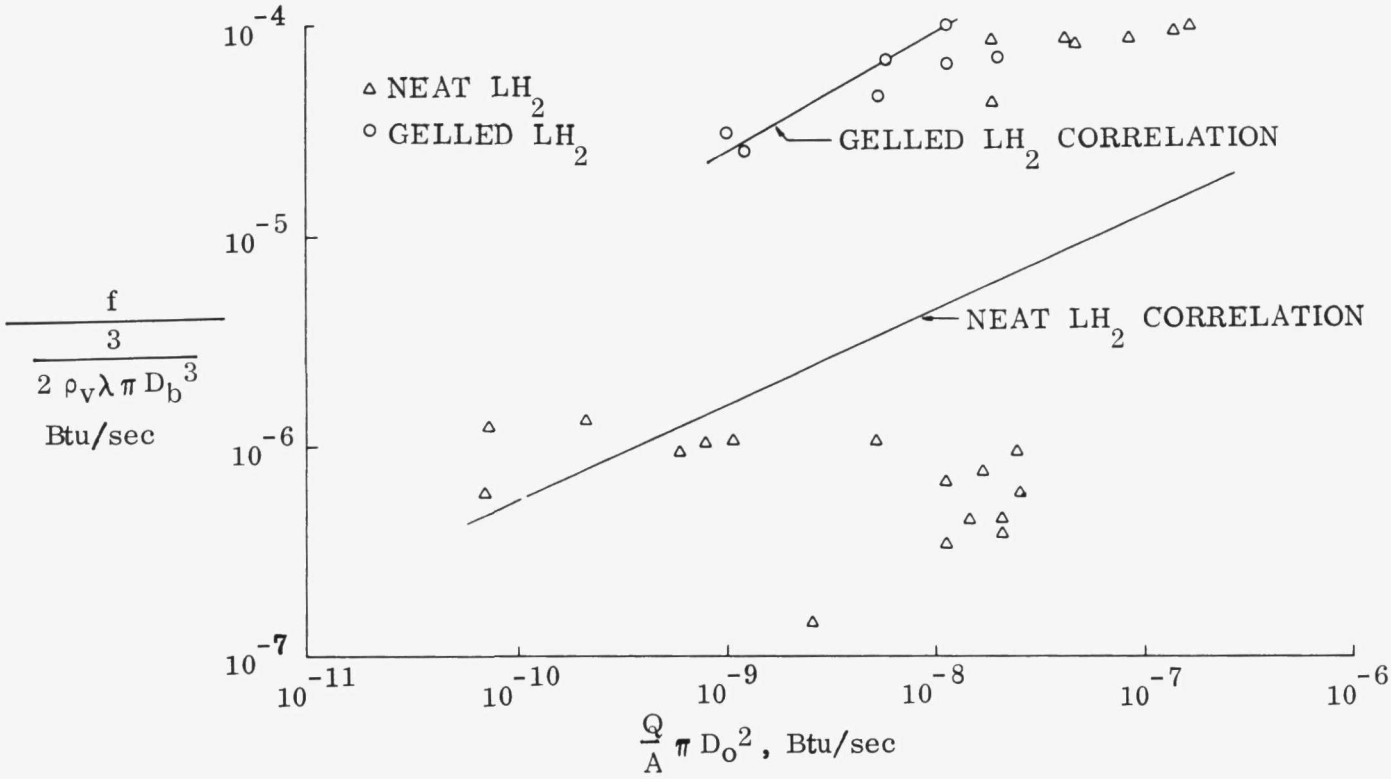

Figure 4-13. Correlation of Bubble Departure Frequency and Cell Heating Rate

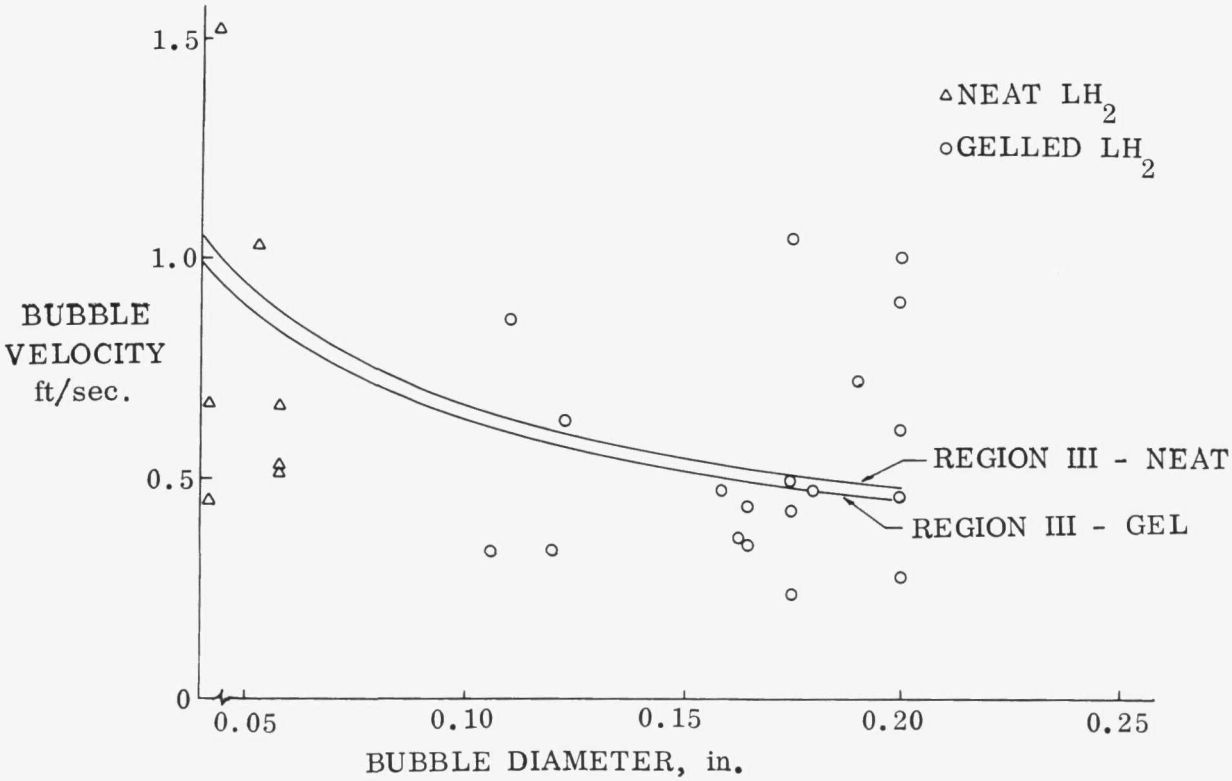

Figure 4-14. Bubble Rise Rate Versus Diameter for Neat and Gelled LH_2

Bubble rise velocities were computed for bubbles leaving the foam and rising in both the gelled and neat LH_2. This data is fitted in Figure 4-14 with predictions of bubble velocity vs diameter obtained from $U = 1.35\ (\sigma\ g_c/(\rho_L R_B)^{1/2}$ which is the prediction equation for region 3. The surface tension used for gel in computing the values shown is identical to the liquid surface tension. This is consistent with the thixotropic nature of the gel. Once bubbles start to rise and move in the gel the surrounding gel shear thins and behaves more like the liquid than it would during bubble breakoff. Actual data was taken by following bubbles individually as they moved through the fluid until they could no longer be visually discerned. This caused the data to be taken near the surface of the foam, perhaps before the bubbles reached terminal velocity. This would cause some scatter, however the major cause for velocity variations in bubbles of like diameters is probably different growth rates. Bubbles being formed faster due to more local cell interconnections or higher local heat flux will have greater inertia leaving the surface of the foam than bubbles formed at a slower rate. It is difficult to determine from the data any difference between bubbles rising in gel or neat LH_2 compared to the analytical model. It should be noted that bubble Reynolds numbers predominately fall within region 3 as defined by Peebles and Garber, Ref. 22, with some Reynolds numbers slightly lower, falling in region 2. This indicates that bubbles are rising where drag and surface forces are most important.

Test results indicated some ethane did initially enter the foam during gelation and immediately thereafter. This appears to be only a transient phenomenon, since the foam subsequently was clean of opaque material. Similarly, no break down of the gel matrix was apparent at the surface of the foam. A further indication of ethane matrix stability is indicated by the fact that temperature profiles within the foam were essentially identical for neat and gelled LH_2. This also implies that the lower boiloff observed with gelled liquid hydrogen is most likely a function of the vertical surfaces of the container rather than the bottom or horizontal surface.

SECTION 5

REFERENCES

1. McKinney, C. D. and Tarpley, W. B., "Gelling of Liquid Hydrogen," Technidyne Inc., West Chester, Pennsylvania, Contract No. NAS3-4186, Report No. NASA CR-54967, June 1966.

2. Kartluke, H., et. al., "Gelling of Liquid Hydrogen," Technidyne Inc., West Chester, Pennsylvania, Contract No. NAS3-2568, Report No. NASA CR-54055, July 1964.

3. VanderWall, E. M., "Carbon Compounds/Liquid Hydrogen Fuels," Technical Report FR02-W396, Contract SNP-1, Aerojet Liquid Rocket Company, October 1970.

4. Globus, R. H., VanderWall, E. M., and Cabeal, J. A., "System Analysis of Gelled Space Storable Propellants," Aerojet Liquid Rocket Company, Contract No. NAS7-473, Report No. AIAA 70-609, June 1970.

5. Gordon, L. J. and Lee, J. B., "Metals as Fuels in Multicomponent Propellants," Aerojet-General Corp., ARS Journal, Volume 32, No. 4, pp 600-606, April 1962.

6. Yates, G. B., "Open Cell Cryogenic Insulation," Convair Division of General Dynamics, Paper L-5, Cryogenic Engineering Conference, June 1970.

7. Yates, G. B. and Bennett, F. O., "Open-Cell Cryogenic Insulation," Convair Division of General Dynamics, GDC-ERR-1586, December 1970.

8. "Design and Development of PPO Foam as a Reusable Internal Insulation for LH_2 Tanks," Phase One Progress Report, Contract NAS8-27566, Convair Division of General Dynamics, June 1972.

9. "Design and Development of PPO Foam as a Reusable Internal Insulation for LH_2 Tanks," Phase Two Progress Report, Contract NAS8-27566, Convair Division of General Dynamics, September 1972.

10. "Space Shuttle Structural Test Program, Final Report - Task 1.1, Cryogenic Tank Structure/Insulation Test," Vols. I and II, Contract NAS9-10960, Convair Division of General Dynamics, March 1972.

11. Rapial, A. S. and Daney, D. E., "Preparation and Characterization of Slush Hydrogen and Nitrogen Gels," Technical Note 378, Cryogenics Division, National Bureau of Standards, May 1969.

12. Globus, R. H., "Process of Forming Particles in a Cryogenic Path," United States Patent Number 3,516,879, June 1970.

13. Chemical Engineers Handbook, Third Edition, McGraw-Hill, N.Y., 1950.

14. Journal of the American Chemical Society, Vol. 52, pp. 611-622, 1930.

15. Journal of the American Chemical Society, Vol. 59, p. 273, 1937.

16. Caine, G., "Test Data Sheet and Performance Curves," Project No. 116124-A, Pesco Products Division, Borg Warner Corp., March 1967.

17. "Flow of Fluids Through Valves, Fittings and Pipe," Technical Paper No. 410, Crane Co., 1969.

18. Masica, W. J., Petrash, D. A., and Otto, E. W., "Hydrostatic Stability of the Liquid-Vapor Interface in a Gravitational Field," NASA-TN-D-2267, May 1964.

19. Tatro, R. E. and Bennett, F. O., "Open-Cell Cryogenic Insulation," GDC-ERR-1650, December 1971.

20. Hughes, R. R., Handlos, A. E., Evans, H. D. and Maycock, R. I., "The Formation of Bubbles at Simple Orifices," Chemical Engineering Progress, Vol. 51, p. 557, 1955.

21. L'Ecuyer, M. R. and Murthy, S. N. B., "Energy Transfer From a Liquid to Gas Bubble Forming at a Submerged Orifice," NASA TND-2547, Purdue University, January 1965.

22. Peebles, F. N. and Garber, H. J., "Studies on the Motion of Gas Bubbles in Liquids," Chemical Engineering Progress, February 1953.

23. Cole, R., "A Photographic Study of Pool Boiling in the Region of the Critical Heat Flux," NASA/LeRC, AIChE Journal, Vol. 6, p. 533, December 1960.

24. Freudlich, H., Colloid and Capillary Chemistry, E. P. Dutton and Co., New York, 1926.

SECTION 6

NEW TECHNOLOGY

In compliance with the New Technology clause of this contract, personnel assigned to work on the program have been advised, and periodically reminded, of their responsibilities in the prompt reporting of items of New Technology. In addition, response is made to all inquiries by the company-appointed New Technology Representative and copies of reports generated as a result of the contract work are submitted to him for review as a further means of identifying items to be reported. When deemed appropriate, conferences are held with the New Technology Representative to discuss new developments arising out of current work that may lead to New Technology items. The New Technology Representative will be responsible for transmitting New Technology to the Technology Utilization Officer.

Contractor plans to continue New Technology monitoring and surveillance as described above in the ensuing period to assure all items of New Technology are reported as they develop.

GENERAL DYNAMICS

Convair Aerospace Division